DEVELOPMENT OF A COMPOSITES MANUFACTURING PROCESS TO MANUFACTURE HIGH QUALITY COMPOSITE LAMINATES: PRESSURIZED VARTM

by

Mehmet Akif Yalçınkaya

A Thesis Submitted to the

Graduate School of Sciences and Engineering

in Partial Fulfillment of the Requirements for

the Degree of

Doctor of Philosophy

in

Mechanical Engineering

April 11, 2017

ABSTRACT

Although vacuum-assisted transfer molding (VARTM) is preferred for manufacturing medium to large composite parts due to its simple tooling and low operational cost, part quality dictated by dimensional tolerances, void content and mechanical properties is usually low due to inherent limitations of the process. In this study, the conventional VARTM process was modified and an alternative process for manufacturing of high quality composite laminates was developed by (i) heating a mold to enable the utilization of a high temperature resin system (EPON 862), and (ii) external pressurization of the mold to increase fiber volume fraction and improve mechanical properties. During post-filling stage, various levels of pressure were applied in a pressure chamber mounted on top of the mold and effect of external pressurization on laminates made of various number of plies was investigated. It was observed that pressurized and heated VARTM led to laminates with less than 1% void content in all laminates manufactured under various external pressure levels. In addition, up to 25% and 13% increase in fiber volume fraction and flexural strength were achieved, respectively. Microstructural analyses, dry and wet compaction characterization of 8-harness satin woven fabric were carried out to understand the void morphology and compaction characteristics of the fabric.

Moreover, the applicability of pressurized VARTM was studied by using another resin type (PRO-SET INF 114) which was processed at low temperatures. It was observed that fiber volume fraction increased similarly to that of EPON laminates and void content of laminates was below 1%. This epoxy resin system had high viscosity which yielded to long mold filling times in conventional VARTM. The pressure chamber was vacuumed at a certain pressure to relax the fabric and increase its permeability which significantly enhanced the resin flow and shortened the mold filling time by 48%. It was concluded that pressurized VARTM could also be implemented to low temperature resins with high viscosity to (i) enhance resin flow, (ii) increase fiber volume fraction, (iii) achieve low void content, and (iv) assure uniform thickness distribution.

ÖZET

Vakum destekli reçine transfer kalıplama (VARTM), basit kalıp ve düşük işletme maliyeti nedeniyle orta ve büyük ölçekli kompozit parçaların imalatında tercih edilen bir imal usulüdür. Fakat bu imal usulünün doğası nedeniyle, boyutsal toleranslar, boşluk oranı ve mekanik özellikler gibi parça kalitesini belirleyen faktörler kısıtlı seviyelerde elde edilebilmektedir. Bu tez çalışmasında, geleneksel VARTM imal usulünde değişiklikler yapılarak, yüksek kaliteli parça imalatı için alternatif bir yöntem geliştirilmiştir. Genellikle oda sıcaklığında ve vakum basıncı ile sınırlanan VARTM'a kıyasla, parçanın elyaf oranını arttırmak ve mekanik özelliklerini iyileştirmek için; (i) kalıbın ısıtılması sayesinde yüksek sıcaklıkta işlenen bir reçine sisteminin (EPON 862) kullanılmasıyla ve (ii) kalıbın dışarıdan basınçlandırılmasıyla, basınçlı VARTM imal usulü geliştirilmiştir. Kalıp dolumu sonrası, kalıbın üzerine yerleştirilen basınç odasına farklı sıkıştırma basıncı seviyeleri uygulanarak, bu uygulamanın farklı sayıda katmanlardan yapılan parçaların özelliklerine etkisi araştırılmıştır. Isıtılmış kalıpta imal edilen tüm kompozit levhalarda, tüm basınç seviylerinde %1'in altında boşluk oranı elde edilmiştir. Ayrıca, basınçsız üretilen parçalara kıyasla, elyaf oranı %25 yükselirken, eğilme mukavemeti de %13'e kadar artmıştır. Mikro-yapısal incelemeler sonucunda, az miktarda olan boşlukların yapısal özellikleri belirlenmiş ve elyaf liflerinin farklı basınçlardaki sıkışması ölçülmüştür. Ayrıca, elyaf dokumalar üzerinde kuru ve ıslak sıkışma deneyleri yapılarak elyafın sıkışma özellikleri tanımlanmıştır.

Bunlara ek olarak, basınçlı VARTM'ın oda sıcaklığı mertebesinde işlenen bir epoksi reçine (PRO-SET INF 114) ile uygulanabilirliği de incelenmiştir. EPON 862 ile üretilen parçalara benzer olarak, elyaf oranı artarken, boşluk oranı da %1'in altında elde edilmiştir. Bu reçine, önceden kullanılan EPON 862 reçinesinden daha yüksek viskoziteye sahip olduğundan, kalıp dolum süresi uzamıştır. Basınç odası vakumlanarak, sıkışmış elyaf rahatlatılımş ve geçirgenliği arttırılarak akış hızlandırılmış, kalıp dolum süresi %48 düşürülmüştür. Sonuç olarak, basınçlı VARTM'ın düşük sıcaklıkta işlenen yüksek viskoziteli reçinelerle uyulanabilirliği; (i) reçine akışı hızlandırılarak, (ii) elyaf oranı arttırılarak, (iii) düşük boşluk oranı ve (iv) düzenli kalınlık dağılımı elde edilerek gösterilmiştir.

Dedicated to my family…

ACKNOWLEDGEMENTS

I would like to thank my advisor Dr. Murat Sözer for all his help and guidance during my studies at Koç University. I am grateful to work with such an encouraging advisor with an admirable personality. He has been more than an advisor and had a significant impact on my research career and personality.

I would also like to express my sincere gratitude to Dr. Cengiz Altan for giving me the opportunity to work with him at the University of Oklahoma (OU) as a visiting researcher. His guidance, enthusiasm and helpful critiques on my research were very valuable for the completion of this dissertation. His willingness to spend his time generously on my research has been very much appreciated and respected. I feel more than lucky to work with such an inspiring person.

My grateful thanks are also extended to the committee members, Dr. Demircan Canadinç, Dr. Can Erkey, and Dr. Nuri Ersoy for their participation and valuable feedback.

Furthermore, I wish to thank my fellow lab-mates, Bekir Yenilmez and Barış Çağlar for their brotherhood and supportive attitude during my studies at Koc University. They were the ones who always encouraged and helped me with anything I struggled during the last six years. Besides, I would like to thank Mert Hancıoğlu for his help and contributions.

Additionally, I thank Görkem Güloğlu, Dr. Youssef Hamidi, Mehrad Amirkhosravi, and Maya Pishvar for their companionship and help during my research at OU Composites Research Group. Also, I would like to thank OU Aerospace & Mechanical Engineering staff, Billy Mays, Greg Williams, and Debbie Mattax for easing my life with all their help and cheerful attitude.

I also thank TÜBİTAK (The Scientific and Technical Research Council of Turkey) for 2214-A scholarship and Koç University for their financial support during my PhD studies.

Finally, I thank my beloved parents, Meral and Nadir Yalçınkaya, my brother, Uğur Alp Yalçınkaya and my wife, Nur Soylu Yalçınkaya for their endless love and support.

TABLE OF CONTENTS

LIST OF TABLES

LIST OF FIGURES

1. INTRODUCTION

1.1. Overview of polymeric composites and manufacturing processes

Polymeric composites have been widely used in many industries such as aerospace, marine, automotive, and defense due to their light-weight and superior mechanical properties. These materials are made of two main components which are the matrix and reinforcement. Matrix materials are usually divided into two main branches as thermoplastic (e.g., polyethylene, polypropylene, polyamide, and etc.) and thermosetting resins (e.g., polyester, epoxy, and vinylester). Most commonly used reinforcement materials are glass, carbon, and aramid (a.k.a. Kevlar) fibers which are available either in chopped strand mat, woven (crimp), or stitched (non-crimp) fabric forms as seen in Figure 1.1.

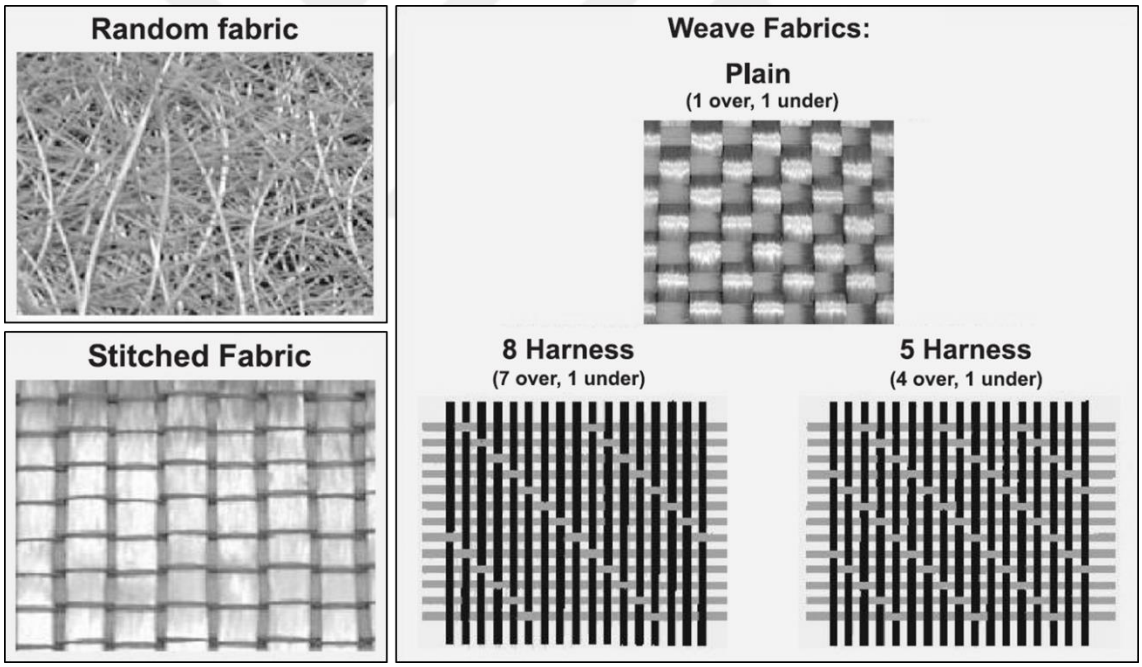

Figure 1.1 - Typical reinforcement fabrics for composites [1]

Most common manufacturing processes for laminated composites are autoclave molding, and Liquid Composite Molding (LCM) processes. Wet-lay-up is the most conventional method in which fabric layers are laid on a mold and they are impregnated with a liquid resin with the help of a brush and/or consolidation roller. Although wet-lay-up is a low cost method, it is labor intensive, parts have high void content, and repeatability of the

process is limited. Therefore, advanced composite materials are manufactured by using autoclave molding or LCM processes.

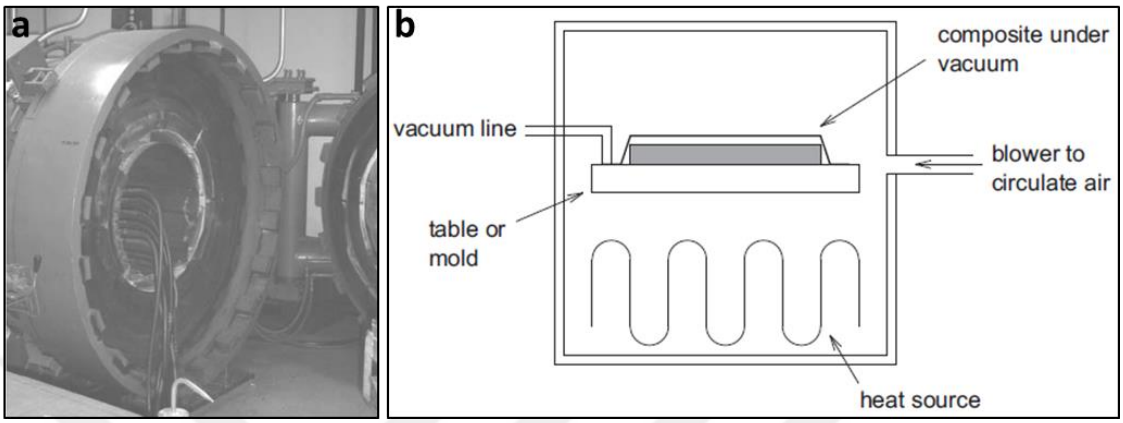

Figure 1.2 - (a) An autoclave and (b) its schematic view [1]

As Figure 1.2 shows, autoclave molding process is performed in a heated pressure vessel to manufacture advanced composites. Pre-impregnated fabric preform (a.k.a. prepreg) is placed on the tool by hand layup or automated tape layup, vacuum bagged, and cured in the autoclave under pressure at certain cure cycles. Low void content, superior mechanical properties and good dimensional tolerances can be achieved in autoclave molding process. However, this process requires high equipment, material, and operational costs which result in expensive products.

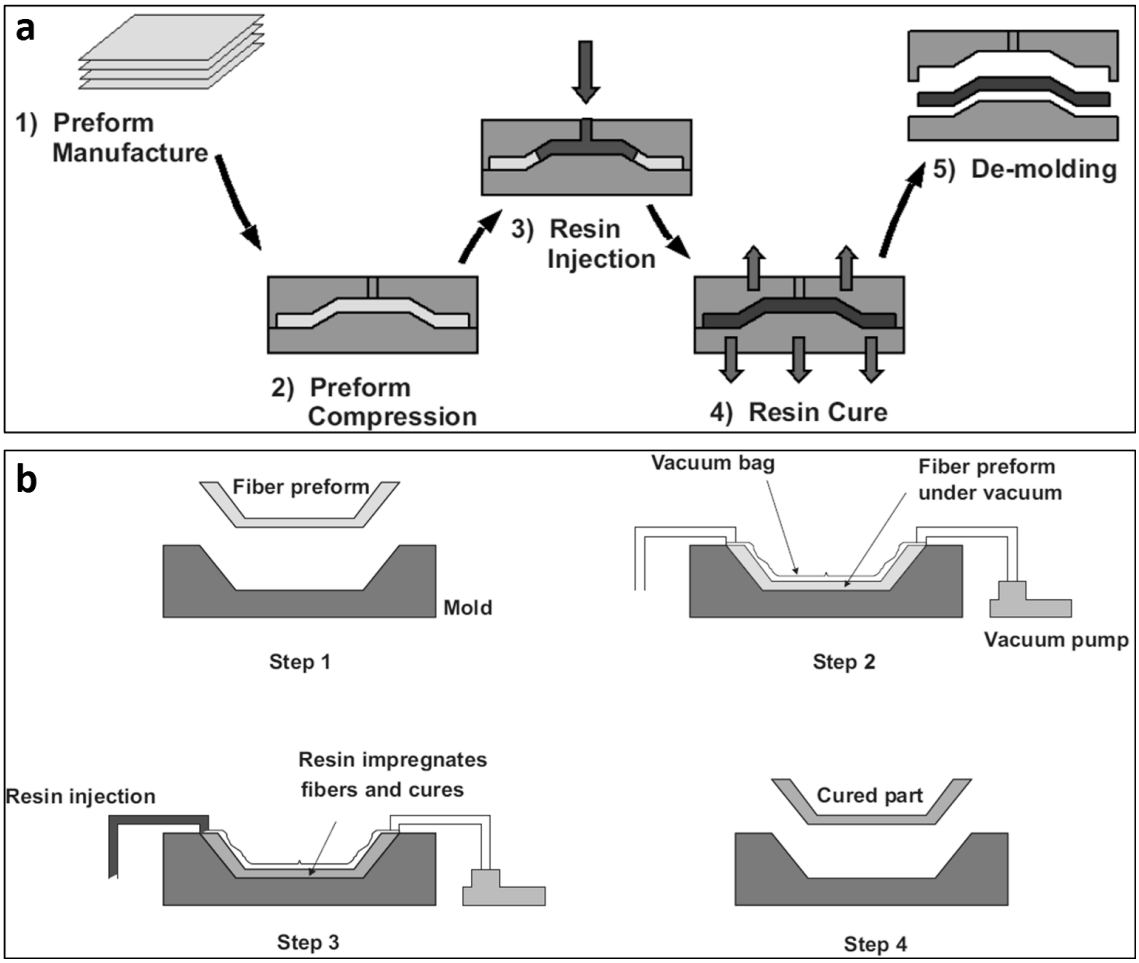

Figure 1.3 - Schematic view of typical LCM processes: (a) RTM and (b) VARTM [1]

LCM processes, such as Resin Transfer Molding (RTM) and Vacuum Assisted Resin Transfer Molding (VARTM, a.k.a. Vacuum Infusion, VI) are potential alternatives to autoclave molding of composite laminates. These LCM processes are also referred as out-of-autoclave manufacturing methods which require relatively lower material, equipment, and operating costs compared to autoclave molding. RTM is a double-sided molding method in which a male and a female mold halves are made of rigid materials (e.g., steel or aluminum). As Figure 1.3(a) shows, a fabric preform is placed into the mold cavity and resin is injected with an injection machine. Small dimensional tolerances and good surface quality can be achieved due to almost rigid mold structure. However, planar dimensions of parts limit the applicability of the process since machining of a double-sided mold is not feasible as the dimensions of mold increase. VARTM is an

advantageous process for manufacturing large parts such as boat hulls and wind turbine blades since it requires only a single sided mold (see Figure 1.3(b)) which significantly reduces the tooling cost. Fabric preform is placed into the mold and sealed under elastic vacuum bag by using a sealant tape. Resin is infused through the preform by using a vacuum pump which creates a pressure differential between the inlet and exit ports of the mold. Details of VARTM process, challenges in terms of part quality and processing related issues will be discussed in the next section.

1.2. Challenges of VARTM and its variants

Although VARTM is an advantageous composites manufacturing process due to its low investment and operational cost, it has various drawbacks such as non-uniform and limited compaction pressure on the fibers which cause in-plane variations of thickness and mechanical properties, and lower fiber volume content compared to RTM and autoclave molding [1]. Typically, fiber volume fractions of 40-50% is achieved in VARTM [2] whereas it can be increased up to 65% and 70% in RTM and autoclave molding, respectively [3]. In addition, the surface at the vacuum bag side has a higher roughness and lower quality due to texture of peel-ply which separates the part from vacuum bag and flow distribution medium, if used.

One of the shortcomings of VARTM is long cycle times due to long mold filling times. Some studies [4,5] used a highly permeable flow distribution medium (DM) on top of fabric preform to reduce the mold filling time by increasing planar resin velocity (see Figure 1.4). This method is known as SCRIMP (Seemann Composites Resin Infusion Molding Process) [6] in which liquid resin flows through the distribution medium and then, impregnates the fabric through-the-thickness (transverse) direction as shown in Figure 1.4(b). Since the flow is not only planar and transverse permeability of the fabric is much lower than the planar permeability, void content may show high variation through the thickness and along the laminate [7], and complete wetting of fibers in thick parts may be difficult to achieve. In addition, the size and placement of the distribution medium should be carefully designed to fill the mold cavity completely and manufacture parts with adequate properties [8]. A peel-ply layer is placed in between the DM and

fabric to enable removal of the DM. The DM and peel-ply are peeled off from the composite after part is demolded which results in a textured surface with high roughness causing deterioration of mechanical properties [9–11].

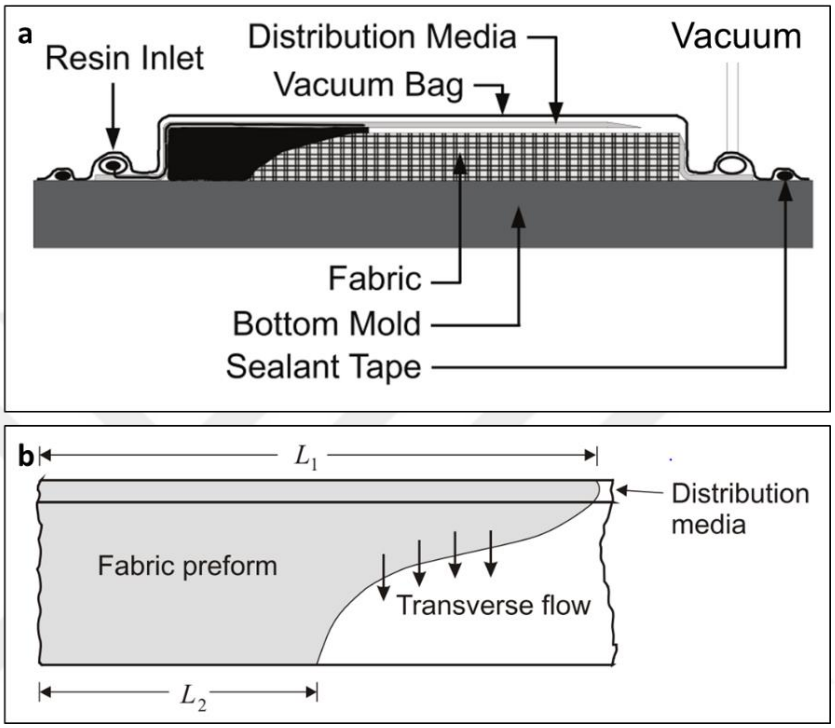

Figure 1.4 - (a) Schematic view of SCRIMP [12] and (b) transverse flow through fabric preform [1]

Alternatively, resin flow can also be manipulated by using various external vacuum chambers placed on top of the vacuum bag to relax the fabric and/or lift the vacuum bag to form a gap for resin to flow through [9,13,14]. The chamber is either placed on the vacuum bag as in Flow Flooding Chamber (FFC), or fixed under a secondary vacuum bag as in Fast Remotely Actuated Channels (FASTRAC), or moved from one location to another to alter the flow pattern as needed in Vacuum Induced Preform Relaxation (VIPR). These processes could be alternatives to SCRIMP by eliminating the distribution medium, however, they also introduce difficulties in processing. For instance, in FFC, the chamber lifts up the vacuum bag and resin enters to a region with almost no resistance against it, thus causing an uncontrolled resin flow. In addition, since the compaction

pressure is locally decreased inside the chamber and increased at the chamber-vacuum bag interface, parts are more prone to local variations.

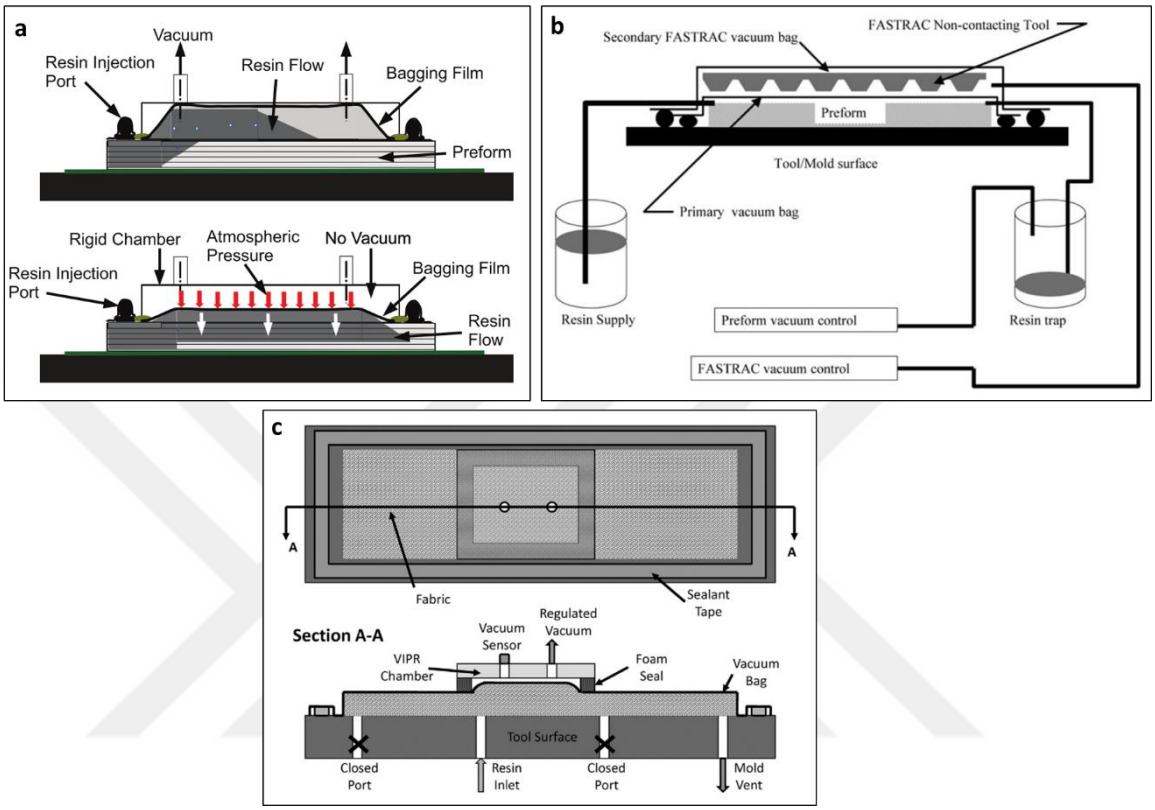

Figure 1.5 – Schematic view of (a) FFC [12], (b) FASTRAC [9], and (c) VIPR [15] processes

Even though these flow enhancement methods enabled faster impregnation of fabrics, they had various shortcomings and were neither practical nor readily applicable to every part geometry. Some studies [16–18] used heated-VARTM [19] to process high-temperature resins without using a distribution medium. On the other hand, some used distribution medium as well since the specific resin systems (LaRC PETI-330, PETI-8 and Cycom 977-20) they used were still too viscous to process even at elevated temperatures [20,21]. In some heated-VARTM studies using various types of resins and fabrics [16,20,22], void content was reduced below 1% whereas some reported higher values up to 7.5% [17,21]. As discussed by various studies [23–25] in detail, capillary number should be around a certain value (~10^{-3}) to achieve complete wetting of fibers

and thus, to hinder inter-tow and intra-tow void formation. Capillary number is linearly related to viscosity and contact angle of resin both of which are significantly dependent on resin temperature. Hence, one can adjust the capillary number by heating the resin if the cure kinetics of the resin allows processing at elevated temperatures. By controlling the viscosity and thus capillary number, the void content of the laminate can be minimized. However, it should be noted that heating the resin accelerates cross-linking reaction in thermosetting polymers and this increases the viscosity of the resin. The overall change in the viscosity due to temperature and cure may cause premature gelation before completing mold filling and post-filling stages. Therefore, resin properties, mold filling and post-filling times should be taken into account before manufacturing with heated VARTM.

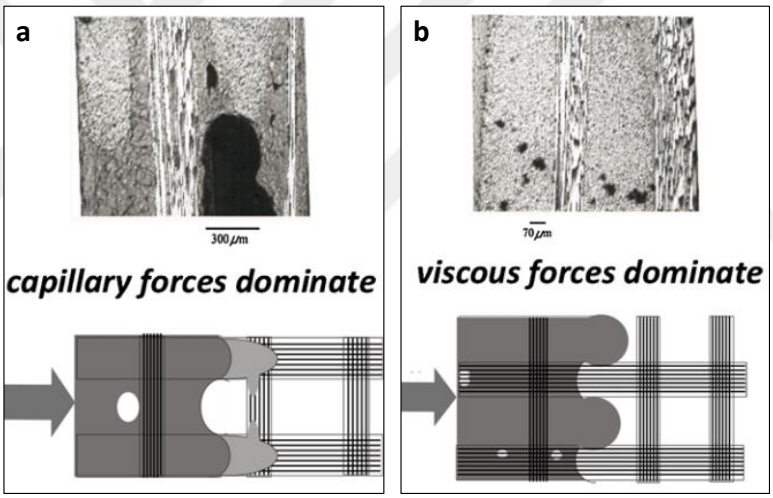

Figure 1.6 - Void formation due to dual-scale flow: (a) inter-tow void formation due to capillary flow, and (b) intra-tow void formation due to viscous flow [23]

Voids are flaws which may significantly affect quality and mechanical performance of composite laminates [26,27]. Voids of different length scales are formed due to: (i) dual scale resin flow through a fiber preform [23,28] (see Figure 1.6); (ii) release of volatiles during curing of the resin [29]; and (iii) dissolved gasses in the resin [30]. A previous study on VARTM [31] investigated the effect of vacuum pressure, inlet pressure, and temperature on the part properties and reported that the following conditions led to low void content: (a) high mold temperature coupled with low gauge vacuum pressure at the

exit, or (b) low mold temperature coupled with high gauge vacuum pressure. The highest fiber volume fraction and lowest void content were achieved when all the following three parameters were controlled by decreasing the *inlet pressure* and keeping the exit at the highest *gauge vacuum pressure* while slightly *heating the mold*. Similarly, various studies [32–35] on RTM and autoclave molding also investigated the effect of process parameters on the void content. Regarding these observations in the literature, it can be concluded that the process parameters during mold filling determine the finished part properties, thus they should be meticulously designed. Besides the process parameters during mold filling stage, post-filling operations also influence the part properties significantly. It was shown that resin bleeding and adding a resistance to flow at the exit not only reduced but also yielded to uniform distribution of voids [7]. Degassing of resin before infusion also has an important effect on reducing the void content of composite laminates as stated in various studies [30,36,37].

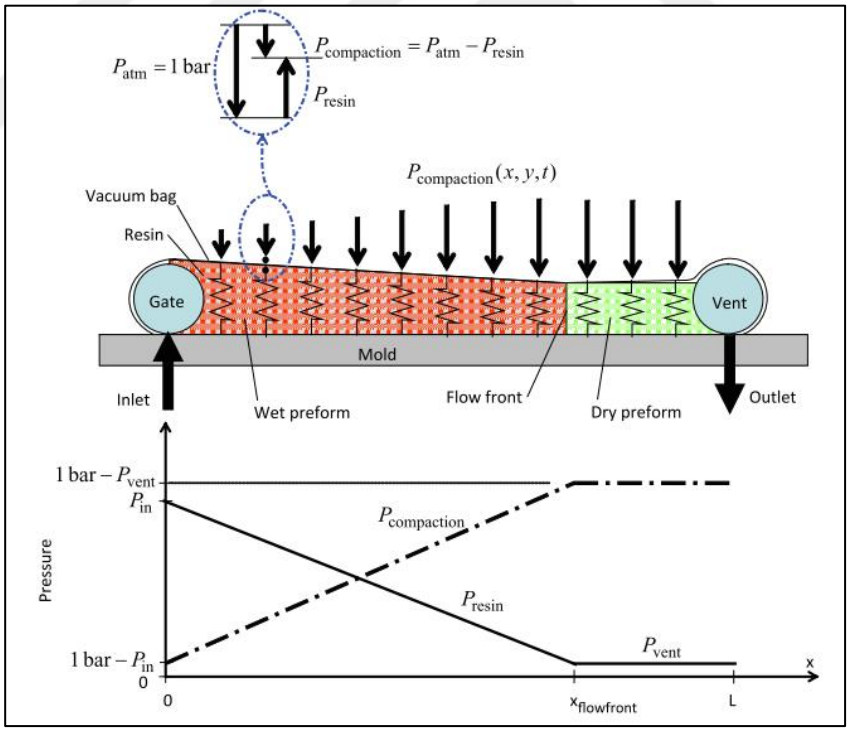

Figure 1.7 - Variation of compaction pressure and thickness in VARTM [1]

Another handicap of VARTM is the thickness and thus, fiber volume fraction variation in the laminate due to varying compaction pressure as illustrated in Figure 1.7 [38–40].

The impregnated preform is thickest at the inlet side, and the thickness gradually decreases towards the exit side due to lower resin pressure causing higher compaction pressure at the exit side [39,41–43]. Various studies [41,42,44,45] showed that applying appropriate post-filling operations such as clamping the inlet and bleeding excess resin from the exit after complete mold filling help to reduce thickness variation by equalizing the compaction pressure on the preform. However, recalling that the maximum compaction pressure on the vacuum bag is limited to atmospheric pressure (~100 kPa), removal of excess resin and equalization of the compaction pressure on the whole part may take long time depending on the fabric permeability and resin viscosity. In various studies, it was documented that equalization of thickness took several times or an order of magnitude longer than the mold filling time [41,45]. In such cases with long post-filling procedures are required, premature resin gelation may occur before the thickness gradient is eliminated.

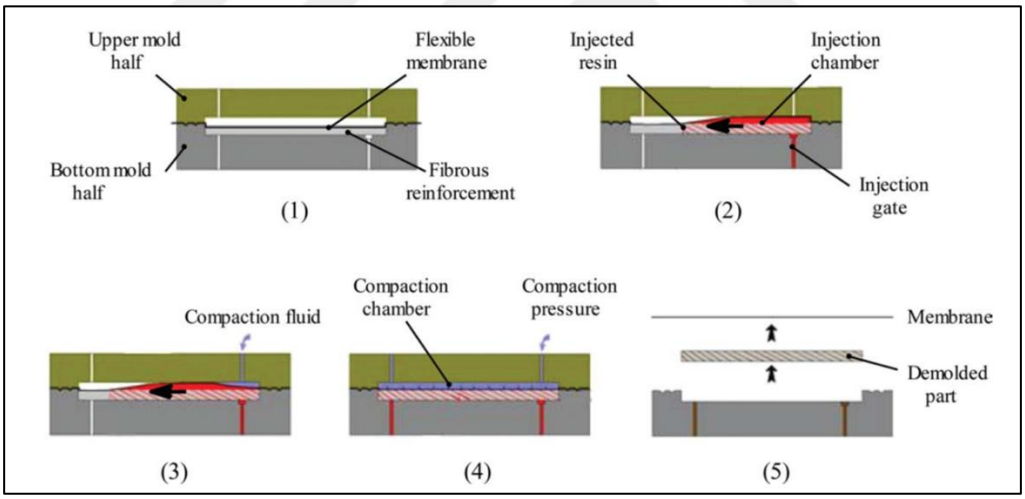

Figure 1.8 - Flexible injection and its main steps [46]

Various studies investigated alternative methods to increase the compaction pressure on the fabric in LCM. Flexible injection was developed to shorten cycle time and increase fiber volume fraction of the laminates [46,47]. As shown in Figure 1.8, a preform was placed under a flexible membrane and resin was injected with an injection machine (at 2 bars of injection pressure in that study). Injected resin lifted the membrane and accumulated near injection port and then, it was distributed by applying compaction

pressure on the membrane with a pressurized silicone oil (at 6 bars in that study). Although, it was concluded that fill time was reduced compared to RTM and uniform thickness was achieved along stair-shaped laminates, this process had various challenges. It was reported that the upper chamber geometry significantly affected the part quality and could cause dry spots in the part [47]. Moreover, the compaction fluid had to be cleaned before removal of the laminate. Another approach to increase the compaction pressure on fabric preform was pressurizing the preform with an inflatable bladder [18]. A fixture was placed on the mold and an inflatable bladder was pressurized under the fixture to consolidate the preform under vacuum bag as shown in Figure 1.9. 20% thickness reduction at 483 kPa of bladder pressure was achieved and tensile strength was increased from 218 to 272 MPa. This process showed the potential of external pressurization on laminate properties. However, applicability of an inflatable bladder could be limited in molds with curvatures and large dimensions.

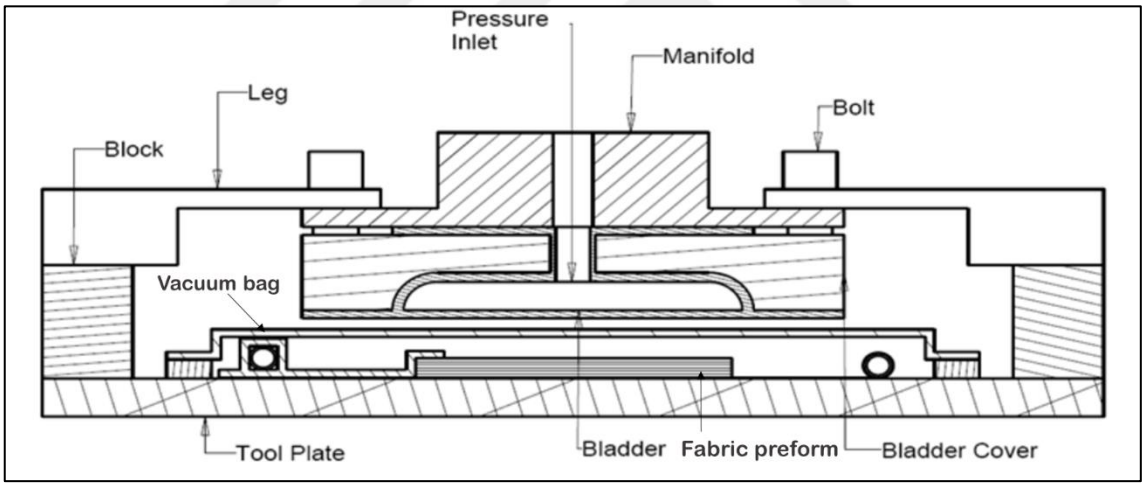

Figure 1.9 - Fabrication of composite laminates by VARTM augmented with an inflatable bladder [18]

1.3. Objective and outline of the dissertation

The objective of this dissertation is to alleviate some of the process related drawbacks of VARTM by developing an externally pressurized variant of VARTM, which can be a low cost alternative manufacturing process for advanced composites. It is aimed to implement a high temperature-processed resin system, decrease void content and

thickness variation, and improve mechanical properties. External pressurization of the preform will increase the compaction pressure and increase fiber volume fraction of the laminate, which will yield to laminates with superior mechanical properties. Moreover, a coupled effect of heat and external pressurization on void content is expected.

An experimental setup for pressurized and heated VARTM is designed and manufactured to fabricate the laminates. In Sections 3 and 4, effect of external pressurization on laminate properties will be investigated. A process window will be developed by implementing resin flushing and external pressurization. Compaction characteristics of various number of plies will be investigated and effect of ply-number on laminate properties will be analyzed. Microstructural properties of laminates will be analyzed under optical microscope to identify voids and their morphology. Consolidation of fiber tows in final laminates under various external pressure levels will be investigated by using micrographs.

Furthermore, applicability of pressurized VARTM on a low temperature resin system with higher viscosity will be studied. Since the viscosity of low temperature-processed resin is higher, it is expected that the mold filling will be longer compared to heated VARTM. It is aimed to enhance resin flow and shorten mold filling time by applying vacuum into the pressure chamber and relax the fabric preform to increase its permeability.

2. EXPERIMENTAL SETUP AND MATERIALS

An overview of the experimental setup for pressurized VARTM and its components are schematically presented in Figure 2.1. The detailed CAD design of the setup was performed in SolidWorks and components such as the mold and pressure chamber were machined in a 3-axis CNC machine. List of components of the experimental setup is given in Table 2.1.

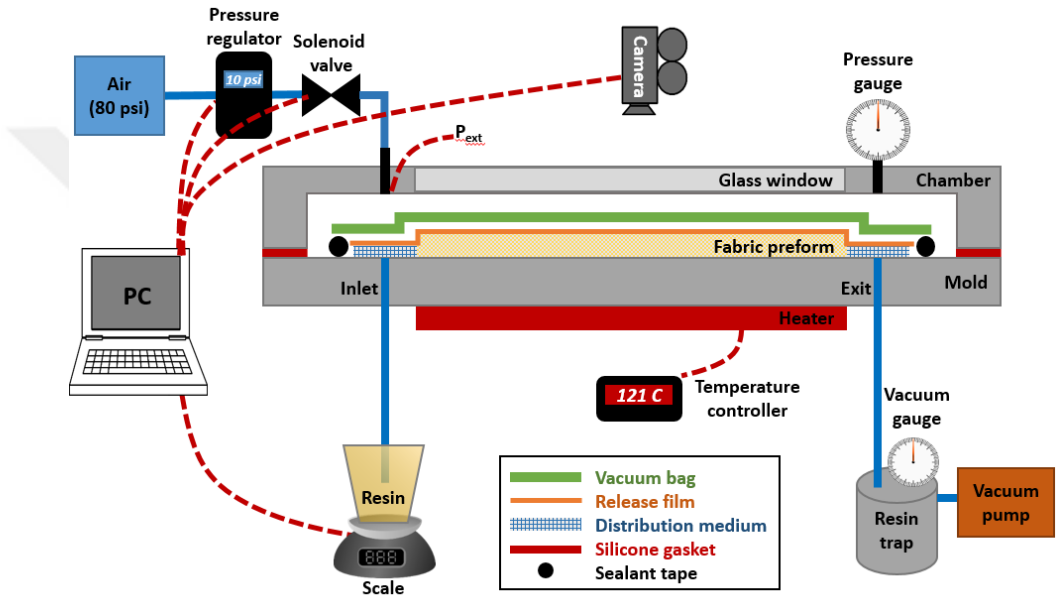

Figure 2.1 - Schematic view of the experimental setup for pressurized VARTM

Table 2.1 - Components of experimental setup

Component	**Brand/Properties**
Pressure regulator	SMC-ITV2050 21N2BL4
Solenoid valve	US SOLID 1/4" Brass Electric Solenoid Valve 24VDC
Scale	OHAUS Pioneer PA313
Temperature controller	Omega DP7002
Heater	McMaster Flexible Silicone-Rubber Heat Sheet, Adhesive Backing
Resin trap	Best Value Vacs 2/3 quart vacuum chamber
Vacuum pump	Best Value Vacs 3CFM vacuum pump
Chamber	In house manufactured
Mold	In house manufactured

2.1. Design and manufacturing of the experimental setup

A 7000 series aluminum lower mold plate with 1 in (25.4 mm) thickness was machined and holes for inlet and exit ports were drilled and threaded to mount barbed fittings as shown in Figure 2.2. Mold material was also aluminum due to its machinability and high heat conductivity.

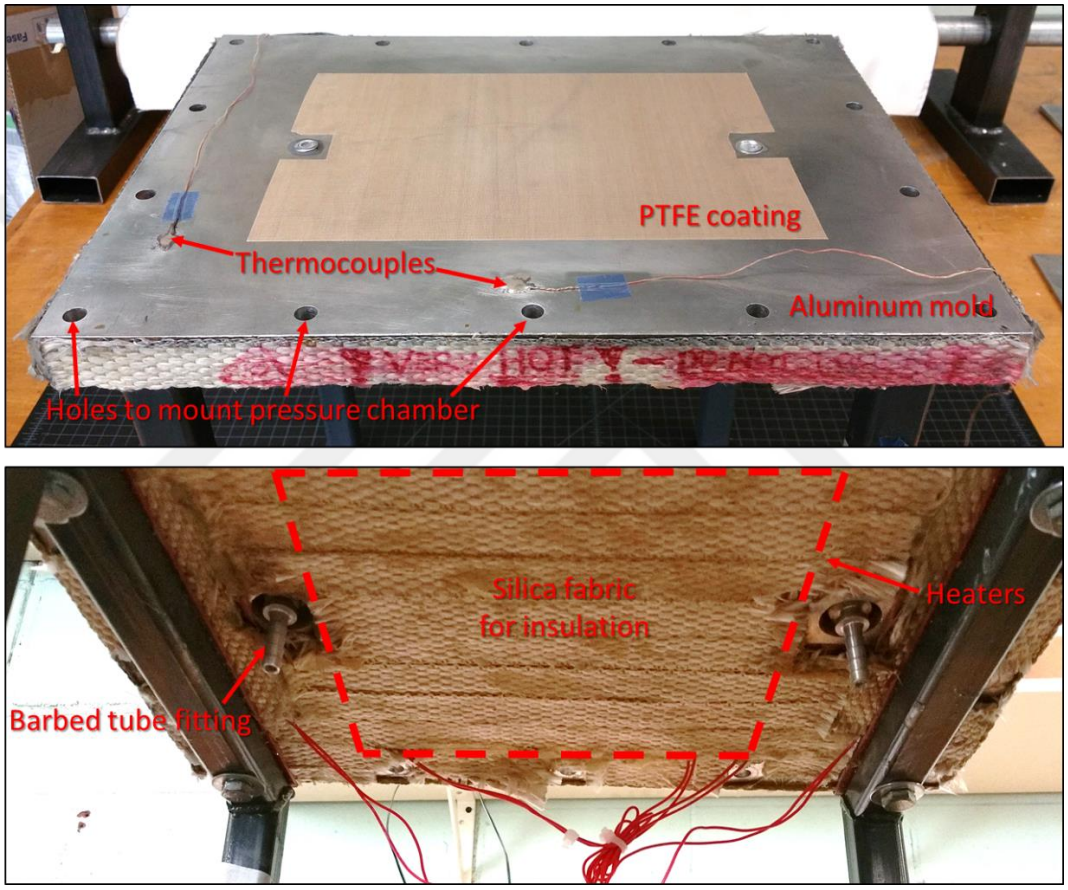

Figure 2.2 - Aluminum mold

Since there was a pressure chamber on top of the mold, the inlet and exit ports were placed under the mold unlike in common VARTM applications as demonstrated in Figure 1.3(b). Fourteen peripheral holes were drilled to bolt the pressure chamber on top of the mold. On the bottom surface of the lower mold, silicone heat sheets with 10 W/in^2 (15.5 kW/m^2) planar heating rate were attached and insulated with a silica fabric. The mold surface was covered with a PTFE coated glass fabric to ease the removal of the manufactured laminates without applying any release agent. The surface temperature was

controlled by on-off temperature controllers which assured uniform temperature distribution on the surface.

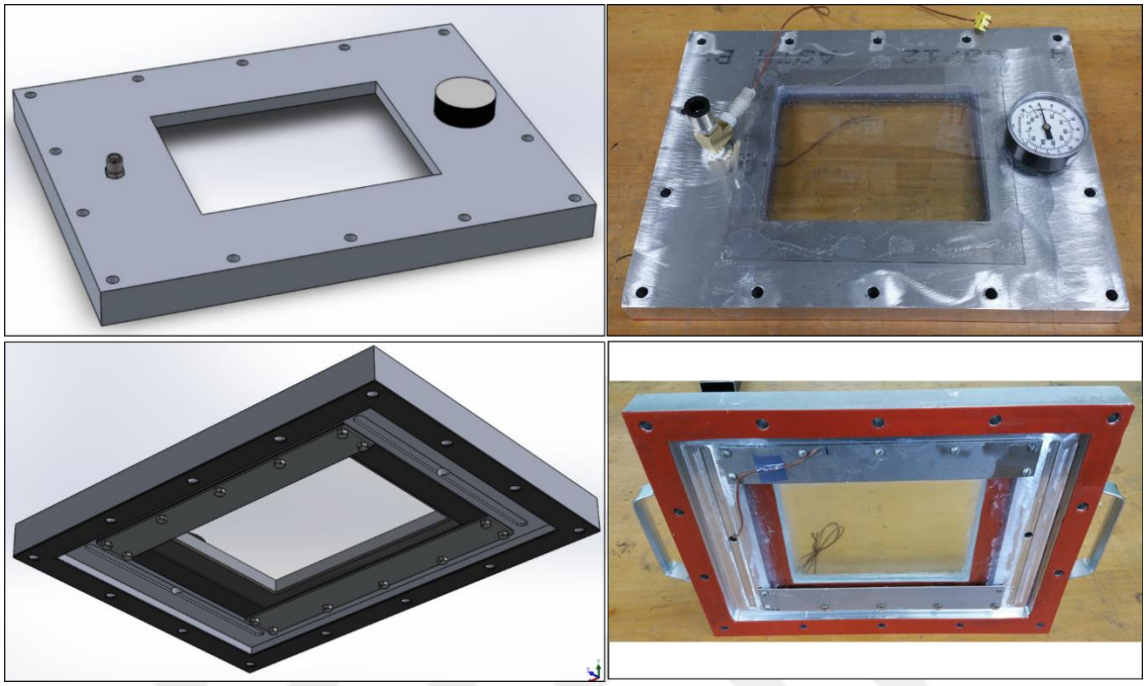

Figure 2.3 - Pressure chamber

Figure 2.3 shows the pressure chamber made of high-strength 7000 series aluminum which was attached to the mold with 3/8 in (~9.5 mm) bolts. A tempered glass window with a thickness of 3/8 in (~9.5 mm) was mounted to the chamber to enable monitoring of resin flow during mold filling. A silicone rubber gasket was glued under the chamber to ensure sealing of the chamber during pressurization. A pressure gauge was mounted to the chamber to monitor the pressure in the chamber. Air pressure was regulated with a pressure regulator and the chamber was pressurized by opening the solenoid valve. In preliminary tests, pressure was increased up to ~550 kPa at 121ºC and there was no air leak or no significant deformation of mold and chamber was observed.

Inlet tube was dipped into the resin reservoir which was placed on an OHAUS Pioneer PA 313 electronic scale to monitor and record the resin mass flow. Exit tube was connected to the resin trap which was vacuumed at a gauge vacuum pressure of ~100 kPa by a vacuum pump. The tubes were made of high temperature silicone to withstand high

temperature at the barbed fittings of the mold. Hose clamps and tacky tape were used to seal fitting-tube interface.

Control of the pressure regulator, solenoid valve, and data acquisition was done using an Arduino Uno controller via an interface created in Labview shown in Figure 2.4. The detailed block diagram of the interface can be found in the Appendix.

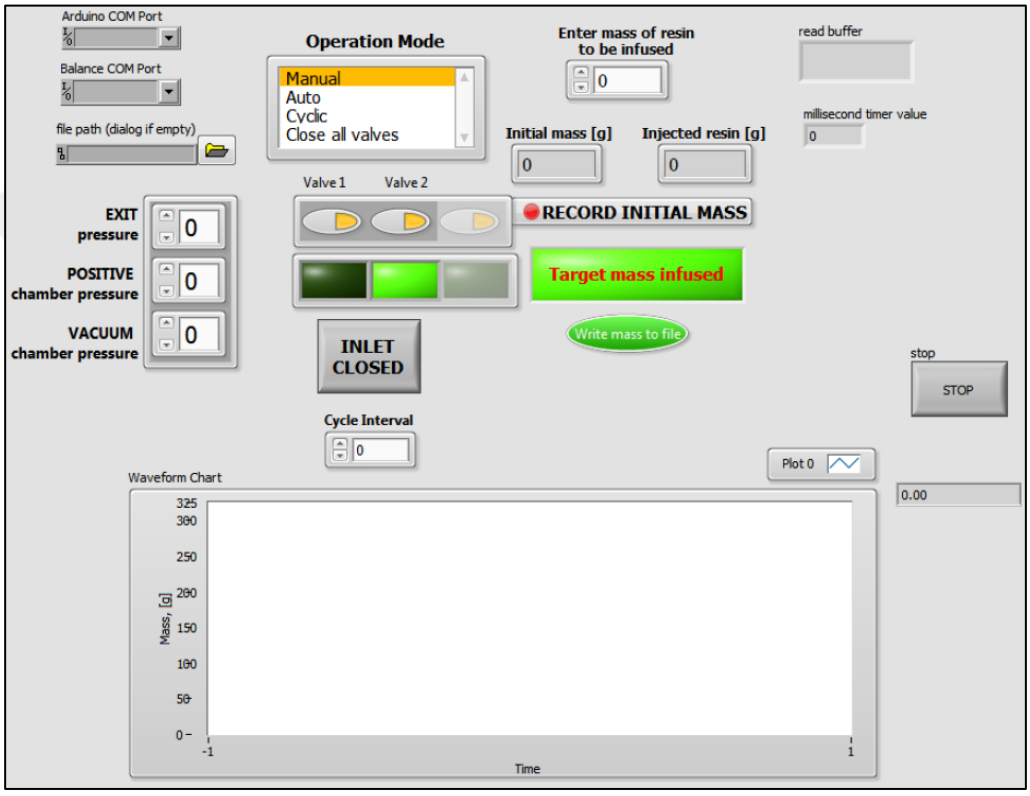

Figure 2.4 - Labview user interface of the experimental setup

2.2. Materials used

The reinforcement material was Fibreglast 8 harness satin woven 7781 E-glass fabric (see Figure 2.5) which has been widely used in aerospace applications. Superficial density of the fabric, ρ_{sup} is 295 g/m^2 as presented in the manufacturer's data sheet [48]. The bulk density of the glass fibers, ρ_{fiber} was measured with a gas pycnometer (AccuPyc II 1340) using 9 samples. Five measurements on each sample were conducted and ρ_{fiber} was found as 2.599±0.012 g/cm^3.

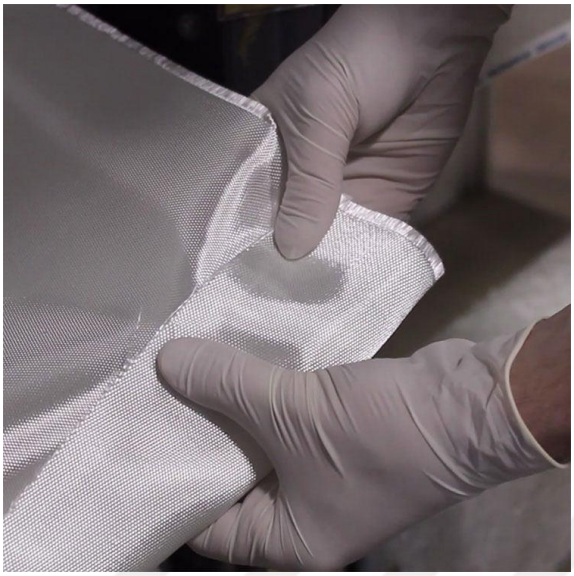

Figure 2.5 - Fibreglast 8HS woven fabric [48]

The matrix material was chosen as a high-temperature-processed epoxy resin which has superior properties compared to polyester or vinyl ester resins which are usually processed at low temperatures, especially for VARTM applications. In this study, EPON 862 epoxy resin and Curing Agent W were used as the resin system (hardener to resin ratio was 26.4/100 by weight). Epoxy and hardener were mixed for 15 minutes at 250 rpm using a mechanical mixer and then, degassed for 2 hours in a vacuum chamber as in another study using the same resin system [49]. According to the manufacturer's datasheet [50], the mixture has a viscosity of 21-23 P at 25°C and it drastically decreases to the order of 10 cP (10 mPa s) at 121°C. Gel time at 121°C is specified as ~95 minutes which allows filling the mold and applying the external pressure for a long enough duration. The cured density of the epoxy was measured according to ASTM D 792 and found as 1.195±0.000 g/cm^3.

3. FABRICATION OF HIGH QUALITY COMPOSITES WITH PRESSURIZED AND HEATED VARTM

3.1. Mold preparation

Six plies of glass fabric with dimensions of 6 in x 8 in (152 mm x 203 mm) were cut along the same direction (i.e., warp direction) of the fabric roll, stacked on top of each other, and placed on the mold surface as shown in Figure 3.1.

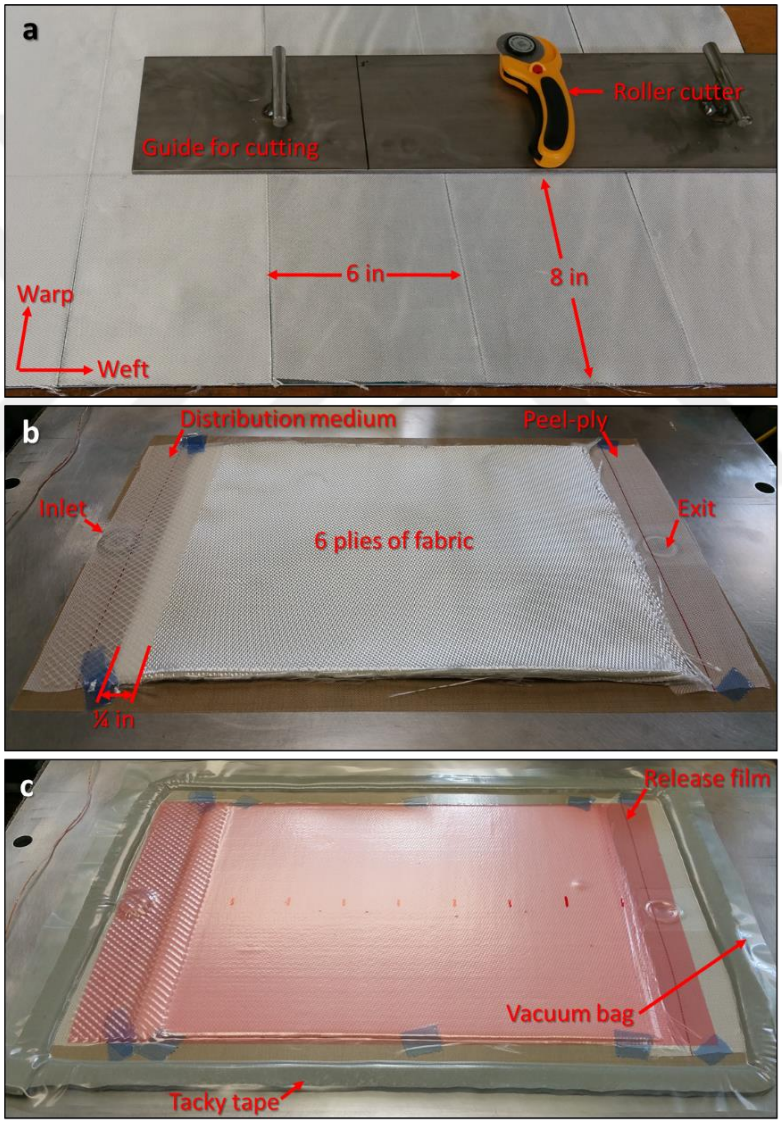

Figure 3.1 - Mold preparation: (a) fabric cutting, (b) stacking and placement of fabric, and (c) vacuum bagging

The distribution medium at the inlet and peel-ply at the exit ports in Figure 3.1 (b) were placed to assure one-dimensional propagation of the resin and hinder blockage of the exit by the vacuum bag, respectively. The fabric and distribution media were covered with a non-perforated release film instead of peel-ply which reduces surface roughness and risk of delamination during removal. It should be highlighted that surface roughness due to peel-ply decreased the flexural strength and stiffness of laminates significantly compared to the ones manufactured using release film [10]. Use of release film reduces the surface roughness, however, in complex geometries it can be challenging to cover the fabric sine wrinkles may form. The whole lay-up was vacuum bagged by applying the tacky tape in between the vacuum bag and the mold which ensured sealing of the mold. The mold was uniformly heated up to 121°C and kept under vacuum for 30 minutes before infusion to assure that there was no leak and the air was fully evacuated from the vacuum bag. This step also ensured that the compaction of the dry fabric was settled and almost uniform before infusion.

The manufacturing of a laminate was divided into 3 stages: (i) mold filling, (ii) flushing, and (iii) external pressurization. The process is outlined in Figure 3.2 for a clear presentation of these stages.

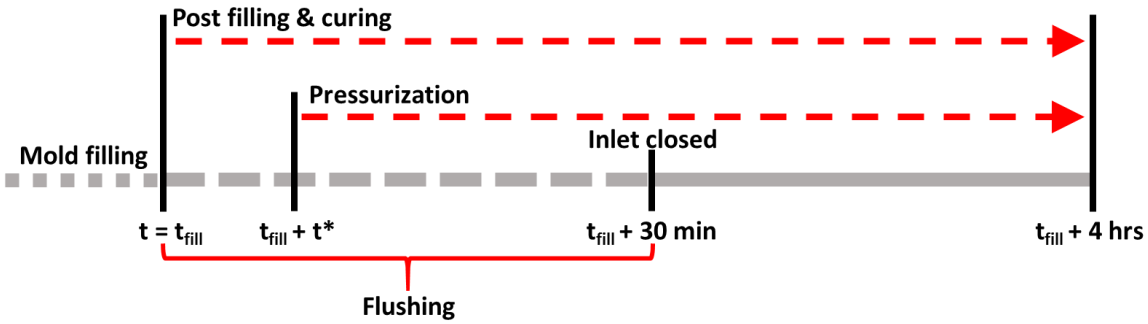

Figure 3.2 - Process outline of pressurized VARTM

3.2. Mold filling

Mold filling was started by unclamping the inlet tube which was dipped into the resin reservoir. Preliminary experiments showed that the mold filling was very fast (~150 s) due to the reduced viscosity at high temperature when an inlet tube with an inner diameter

of 1/4 in (6.4 mm) was used. Therefore, a tube with smaller inner diameter of 1/16 in (1.6 mm) was used to slow down the mold filling by inducing a higher resistance to flow and reduce the time between complete mold filling and the gel point of resin. In addition, the same tube was used at the exit to create a resistance against the outflow of resin which was proven to reduce void content [7]. As the tube diameter was decreased, average mold filling time of the repeated experiments increased to 482±17 seconds. The arrival of flow front at every 1 inch of the preform was recorded in every experiment to monitor to verify that mold filling time was similar in every experiment.

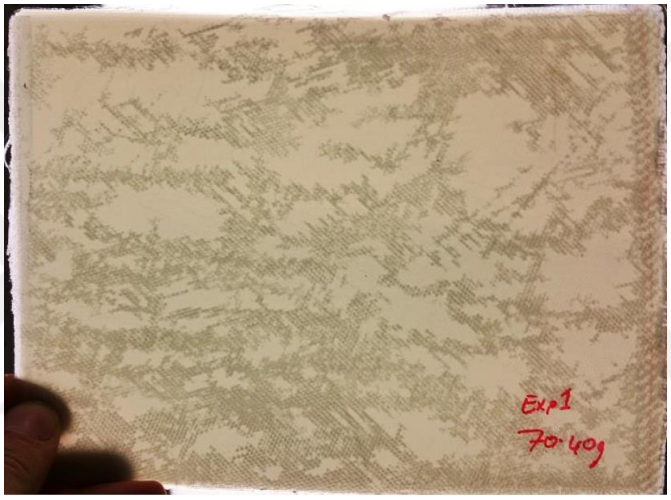

Figure 3.3 - Defective laminate: dark regions are voids

In preliminary experiments, inlet tube was clamped immediately after complete mold filling and exit was continued to be vacuumed. However, this caused parts with too many voids as shown in Figure 3.3. This was most possibly due to capillary flow causing inter-tow voids in between the fiber tows, which could be eliminated by taking appropriate post-filling actions such as flushing (i.e., continuing the resin infusion after complete mold filling).

3.3. Flushing

In LCM, void formation mechanisms during mold filling should be identified to take appropriate post-filling actions for removal of the voids. To investigate and understand the formation of voids seen in Figure 3.3, a capillary number analysis was performed. The average macroscopic resin velocity, V was calculated as 6×10^{-4} m/s by dividing the

length of preform to average mold filling time; the viscosity of resin, μ and surface tension, γ were taken as ~50 cP and ~35 mN/m (typical for similar EPON resins [51]), respectively. The dimensionless capillary number, $Ca = \mu V/\gamma$ was approximately calculated as ~8.5 x 10^{-4} which was slightly lower than the critical range of Ca ≈ 10^{-3} stated in various studies [23,52,53]. The low *Ca* indicated that the flow was governed by the capillary forces and faster in the tows than in between the tows, which could cause entrapment of voids in between the tows as also widely studied in the literature [23,24].

One of the efficient ways for void mobilization and removal in a saturated preform is to continue resin infusion (flushing) after complete mold filling as discussed in previous studies [31,33]. Voids move with the flushed resin and exit through the vent of the mold which reduces the void content of the laminate. The voids in between the tows (i.e., inter-tow voids) could be already mobilized during mold filling towards the exit at the calculated *Ca* which was similar to the critical *Ca* for void mobilization in Ref. [54]. By continuing resin infusion during flushing, these mobilized voids would be removed through the exit of the mold. In this study, voids were removed with resin flushing during which inlet was kept open and infusion was continued for 30 minutes after complete mold filling. Figure 3.4 shows that ~70% of the resin mass for complete mold filling was infused during 30 min flushing of non-pressurized laminates.

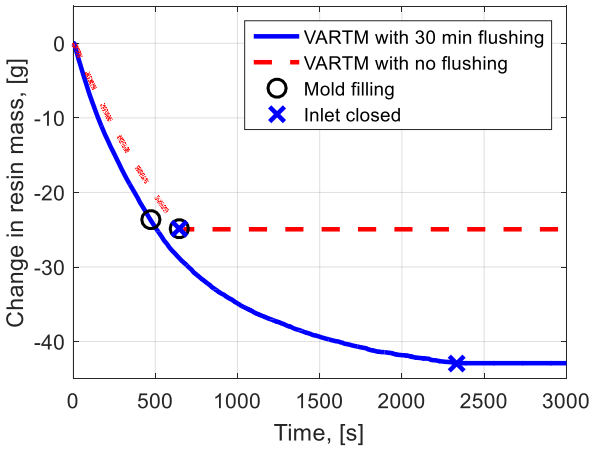

Figure 3.4 - Effect of flushing on the resin mass at the inlet resin reservoir

To investigate the effect of flushing and external pressurization on the laminate properties, and verify if the analysis and statements above were valid; four different cases

were studied by applying various combinations of external pressurization (non-pressurized, NP and pressurized, P) and flushing (non-flushed, NF and flushed, F). Laminates were manufactured according to these cases and they were scanned in a laser scanner. Since they were as thin as ~1 mm, voids through the thickness were captured and presented in Figure 3.5.

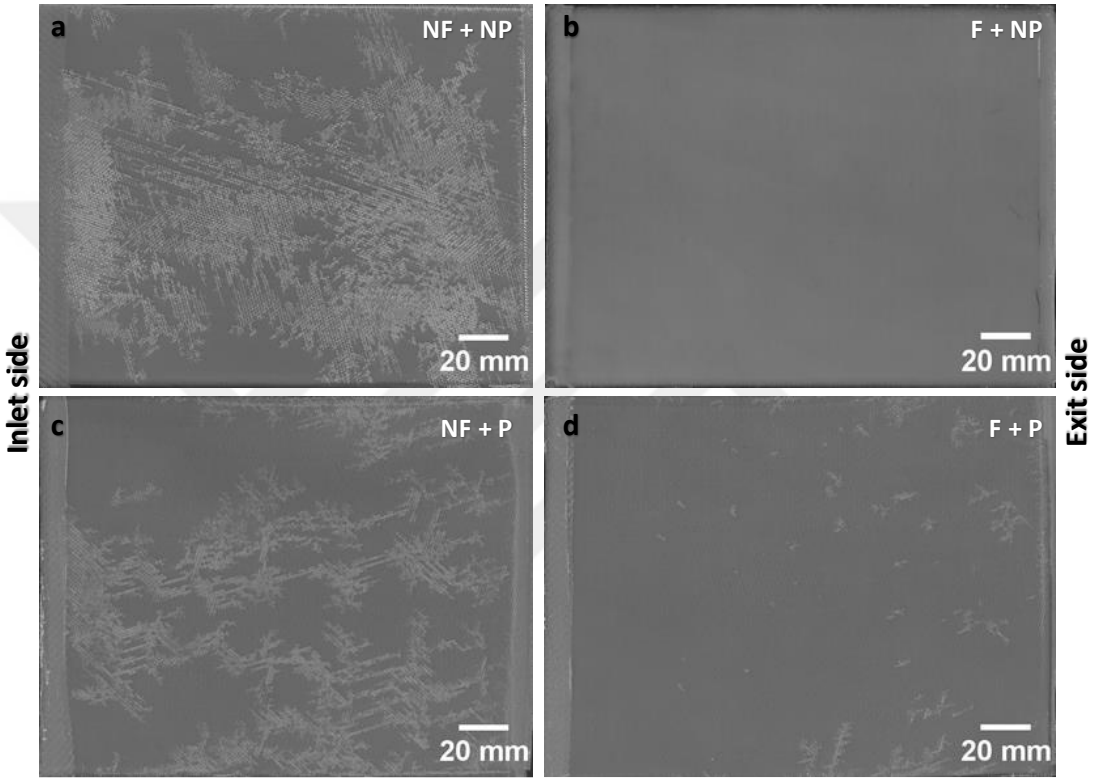

Figure 3.5 - Effect of flushing and external pressurization on the part quality: (a) Non-flushed and non-pressurized laminate, (b) Flushed and non-pressurized laminate, (c) Non-flushed and pressurized laminate, and (d) Flushed and pressurized laminate

Figure 3.5(a) shows that during manufacturing of non-pressurized (NP) laminates, flushing significantly removed the voids which were densely present in non-flushed (NP+NF) laminates seen in Figure 3.5(b). It is also seen that, external pressurization on its own also reduced the voids when Figure 3.5(a) and (c) are compared. Furthermore, when flushing was applied to pressurized laminates, these voids were further removed as seen in Figure 3.5(d). In Figure 3.5(c), it was observed that voids were branched in various directions due to the woven fabric architecture having gaps in between warp and

weft tows suitable for voids to mobilize which was also reported in the literature [55]. To quantify the visual observations, various tests and microscopy analysis were performed.

Two laminates for each case were manufactured and resin burn-off (ASTM D 3171) and flexural testing (ASTM D 790) tests were conducted on specimens which were cut and prepared according to the cutting template shown in the Appendix. Thickness of the specimens were measured at 35 locations with a micrometer. The results of these tests are presented in Figure 3.6, and Table 3.1. Figure 3.6(a-b) illustrates the results using "Box and Whisker Plot" which will be used frequently throughout this thesis work. Details about "Box and Whisker Plot" is attached to the Appendix.

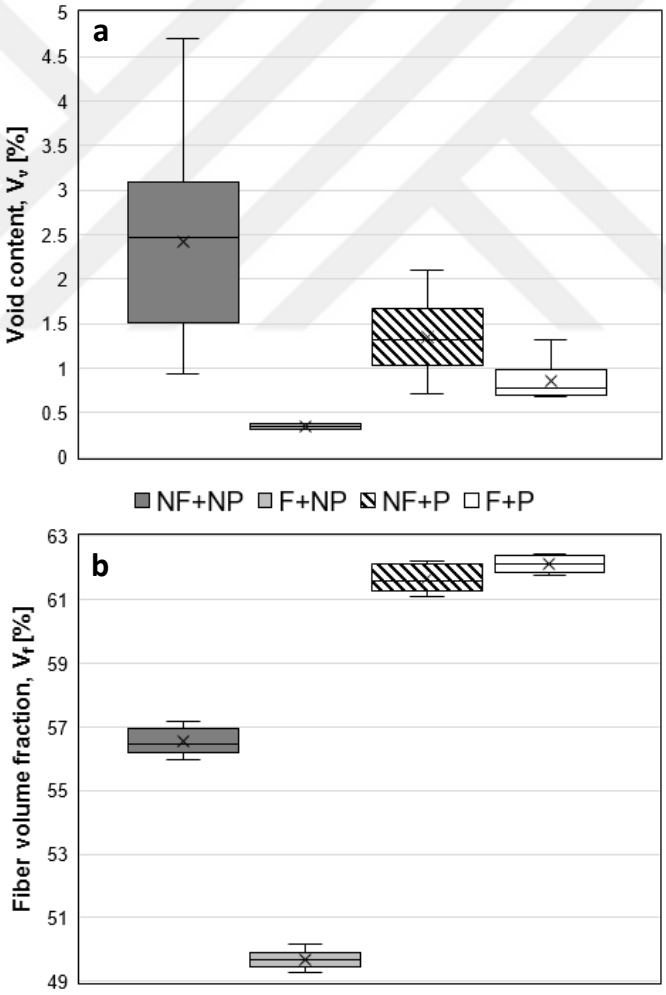

Figure 3.6 - Effect of flushing and external pressurization on (a) void content and (b) fiber volume fraction

Void content and fiber volume fraction were determined according to ASTM D3171 burn-off tests. Void content was as high as 4.7% in the NF+NP laminates whereas the highest void content was 0.38% in the F+NP laminates as depicted in Figure 3.6(a). This assured that the voids were successfully mobilized and removed by resin flushing which validated the visual observations. Figure 3.6(a) shows that external pressurization on its own (NF+P) reduced the average void content from 2.4% to 1.4% and its variation in the tested samples compared to NF+NP laminates. When external pressure was applied together with resin flushing (F+P), further reduction in void content (<1%) compared to NF+P laminates was achieved as also shown in Figure 3.5(d). Figure 3.6(b) clearly shows that the fiber volume fraction, V_f of laminates was significantly increased above 62% with external pressurization whereas flushing caused a reduction in V_f. It is also seen that pressurization suppressed the negative effect of flushing on V_f while yielding to very low void content below 1%.

Table 3.1 - Thickness and mechanical properties of the laminates manufactured with various combinations of flushing and external pressurization

	Thickness, h [mm]	Flexural strength, [MPa]	Flexural stiffness, [GPa]
NF + NP	1.246 ± 0.005	629 ± 26	26.4 ± 0.4
F + NP	1.401 ± 0.003	650 ± 6	24.3 ± 0.3
NF + P	1.106 ± 0.004	730 ± 12	30.6 ± 0.6
F + P	1.137 ± 0.003	736 ± 27	29.1 ± 0.6

Despite the fact that fiber volume fraction was reduced from 57% (NF+NP) to 50% (F+NP) due to excess resin intake during flushing, the increase in average flexural strength seen in Table 3.1 was noteworthy. Here, it could be stated that the high void content of NF+NP laminates caused a significant reduction in flexural strength. In addition, external pressurization increased the flexural strength significantly and when coupled with flushing, further improvement was achieved. F+P and NF+P parts had similar fiber volume content (see Figure 3.6(b)), but a slight decrease in the flexural

strength of the NF+P parts was observed which was possibly due to the higher void content of the NF+P parts. In summary, it was observed that 17% improvement in flexural strength was obtained when NF+NP and F+P laminates were compared. Similar improvement in flexural stiffness was also documented in Table 3.1.

To gain a more comprehensive understanding of the effect of flushing, NF+NP and F+NP laminates seen in Figure 3.5(a) and (b) were examined under a light microscope. Micrographs shown in Figure 3.7 show the microstructure of these laminates. Figure 3.7(a) validated the capillary number analysis at the beginning of this section by showing that voids were formed in between the fiber tows. This clearly indicated that flow was governed by the capillary forces which caused the entrapment of voids in inter-tow regions during impregnation. Additionally, Figure 3.7(b) shows that, flushing removed the voids located in between the tows which was in agreement with the resin burn-off results given in Figure 3.6.

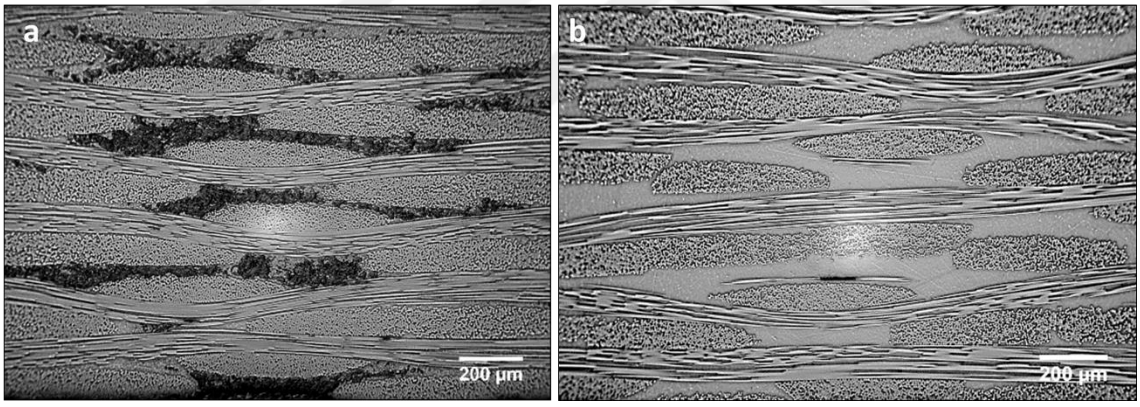

Figure 3.7 - Effect of flushing on the microstructure of laminates: (a) flushed laminate with void-free section, and (b) non-flushed laminate with inter-tow voids

3.4. External pressurization

In the previous section, it was shown that external pressurization led to significant increase in fiber volume fraction. In this section, effect of two major parameters regarding pressurization on laminate properties were investigated: (i) level of pressure, and (ii) instant when pressure was applied (t^* in Figure 3.2).

Various external gauge pressure levels, P_{ext} = 5, 10 and 20 psi (34.5, 69, and 138 kPa) were applied at t^* = 5 min to investigate the effect of external pressurization on the part properties. Figure 3.8(a) shows the mass change at the inlet resin reservoir during both standard VARTM (i.e., no externally pressurized chamber was used) and pressurized VARTM processes. It was observed that when external pressure was applied on the laminate during flushing, some resin was evacuated through the inlet port. In Figure 3.8(a), it can be seen that the amount of resin flushed until the inlet tube was clamped (shown with red, green, and black curves for the three external pressure levels) was significantly reduced due to external pressure compared to the VARTM experiment (shown with a blue curve). As the external pressure was increased, amount of resin removal through the inlet port increased as well. Effect of reduction in flushed resin mass on the laminate properties will be investigated in the next section.

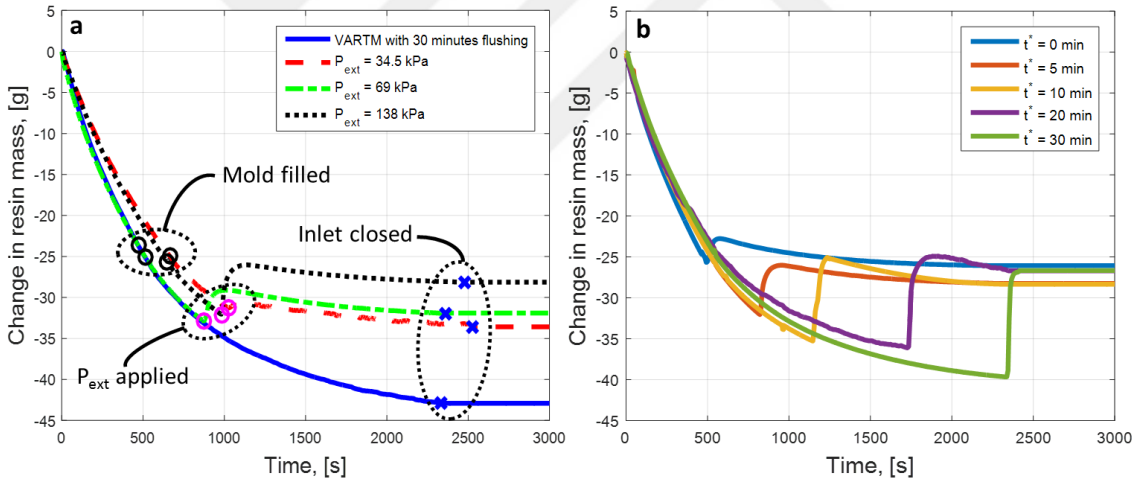

Figure 3.8 - Change in resin mass in the reservoir for (a) various Pext and (b) various t*

The chamber was pressurized at various instants (i.e., t^* = 0, 5, 10, 20 and 30 min) after the complete mold filling during flushing. P_{ext} was chosen as 138 kPa Figure 3.8(b) shows the mass change at the inlet reservoir when P_{ext} was applied at various t^* and it was observed that the final resin mass in the reservoir was very similar for every t^* which implied that resin removal through inlet port did not significantly depend on t^* but the level of P_{ext}. The effect of various t^* on laminate properties will be discussed in the next section.

For each external pressure value and application instant, two laminates were manufactured. It should be noted that the inlet was always clamped 30 minutes after the complete mold filling (i.e., 30 min flushing) as illustrated in Figure 3.2. However, when pressure was applied at t^* = 30 min, a modification was made since the pressurization coincided with the end of resin flushing (i.e., inlet closing). In this case, resin removal through the inlet was allowed for an additional minute. The parts were cured at 121ºC for 4 hours in the mold after complete mold filling and exit port was vacuumed during the curing.

3.5. Results and discussion

3.5.1. Laminate thickness

Thickness was measured with a micrometer at a grid of 35 uniformly distributed locations (5 x 7) along the width and length of the laminates according to the template in Appendix. Figure 3.9(a) and (b) show the average thickness values of laminates manufactured under (a) different external pressures (P_{ext}) and (b) P_{ext} = 138 kPa applied at different t^* during 30-minutes flushing, respectively.

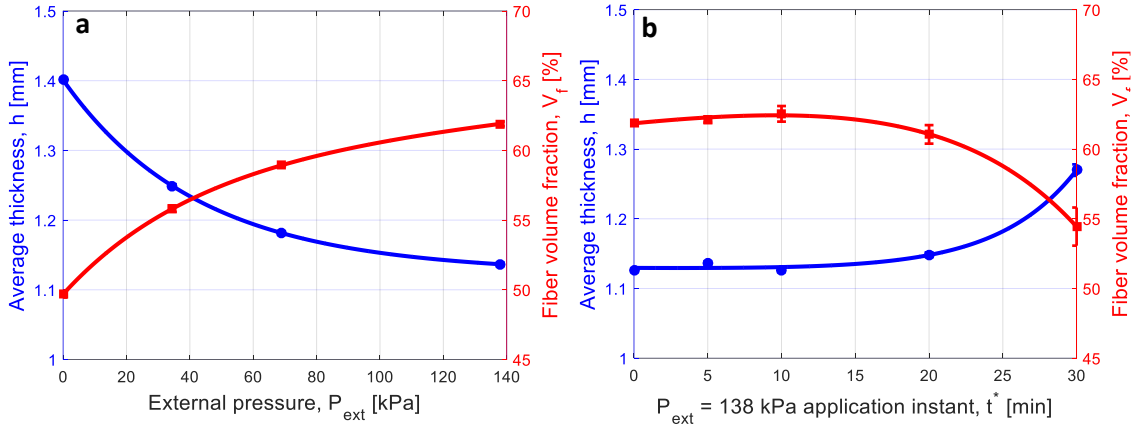

Figure 3.9 - Effect of (a) external pressure, and (b) external pressure application instant on the part thickness and fiber volume fraction obtained by resin burn-off

As seen in Figure 3.9 (a), external pressurization reduced the average part thickness and thus, increased the fiber volume fraction from an initial value of 50% to 62%. Average thickness values were 1.401±0.003 mm, 1.249±0.004 mm, 1.181±0.003 mm and 1.134±0.003 mm for 0, 34.5, 69 and 138 kPa external pressure values, respectively. The

minimum thickness and highest fiber volume fraction were achieved under the highest external pressure of 138 kPa. The exponential decay in thickness with P_{ext} shows that there is a limit for the minimum laminate thickness thus; increasing the external pressure above a certain value will not result in a thinner laminate.

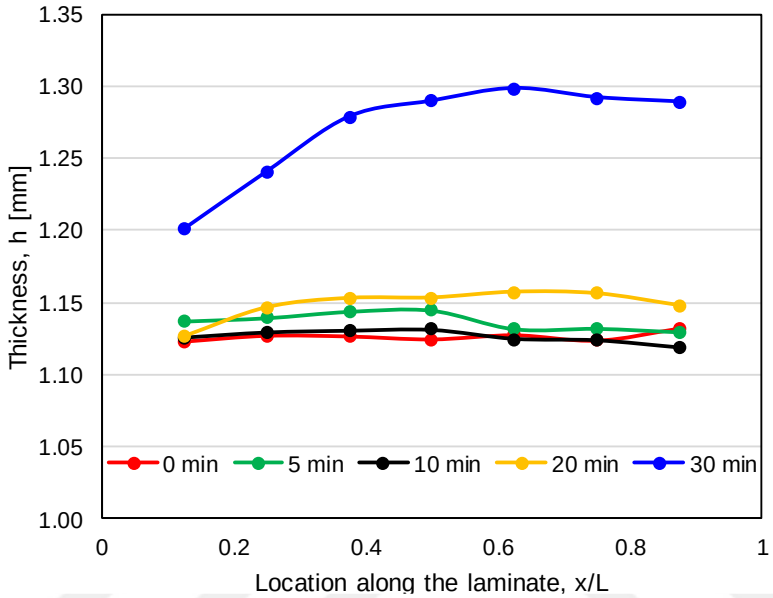

Figure 3.10 - Effect of various t* on thickness distribution of laminates

The effect of t^* on average laminate thickness is presented in Figure 3.9(b) and Figure 3.10. Figure 3.10 shows that, (1) at early stages of flushing, similar thickness and its distribution are observed (shown with green, red and black), and (2) when $t^* \geq 20$ min, higher thickness and its significant variation were measured (shown with yellow and blue). This can be attributed to two possible factors: (i) the viscosity of the resin increased considerably due to cross-linking reaction and it became harder to remove the excess resin through the inlet and exit ports, and/or (ii) the duration of inlet port being open was not long enough to remove sufficient amount of resin through the inlet port. The second possibility does not comply with Figure 3.8(b) which shows that the evacuated resin amount through the inlet was not significantly affected by t^*. Furthermore, the thickness distribution of laminates manufactured by applying pressure at $t^* \geq 20$ min showed that the laminates were thicker at the exit than the inlet side as seen in Figure 3.10. This indicated that when P_{ext} was applied late (i.e., $t^* \geq 20$ min), resin removal through exit port

was reduced which was possibly due to increased resin viscosity with time. Therefore, external pressure should be applied at the earlier stages of post filling to achieve uniform thickness distribution. Please see the change in viscosity of resin with time and temperature in the Appendix for detailed information.

The thickness variation in each part was so small that most of the error bars in Figure 3.9(a) and (b) are barely noticeable. Although, variation in part thickness is a drawback of VARTM process due to the varying compaction pressure on the preform [38,39,56,57], if appropriate post-filling actions are taken, the thickness variation can be minimized as shown in some studies [41,42,44,45]. Most of these studies used a non-curing test fluid such as corn syrup or various types of oils and assumed that the viscosity stays the same during post-filling which is not the case in a real manufacturing environment. In addition, adding a cover mold or caul plate is shown to result in more uniform thickness distribution [58]. In this study, viscosity of the resin in the heated mold was lower than typical resin viscosity used in VARTM at room temperature, and this enabled an easier resin flow during the post-filling stage. Therefore, thickness of a laminate was very uniform and no significant variation was observed if P_{ext} was applied at $t^* \leq 20$ min. Regarding the results shown in Figure 3.9(a) in which external pressure was applied at $t^* = 5$ min, maximum variation in thickness in two parts manufactured under the same external pressure was calculated as ±0.004 mm within the 95% confidence interval. These results confirm the dimensional repeatability of the parts made by pressurized VARTM.

3.5.2. Resin burn-off results

To determine the fiber volume fraction and void content of laminates, resin burn-off procedure was conducted according to ASTM D 3171. Three burn-off samples with dimensions of 0.75 in x 2 in (19.1 mm x 50.8 mm) from each laminate were cut along the flow direction using a diamond cutter (IsoMet 1000 Precision Cutter). These samples were cleaned and dried for 24 hours in a vacuum furnace to remove any moisture which may have been absorbed during cutting. Then, they were weighed on a precision balance (OHAUS Adventurer AX 124) and their densities were measured according to ASTM D 792. The samples were placed in borosilicate glass or ceramic beakers and kept in a

furnace at 600°C for 2 hours to remove the epoxy matrix completely. The remaining fibers were weighed and fiber volume fraction and void content of samples were calculated as guided in ASTM D 3171 and seen in Figure 3.11. Thermogravimetric analysis (TGA) were run on the fibers to see if they lose any weight due to the sizing being burned off at 600°C and no significant mass change was observed, meaning that the effect of sizing on the resin burn-off results was negligible according to ASTM D 3171.

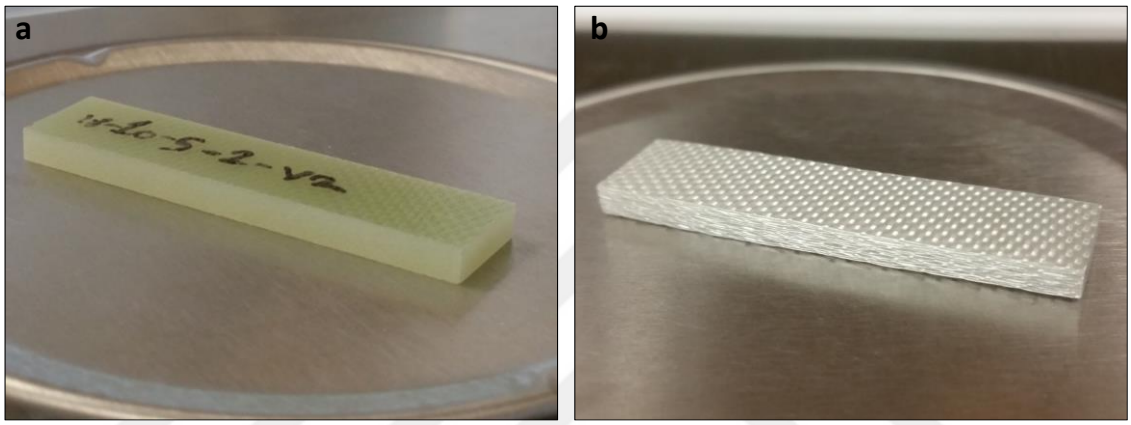

Figure 3.11 - Burn-off sample: (a) before and (b) after resin burn-off

Figure 3.9(a) shows that V_f of samples manufactured under 34.5, 69 and 138 kPa external pressure were 56, 59 and 62% (compared to V_f = 50% in VARTM with no external pressure), respectively. In addition to the increase in V_f, variation in V_f was insignificant so that the error bars in Figure 3.9 (a) are not noticeable. However, when t^* was over 20 minutes, the increase in V_f was not as big as the values mentioned above and planar variation of V_f increased as seen in Figure 3.9(b). In order to corroborate the resin burn-off results, one may calculate the fiber volume content using the geometrical properties of the samples as $V_f = (N\ \rho_{sup}) / (\rho_{fiber}\ h)$ where N is the number of plies, ρ_{sup} is the superficial density of a single ply, ρ_{fiber} is the fiber density and h is the thickness of the laminate. The average percent difference between burn-off and geometrical V_f results was 1.5% which further validated the burn-off results.

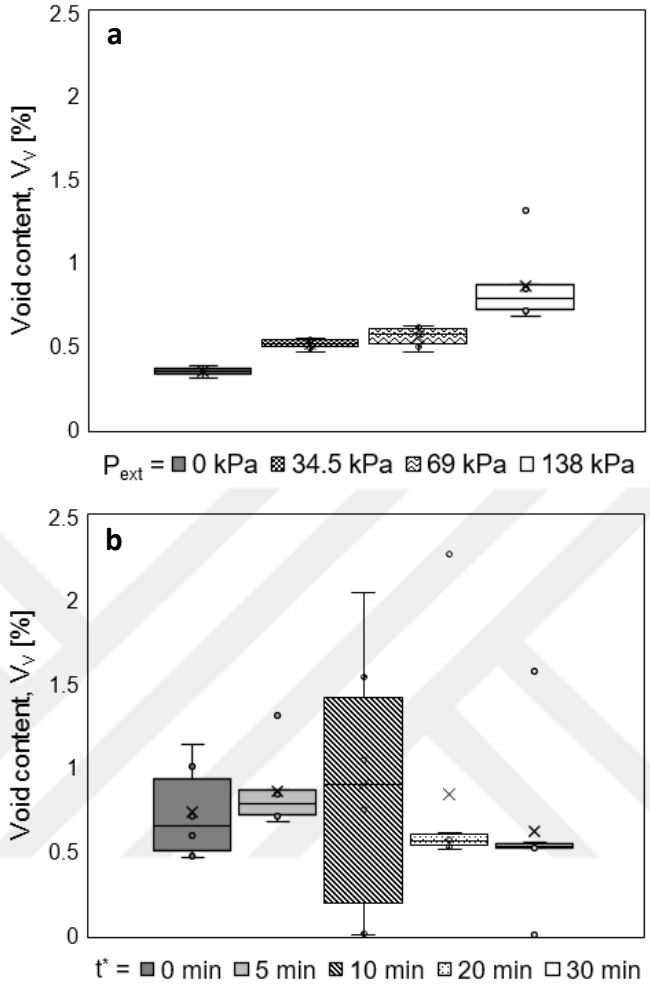

Figure 3.12 - Effect of (a) external pressure and (b) external pressure application instant on the average void content and its variation

Void contents of the laminates manufactured under various external pressures and pressurization instants are shown in Figure 3.12(a) and (b), respectively. It is seen that the void content increased slightly from 0.35% to 0.86% with increasing external pressure. Figure 3.12(a) shows that regardless of the external pressurization level, pressurized and heated VARTM process led to average void content values less than 1%. This accomplishment is a very significant and promising outcome of the externally pressurized and heated VARTM process since higher void contents could be commonly observed in the literature for various types of materials and process parameters [7,21,31]. However, the slight increase in void content should be analyzed and discussed by

investigating the coupled effect of flushing and pressurization on the void content. The increase in void content with increasing P_{ext} could be attributed to two phenomena: (i) reduction of flushed resin mass, m_f with P_{ext} as seen in Figure 3.8(a) and (ii) local entrapment of mobilized voids due to squeezed inter-tow regions. m_f was normalized by the infused resin mass when the preform was completely impregnated, m_p as seen in Figure 3.13(a) to show the relation between P_{ext} and m_f. As P_{ext} increased, the permeability of saturated fabric decreased which caused the reduction of m_f. To account for the coupled effect of flushing and pressurization, a dimensionless parameter of α = P/M was introduced. In Figure 3.13(b), it is clearly seen that as α increased, the void content increased which signified that the flushed resin mass and P_{ext} should be carefully determined to achieve low void content in pressurized VARTM. The second phenomenon was also possible since few samples manufactured under P_{ext} = 138 kPa had void contents exceeding 1% as illustrated by the upper bounds and outlying data in Figure 3.12(b). The presence of localized voids will be investigated and discussed in more detail by analyzing the micrographs in the following section.

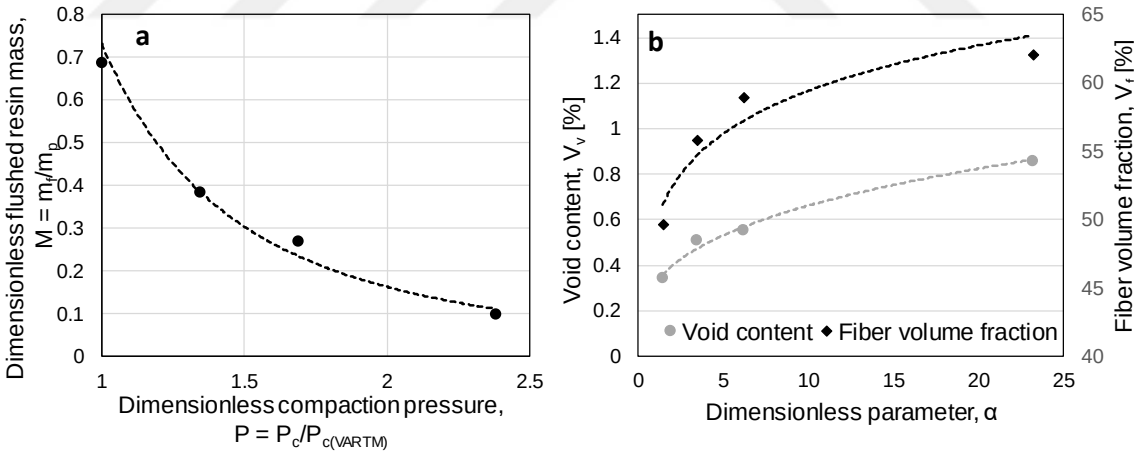

Figure 3.13 - a) Effect of external pressure on flushed resin mass and b) coupled effect of flushing and pressurization on the void content and fiber volume fraction of laminates

3.5.3. Microscopy examination

Microscopy examination was reported to be one of the most reliable methods to acquire information about the microstructure, void morphology and content of a laminate [7,59]. Some studies in the literature [7,31] carried out the analysis by sampling images from certain locations in a cross-section, whereas a few others [25,26,59] examined the whole sample.

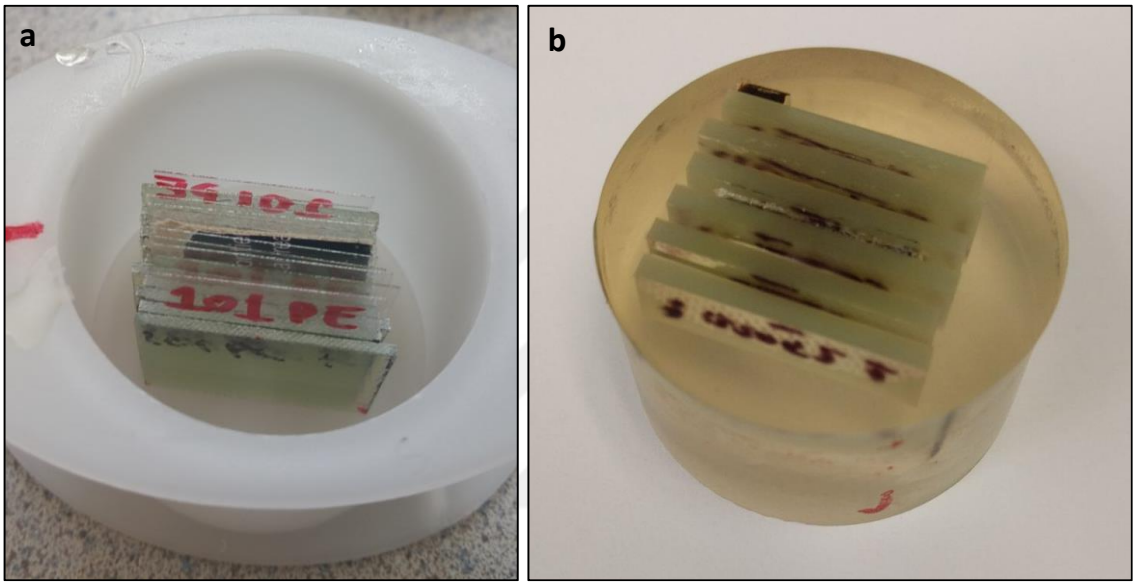

Figure 3.14 - Microscopy sample: (a) embedding into acrylic, and (b) polished sample

In this study, six-inch (152 mm) long samples were cut right next to the burn-off samples along the laminates and each sample was divided into 6 equal pieces according to the cutting layout shown in Appendix. Samples were placed in a special mold and embedded in acrylic as seen in Figure 3.14(a). Then, they were polished by using Struers Labopol-5 polishing machine. The whole cross-section was analyzed at different magnifications ranging from 50X to 500X, to capture all identifiable voids and have a more comprehensive investigation of the microstructure and void morphology. Micrographs were taken with a digital microscope camera mounted on a MEIJI optical microscope.

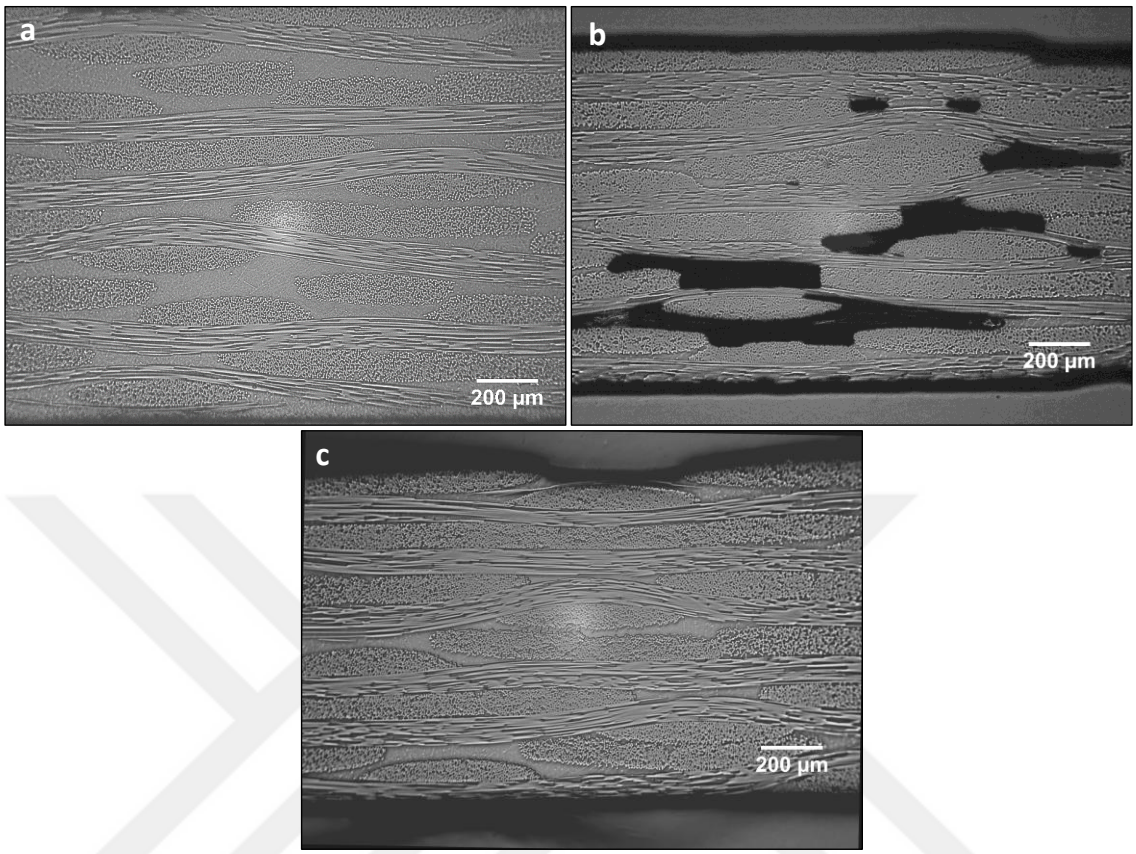

Figure 3.15 - Micrographs of various laminates: (a) void free cross section of a non-pressurized laminate, (b) localized void clusters from a 138 kPa pressurized laminate, and (c) void free cross-section of a 138 kPa pressurized laminate

Figure 3.15(a) and (b) show the micrographs of a non-pressurized VARTM laminate and pressurized at 138 kPa right after complete mold filling, respectively. These micrographs were taken under the same magnification to show the microstructure of the laminates comparatively. While Figure 3.15(a) shows a void-free cross section, Figure 3.15(b) shows inter-tow voids entrapped and squeezed in between the tows. The voids seen in Figure 3.15(b) were localized and not evenly distributed along the part. Figure 3.15(c) shows another image taken from the same sample shown in Figure 3.15(b), depicting a void free region. The thickness reduction with the effect of external pressure is also noticeable and this is mainly due to the consolidation of resin rich inter-tow regions rather than compression of tows. A close-up image of an entrapped inter-tow void is shown in Figure 3.16(a).

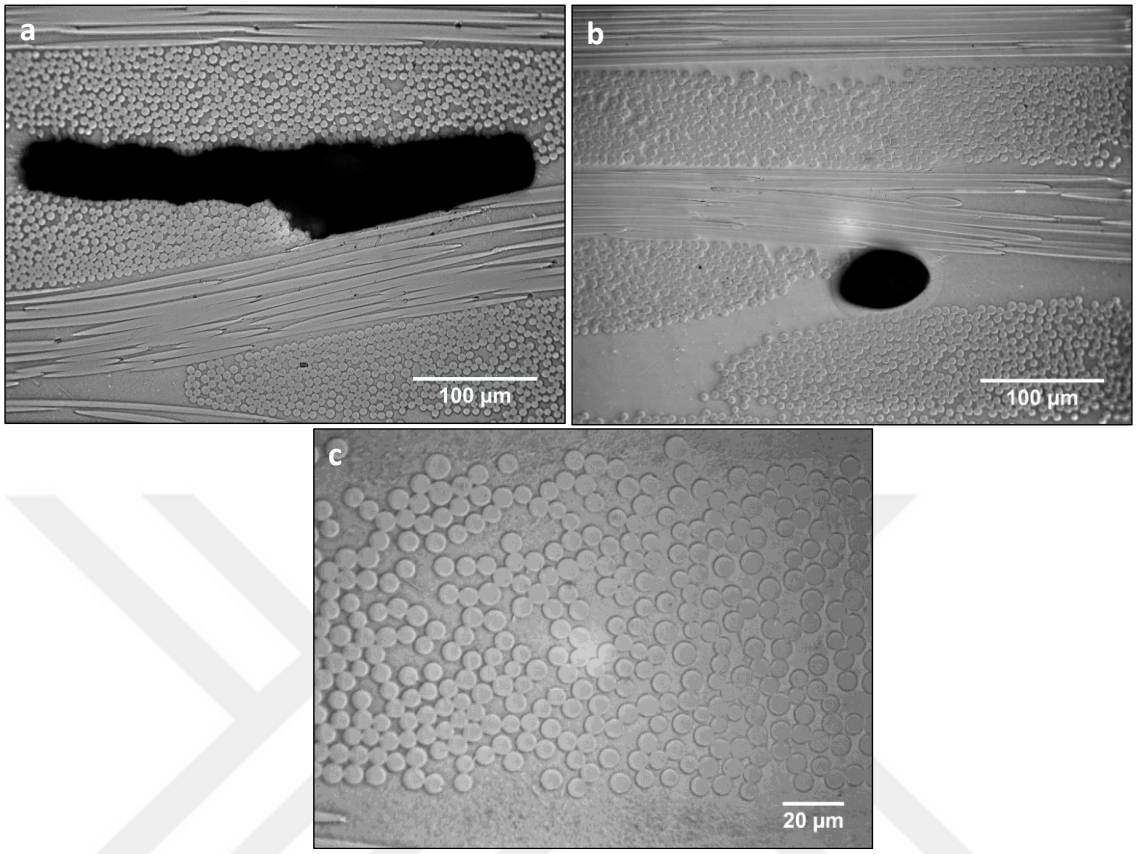

Figure 3.16 - Close-up micrographs of (a) an entrapped inter-tow void which took the shape of the gap between the tows, (b) a spherical matrix void and (c) a fully wetted tow with no intra-tow voids

The inter-tow voids in pressurized parts were squeezed laterally and elongated in the flow direction, taking the shape of the inter-tow region. Obviously, these voids could not penetrate into the tows during flushing and external pressurization. There were also some almost spherical voids in the matrix as shown in Figure 3.16(b) which were representative of voids observed in the part pressurized at P_{ext} = 34.5 kPa. In contrast to Figure 3.16(a), Figure 3.16(b) shows that the inter-tow region was not consolidated enough to compress the void and conform its shape according to the narrowed-down inter-tow gap. On the other hand, the tows were carefully examined for intra-tow voids as small as a few microns using a higher magnification (i.e., 500X). However, no intra-tow void was present in any laminate regardless of external pressure level or its application time. Figure 3.16(c) shows a representative micrograph of a tow which did not include any void. In

addition, it can be seen that the fiber diameter did not show a significant variation which could otherwise create uneven channels and variation of permeability within a tow during resin flow causing intra-tow voids. This image also shows that tows were perfectly wetted by resin which validated the capillary analysis indicating that the flow was governed by the capillary flow through the fiber bundles.

In addition to using the resin burn-off method, the void content was also calculated using an image processing tool, ImageJ by selecting all identifiable voids present on the examined cross-sections and dividing the total void area to the total cross-sectional area of a specimen. For all samples, the results of the void volume fraction obtained from image processing agreed well with the burn-off results. Similar to various studies [7,60], there was no apparent trend in void distribution along the flow direction and it was seen that the voids were localized as clusters and not distributed evenly throughout the composite. Another important observation was that voids were not observed in non-pressurized and flushed parts whereas small amounts of localized voids were formed with increasing external pressure. The formation of localized voids was probably due to the further compaction of fabric layers which squeezes voids between the tows and restrain their mobility by collapsing the flow channels through which voids could move towards the exit. In addition, during external pressurization, the resin in-flow through the inlet was limited due to decreased permeability of the fabric causing less resin to be flushed until the inlet tube was clamped as seen in Figure 3.8(a). It should also be highlighted that, in pressurized parts, the void clusters seen in Figure 3.15(b) were observed less with decreasing external pressure. The effect and importance of flushing were previously discussed and therefore, it was expected that some of the voids were not removed in highly pressurized (i.e., 138 kPa) parts whereas more flushing and less compaction led to more void mobility and lower void levels in the less pressurized parts. Another reason for presence of voids in the pressurized parts can be the excessive resin bleeding due to maintaining the vacuum at the exit port throughout the whole process [61].

3.5.4. Flexural properties

Eight samples from each laminate were cut and tested according to ASTM D 790 using a Universal Test Machine (UTM) with a 3-point bending fixture as seen in Figure 3.17. Span to thickness ratio of 24:1 was used, and the span was adjusted within ±1% of the calculated value.

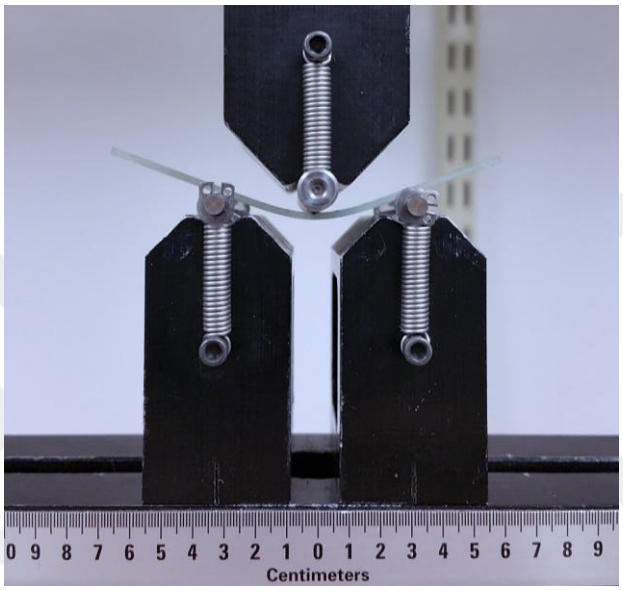

Figure 3.17 - Flexural testing

The average flexural strength of the 16 samples cut from 2 laminates manufactured by applying the same process parameters are measured according to ASTM standard. The results are presented in Figure 3.18. Error bars show 95% confidence interval of the experimental data.

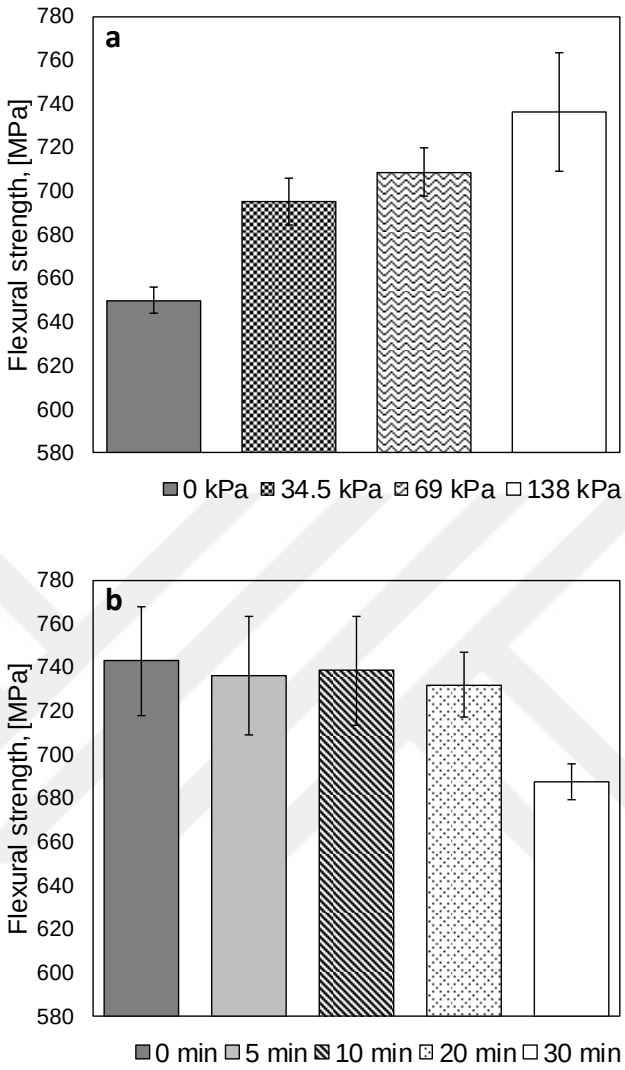

Figure 3.18 - Effect of (a) external pressure and (b) external pressure application instant on flexural strength

External pressurization of a laminate increased the average flexural strength from 650 MPa to 695, 709 and 736 MPa when P_{ext} = 34.5, 69 and 138 kPa was applied, respectively, as seen in Figure 3.18(a). This corresponds up to 13% increase in flexural strength at the highest P_{ext}, which can be correlated with the increase in V_f due to P_{ext}. At this point, it could be argued that not only the increase in V_f but also void content (see Figure 3.12(a)) may have caused a coupled effect on the flexural properties. However, it should be noted that void content below a certain limit does not effect the mechanical properties significantly as also reported in the literature [26]. Therefore, it could be concluded that

increase in P_{ext} and thus V_f improved the flexural properties of laminates. On the other hand, it should also be recalled that, flexural strength was not governed by V_f when void content was very high as shown in Figure 3.6(a) and Table 3.1. Furthermore, the variation in void content (Figure 3.6(a)) due to localized voids caused the variation in flexural strength of laminates manufactured under P_{ext} = 138 kPa. As Figure 3.18(b) shows, a decrement in the flexural strength was observed due to insufficient removal of excess resin when $t^* \geq 20$ min. This also corroborated that at low void contents, V_f significantly affected the flexural strength.

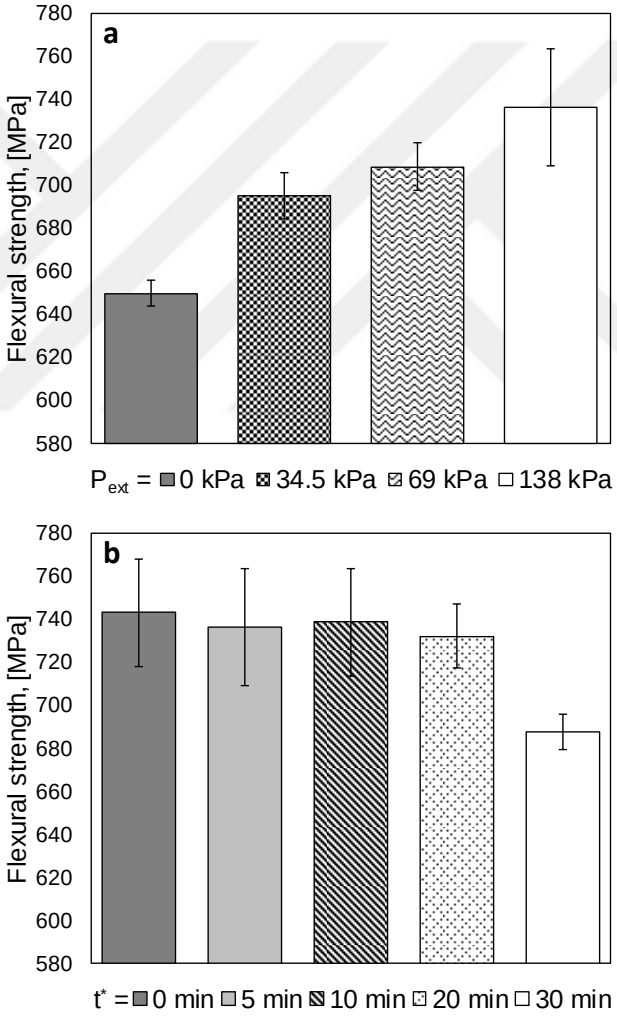

Figure 3.19 - Effect of (a) external pressure and (b) external pressure application instant on flexural stiffness

Flexural stiffness of the laminates also showed a robust positive trend with applied pressure, similar to that of flexural strength. Figure 3.19(a) demonstrates that 34.5, 69 and 138 kPa external pressurization increased the flexural stiffness by 11, 16 and 20%, respectively compared to non-pressurized laminates. Moreover, it was observed that flexural stiffness was almost linearly related to V_f which verified the validity of rule of mixtures. This is a strong sign of a proper resin-matrix interface in the laminates which also supports the findings presented in microscopy analysis. Therefore, it can be concluded that the interfacial bonding of fibers and resin was not affected by the external pressurization and dominated by the resin fiber bonding. In addition, effect of pressurization instant on the stiffness shown in Figure 3.19(b) followed a similar trend as flexural strength.

In addition, the coupled effect of flushing and pressurization on the flexural properties of laminates was analyzed in Figure 3.20. The dimensionless parameter α was previously introduced in Section 3.5.2. It was observed that both strength and stiffness of laminates followed a similar trend with increasing α as previously shown for fiber volume fraction and void content.

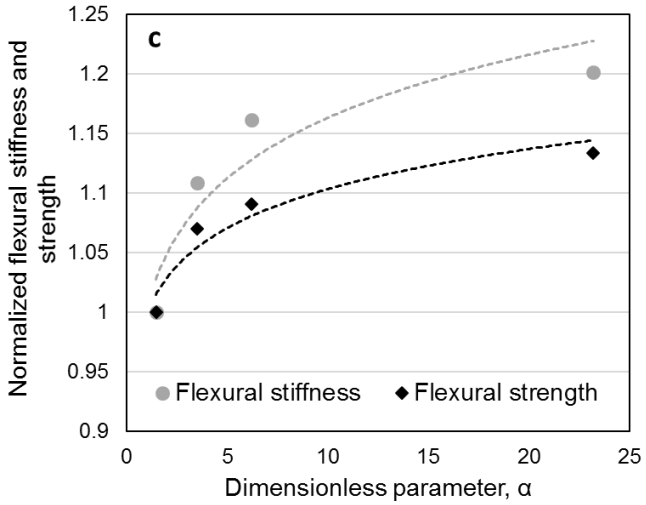

Figure 3.20 - Coupled effect of flushing and pressurization on flexural properties

4. AN EXTENSIVE STUDY ON PRESSURIZED AND HEATED VARTM: EFFECT OF NUMBER OF PLIES ON THE LAMINATE PROPERTIES AND COMPACTION BEHAVIOR

4.1. Objective of the extensive study

In Section 3, externally pressurized variant of heated VARTM process was introduced and it was shown that fiber volume fraction and mechanical properties of laminates were significantly improved while void content levels below 1% were achieved as compared to conventional VARTM. However, it was not obvious whether similar improvement would be obtained for thicker laminates since the compaction behavior of higher number of plies of the fabric under same compaction pressure is not known. This study aims to extend the applicability of pressurized and heated VARTM by

- compaction characterization of various number of fabric,
- manufacturing of 12- and 18-ply laminates (recall that 6-ply laminates were manufactured in Section 3) and investigating the effect of external pressurization on thickness, fiber volume fraction, void content, microstructure, and mechanical properties on these laminates,
- comparison of physical, microstructural, and mechanical properties of 6-, 12-, and 18-ply laminates,
- performing a detailed microstructural analysis to investigate the compaction of fabric layers in final part and void morphology.

4.2. Compaction characterization of the fabric

Dry compaction characterization experiments for various number of plies of the fabric were conducted under unloading conditions using the experimental setup shown in Figure 4.1. The aim of dry compaction characterization was to investigate (i) the effect of number of plies on the compaction behavior of the fabric, and (ii) whether the part thickness could be correlated to the dry compaction behavior of the fabric preform made of various number of plies.

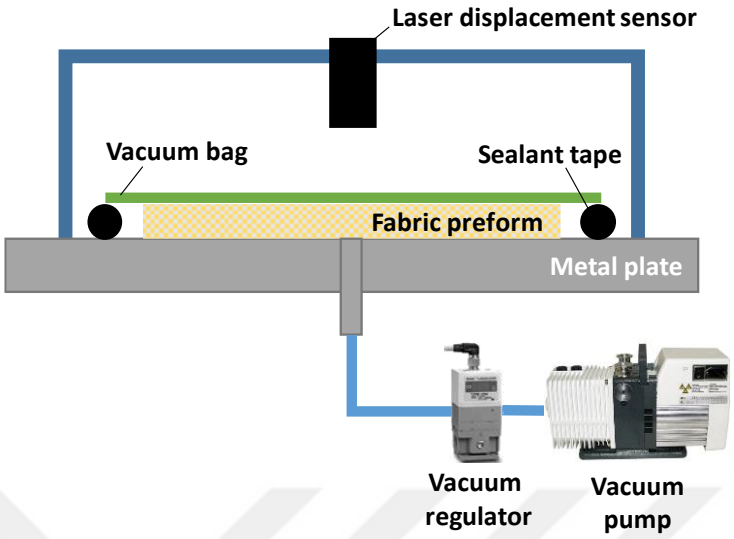

Figure 4.1 - Experimental setup for compaction characterization of fabrics

Specimens with a size of 100 mm by 100 mm for each ply configuration were placed and vacuum bagged on a platform which had a laser displacement sensor (OMRON Z4M-W40RA) on top as shown in Figure 4.1. The fabric was kept under 96 kPa gauge vacuum pressure (i.e., 96 kPa compaction pressure, P_c) for 5 minutes and thickness change with time was monitored as shown in Figure 4.2(a) for a 12-ply fabric preform as an example. It was observed that for the fabric type used here, the thickness settled rapidly and did not decrease further after being loaded at the highest compaction pressure whereas various types of fabrics (e.g., random mat) showed a more dominant viscoelastic behavior causing significant change in thickness with time as studied in literature [39,62]. After 5 minutes of loading, the compaction pressure was decreased gradually down to 2 kPa with a decrement of 2 kPa at every step as seen in Figure 4.2(b). Pressure under the vacuum bag was measured and recorded by using a pressure transducer. Measurements were taken 30 seconds after the pressure was set so that it was ensured that the compaction pressure and fabric thickness were settled. An example of thickness versus compaction pressure during unloading stage is presented in Figure 4.2(c).

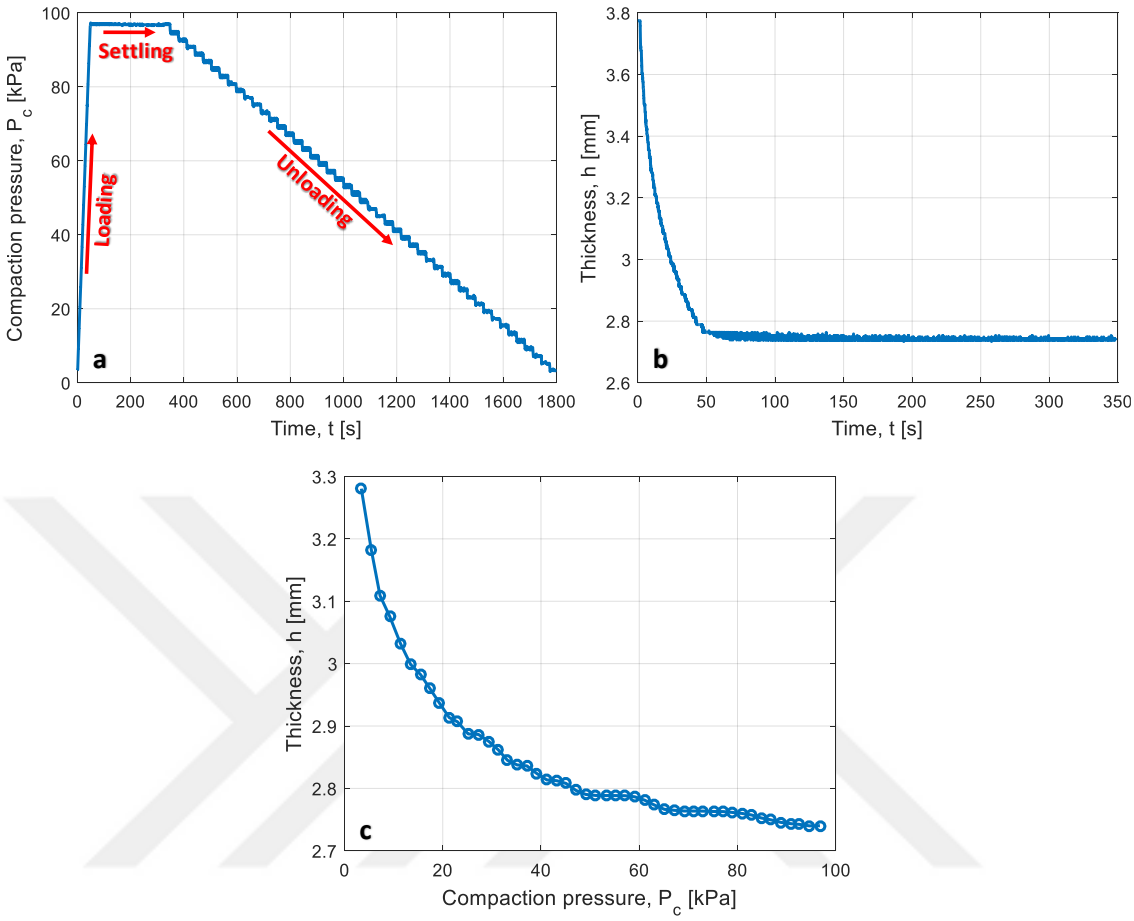

Figure 4.2 – (a) Pressure schedule during compaction characterization, (b) thickness of a 12-ply fabric preform during loading and settling, and (c) thickness during unloading from 96 kPa to 2 kPa

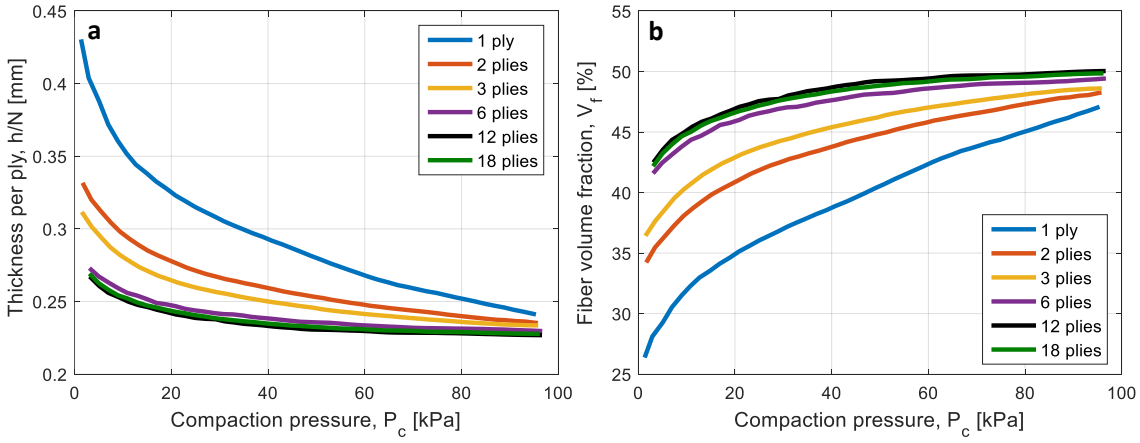

Figure 4.3 - Compaction characterization of fabric preforms made of various number of plies; *N* is the number of plies

Three experiments were repeated for each number of plies. Figure 4.3 shows the per-ply thickness and corresponding fiber volume fraction of fabric preforms made of 1, 2, 3, 6, 12, and 18 layers. Fiber volume fraction was calculated as $V_f = (N\ \rho_{sup})/(\rho_{fiber}\ h)$ where N is the number of plies. It was clearly seen that as the number of layers increased per-ply thickness decreased. This happened due to different levels of nesting of fabric layers which was absent for 1-ply preform shown with blue curve and minimal for a few ply cases. However, as the pressure increased, the difference between per-ply thickness curves decreased. Moreover, it was also observed that similar compaction behavior was reported for 6, 12, and 18 plies which showed that as the number of plies increased, effect of nesting on the compaction behavior was reduced as also reported in various studies [63–65]. Thicker samples with more than 18 layers could not be tested to further validate this assumption, since the range of laser displacement sensors were not suitable for such samples.

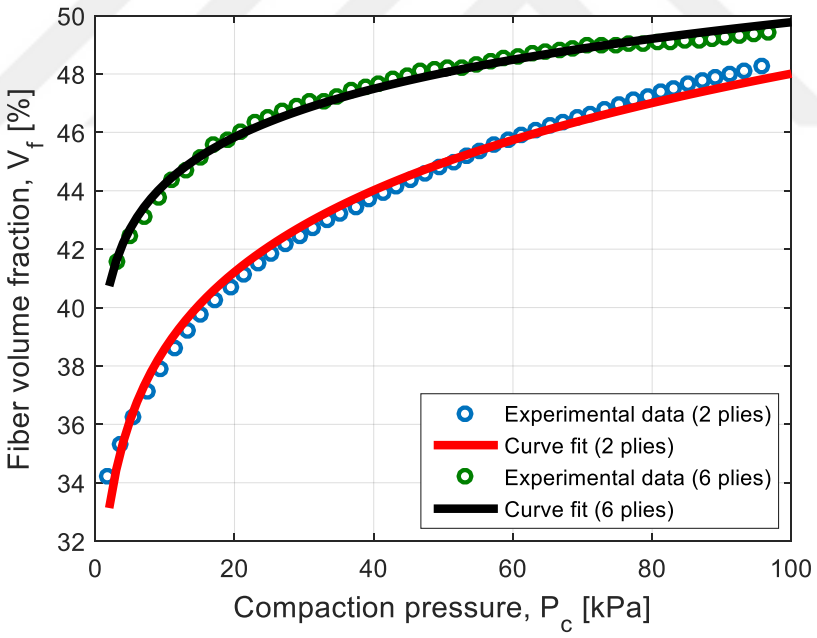

Figure 4.4 - Curve fitting to experimental compaction characterization data

An exponential curve was fitted for all number of plies and examples are seen in Figure 4.4 for 2 and 6 plies. The function $V_f = AP_c^B$ was commonly used by many studies to model the non-linear elastic compaction behavior of fabric preforms [38,66–68]. Curve

fit constants, A and B for all number of plies are tabulated in Table 4.1 where V_f is in [%], and P_c is in [kPa].

Table 4.1- Curve fit constants for compaction characterization

Number of plies	A		B	
1	22.9		0.1493	
2	31.0		0.0948	
3	34.0		0.0785	
6	Dry	Wet	Dry	Wet
	39.3	42.9	0.0512	0.0619
12	40.6		0.0477	
18	40.2		0.0487	

Compaction behavior of the fabric impregnated with resin was also characterized by running wet-compaction characterization experiments on 6-ply preforms under unloading condition. Dry preform was kept under P_c = 96 kPa for 2 minutes and then wetted with a test fluid which had a viscosity of ~100 cP. Wetting was completed in 30 seconds and wet preform was kept under P_c = 96 kPa for 5 minutes. Then, the preform was unloaded as done in dry compaction characterization experiments. An example of wet compaction characterization experiment is presented in Figure 4.5(a) and average of three experiments for wet-unloading stage is shown in comparison with the dry compaction characterization in Figure 4.5(b). Curve fit constants for wet compaction characterization are given in Table 4.1. It was observed that the thickness of fabric preform significantly reduced (~14%) due to lubrication effect when wetted. In addition, thickness of the wet preform under 96 kPa was settled quickly after wetting was completed.

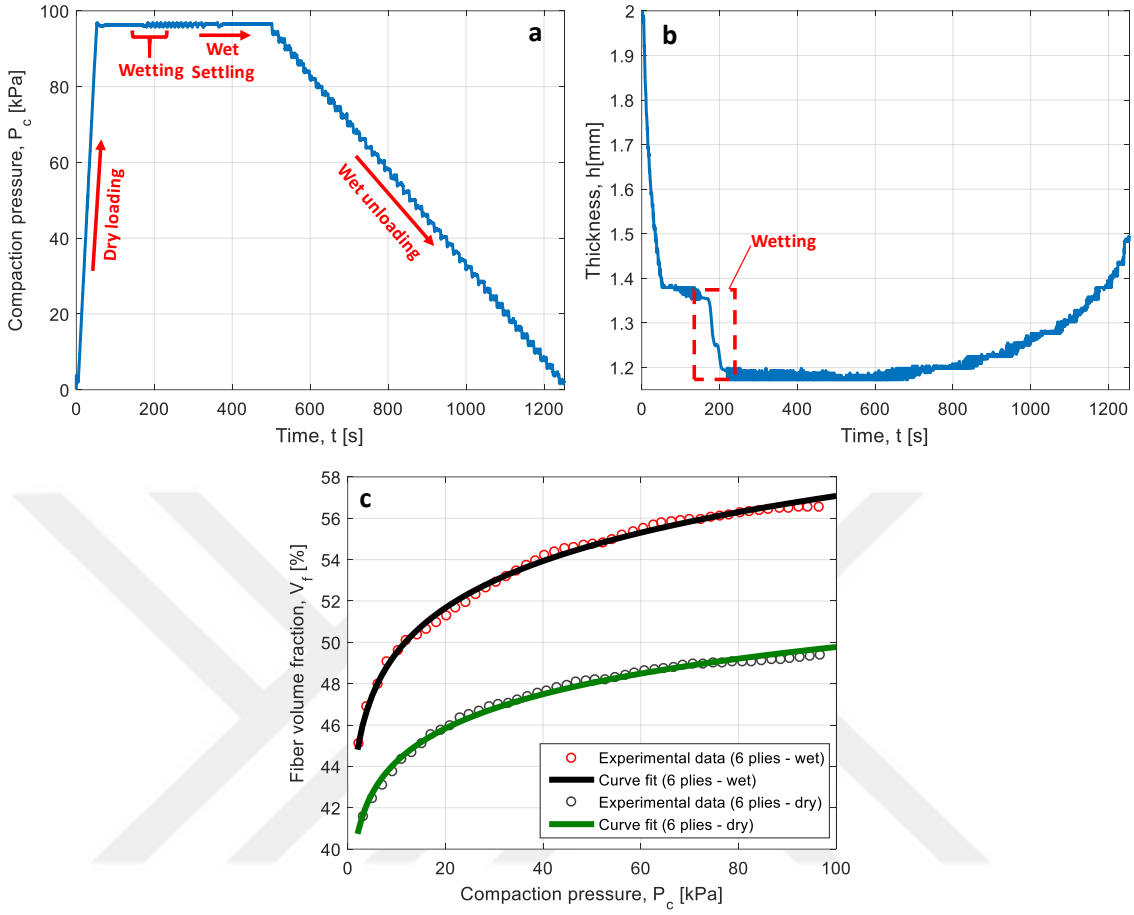

Figure 4.5 - Wet compaction characterization of a 6-ply preform: (a) pressure schedule and (b) thickness of a fabric preform during an experiment, and (c) curve fitting to wet-unloading stage and comparison of wet and dry compaction behavior of the fabric

4.3. Laminate manufacturing

Manufacturing of laminates was described in Section 2 in detail and it will be shortly outlined here as well. In this study, composite laminates made of 12 and 18 plies of the fabric were manufactured under different external pressure levels, P_{ext} by using the experimental setup shown in Figure 2.1 and following the same procedure demonstrated in Figure 3.2. The following parameters were chosen the same for 6-ply laminates to compare the results fairly:

- total flushing duration = 30 min after complete mold filling
- external pressurization instant, t^* = 5 min (see Figure 3.2 for t^*)

- P_{ext} = 0, 34.5, 69, and 138 kPa
- planar dimensions of the laminates: 6 in (152 mm) in width and 8 in (203 mm) in length

The mold was prepared according to the procedure explained in Section 3.1 and infusion was started by unclamping the inlet tube. For the pressurized laminates, significant amount of excess resin removal through the inlet port was observed as shown in Figure 4.6.

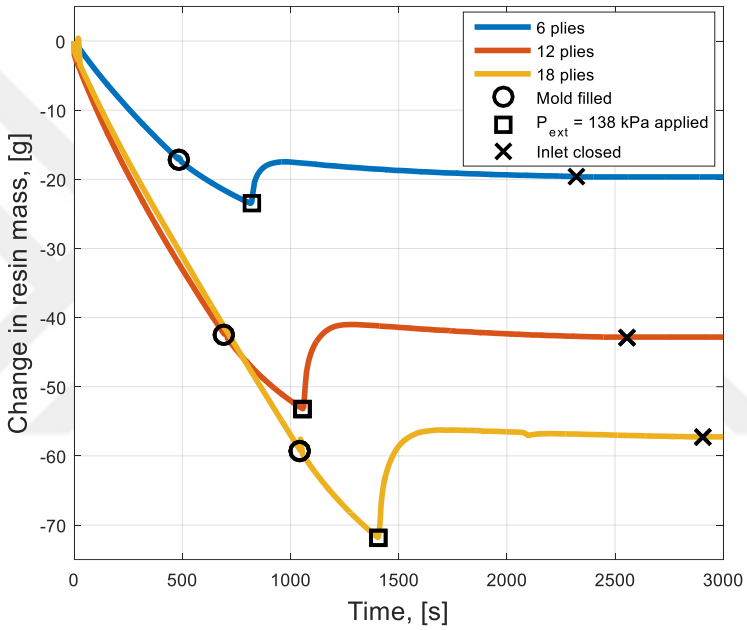

Figure 4.6 - Mass change in the resin reservoir during manufacturing of 6-, 12-, and 18-ply laminates (P_{ext} = 138 kPa)

In addition, it was also observed that the mold filling time for 12- and 18-ply laminates was longer than 6-ply laminates. Assuming that the permeability of a fabric preform is significantly dependent on V_f but not the number of plies, this seemed to contradict with Darcy law. Under constant injection pressure boundary condition, the fill time for 6-, 12- and 18-ply laminates should have been similar according to Darcy law. The increase in fill time could be caused by the very thin tube attached at the inlet which limits the flow rate as shown in Figure 4.6. Although, the flowrate should linearly increase with the increasing thickness (and thus, volume to be filled per cross-sectional area) under

constant pressure injection boundary condition, it was observed that the flowrate during filling of 12- and 18-ply preforms were almost the same. To investigate this phenomenon and verify the effect of tube diameter on fill time, mold filling experiments were conducted by using the wide tubing.

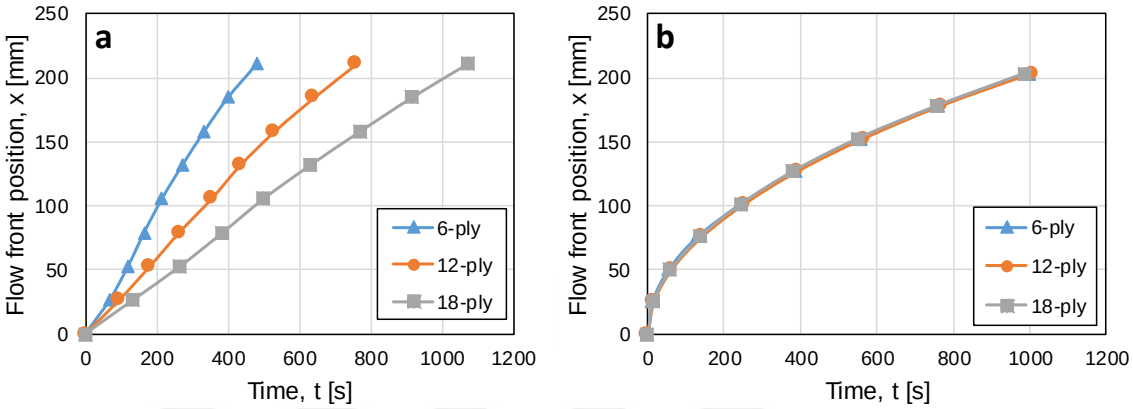

Figure 4.7 - Mold filling times for 6-, 12-, and 18-ply laminates using (a) small diameter tubing, and (b) large diameter tubing

The experiments in Figure 4.7(b) were conducted by using diluted corn-syrup with a viscosity of ~100 cP at room temperature whereas Figure 4.7(a) shows the fill times for EPON 862 resin with a viscosity of ~50 cP at 121 ºC. This figure shows that the difference in fill times for 6-, 12-, and 18-ply laminates was due to the small diameter tubing. Recall that smaller diameter tubing was intentionally to slow down the mold filling. In addition, Figure 4.7(b) validated that the permeability of the fabric was not significantly dependent on the number of layers. Although this analysis was important to understand the difference in fill times, it was beyond the scope of this thesis work to investigate this phenomenon further.

4.4. Results and discussion

4.4.1. Laminate thickness, fiber volume fraction and void content

Figure 4.8(a) and (b) presents the average thickness values with 95% confidence interval shown with error bars which are barely visible due to uniform thickness distribution within the parts. Under 138 kPa external pressure, significant decrease in thickness up to 19% and 17% for 12- and 18-ply laminates was achieved, whereas it was 19% for 6 plies.

At this point, it could be argued that pressurizing the laminate with a slower rate could lead to more thickness reduction. However, for satin woven fabric architecture it was shown that compression speed did not make a significant difference as in other fabric types [69]. Figure 4.8(c) shows that the per-ply thickness values of 6-, 12-, and 18-ply laminates under certain P_{ext} was very similar and did not depend on the number of plies. This indicated that regardless of the number of plies of the selected glass fabric, similar thickness reduction could be achieved at various P_{ext} levels in pressurized VARTM.

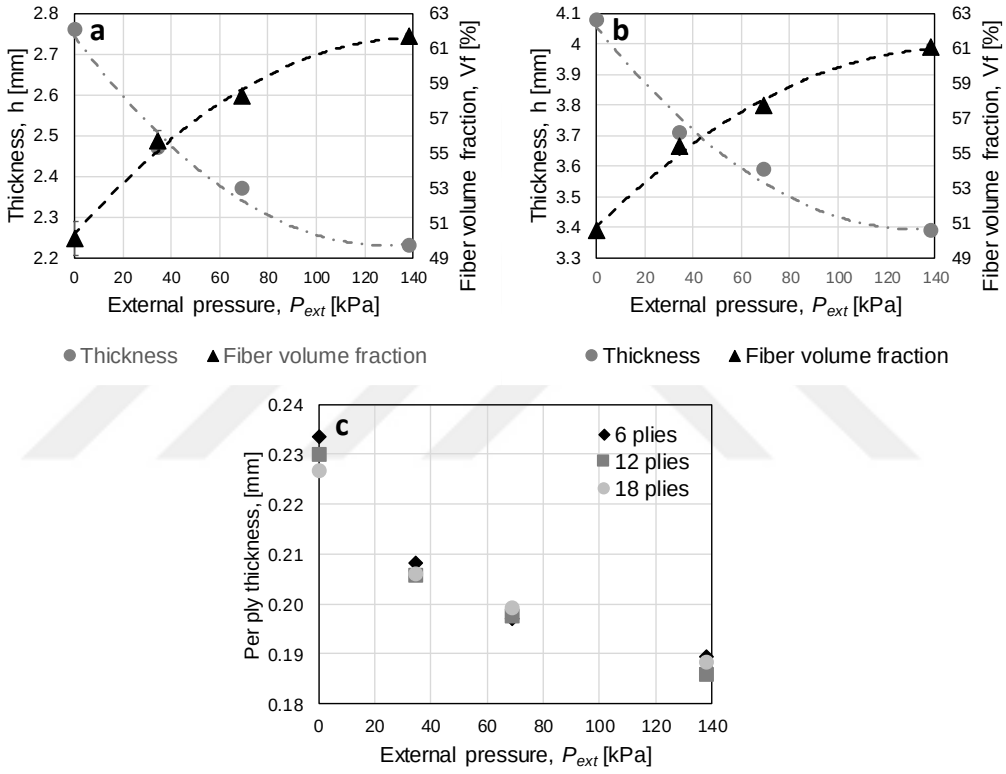

Figure 4.8 - Effect of external pressure on the part thickness and fiber volume fraction of (a) 12 plies and (b) 18 plies, and (c) per-ply thickness of 6-, 12- and 18- plies

To measure the V_f and void content, V_v three specimens with dimensions 0.5 in x 2 in (13 mm x 51 mm) from each laminate were cut according to the cutting template presented in Appendix. The same resin burn-off procedure (ASTM D 3171) was followed to measure V_f . Figure 4.8(a) and (b) shows the effect of P_{ext} on V_f of 12- and 18-ply laminates, respectively. VARTM laminates (i.e., P_{ext} = 0 kPa) had V_f values of 50% and 51% which increased up to 62% and 61% when 138 kPa of external pressure was applied

on 12- and 18-ply laminates., respectively. As reported in Section 3.5.2, 6 ply laminates had an increase from 50% to 62% under the same conditions which shows that the increase in V_f was not significantly dependent on the number of layers as also depicted in various studies [69,70]. However, the negligible effect of ply number may be not valid if the number of plies are excessively increased as discussed in Ref. [70] which showed that when the number of plies increased from 16 to 100, lower V_f values were achieved under same compaction pressure.

Compaction characterization experiments and average laminate thickness values were analyzed together to investigate whether there was a relation between them. Figure 4.9(a-c) shows that V_f of 6-, 12-, and 18-ply laminates externally pressurized under P_c > 34.5 kPa followed a different trend compared to dry compaction characterization behavior of the fabric. This could be explained by the fact that V_f of fabric preform was significantly increased when wetted as shown in Section 4.2. Note that the compaction pressure on the manufactured part was calculated by adding the external pressure value to the gauge vacuum pressure (for instance, 138 kPa + 100 kPa = 238 kPa). It could be expected that the wet compaction characterization would mimic the externally pressurized laminates' compaction behavior, however, V_f of laminates at low P_{ext} (0 and 34.5 kPa) were lower compared to the extrapolated curve fit in Figure 4.9(d). Recalling that V_f of non-pressurized and non-flushed 6-ply laminates was ~57% which was very similar to V_f of wet fabric preform (~57%) under ~100 kPa as seen in Figure 4.9(d), it could be suspected that flushing caused deviation from wet compaction characterization. When flushing was implemented, V_f of the non-pressurized laminates decreased from ~57% to ~50% as reported in Section 3.3 and seen in Figure 4.9(d). Since the compaction pressure in both cases was almost equal (i.e., P_c = 100 kPa ≈ P_{atm}), this could be explained by the additional resin intake during flushing and limited removal of excess resin due to increased viscosity of the resin with time. Therefore, it could be concluded that at no- or low-P_{ext}, compaction pressure was supported not only by the fiber bed but also by the resin. On the other hand, at high P_{ext} (138 kPa), it was observed that V_f of laminates was slightly above the compaction characterization curve. This could be due to debulking of the preform which was caused by the cyclic loading-unloading of preform. Debulking

increased V_f (and decreased thickness) further by enhancing nesting of fiber tows as also shown in various studies [71,72]. In pressurized VARTM process, the preform relaxed (unloaded) during mold filling due to increasing resin pressure and decreasing compaction pressure, and then, it was further compressed (loaded) due to external pressurization which yielded to higher V_f.

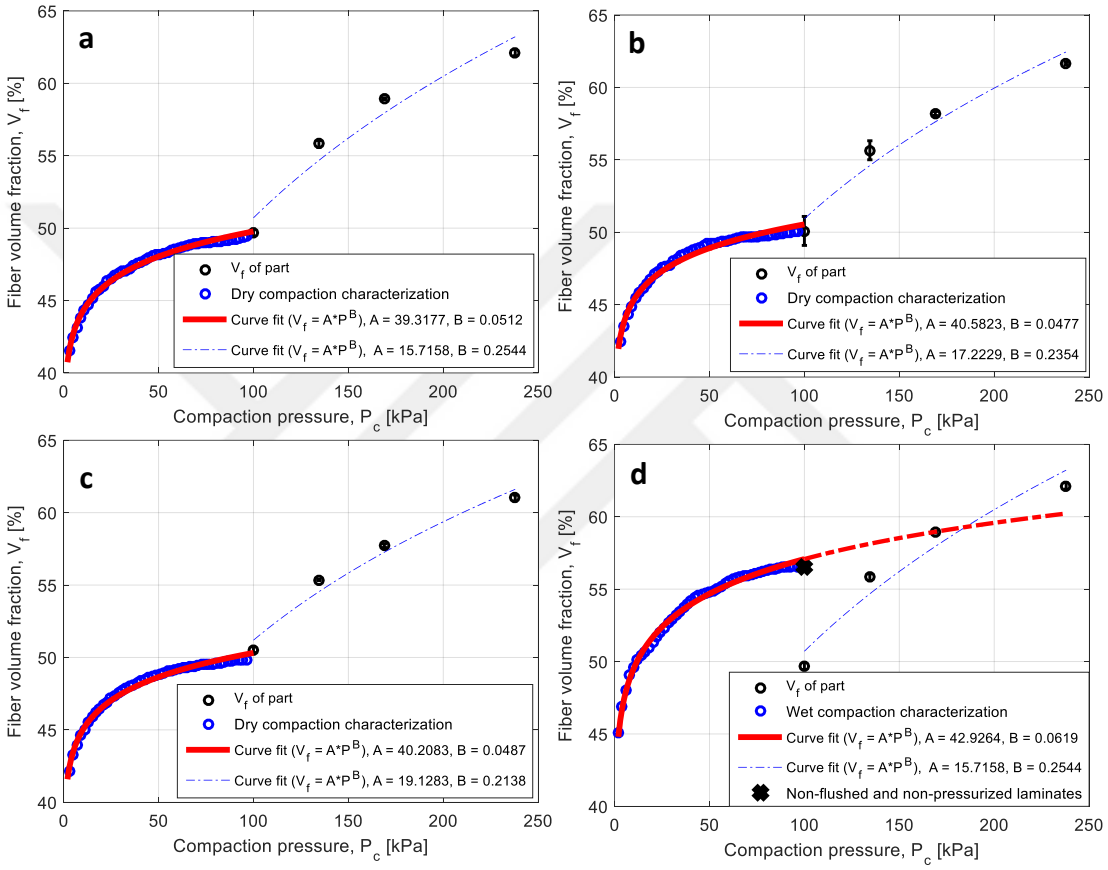

Figure 4.9 - Comparison of compaction characterization and V_f of laminates: (a) 6 (dry), (b) 6 (wet), (c) 12, and (d) 18 plies. In curve fits, V_f is dimensionless and P is in [kPa]

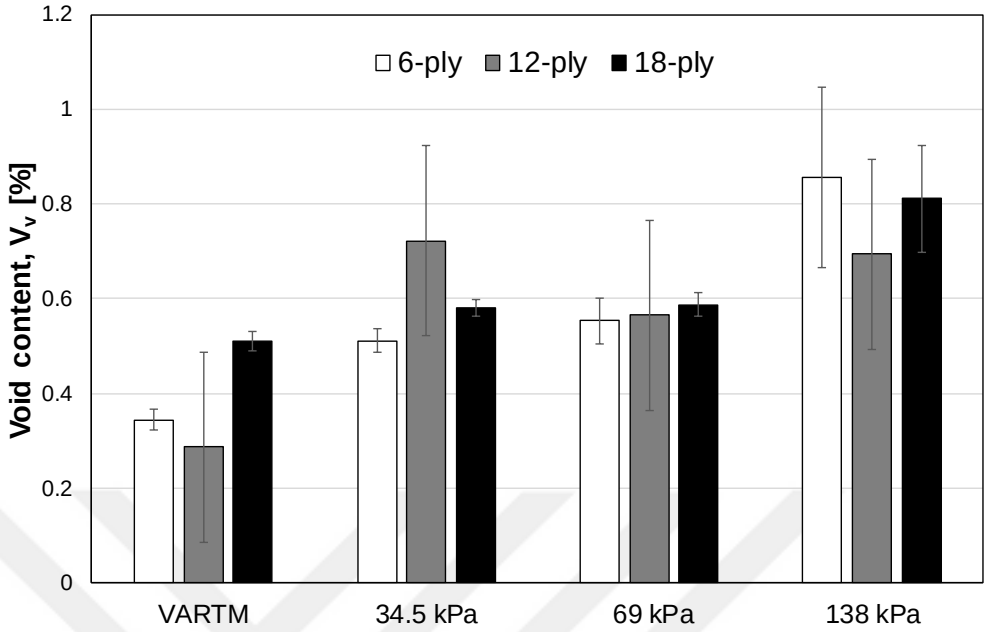

Figure 4.10 - Comparison of the void content of 6-, 12-, and 18-ply laminates manufactured under various external pressure levels

To determine the void content volume of the burned-off matrix and remaining fibers were subtracted from the total volume of the sample and the remaining volume corresponded to voids. The ratio of the void volume to the total volume of the sample was V_v of the sample. Figure 4.10 shows the average V_v with the 95% confidence interval for 6-, 12- and 18-ply laminates, respectively. It is seen that the average V_v of all laminates was below 1% for all external pressure values. A minor increase in V_v was observed in all laminates with increasing P_{ext} which could be due to mobilized voids being stuck in between the tows during flushing and pressurization. To fully understand the phenomenon and verify that the V_v was accurately determined, the microstructure of the samples will be analyzed in the next section.

4.4.2. Microscopy analysis

To investigate the microstructural properties of laminates, a 6 in (152 mm) long sample from each laminate was cut and prepared as described in Section 3.5.3. Samples were analyzed under a MEIZU light microscope using magnifications between 50X and 500X to investigate the (i) void morphology and (ii) tow consolidation.

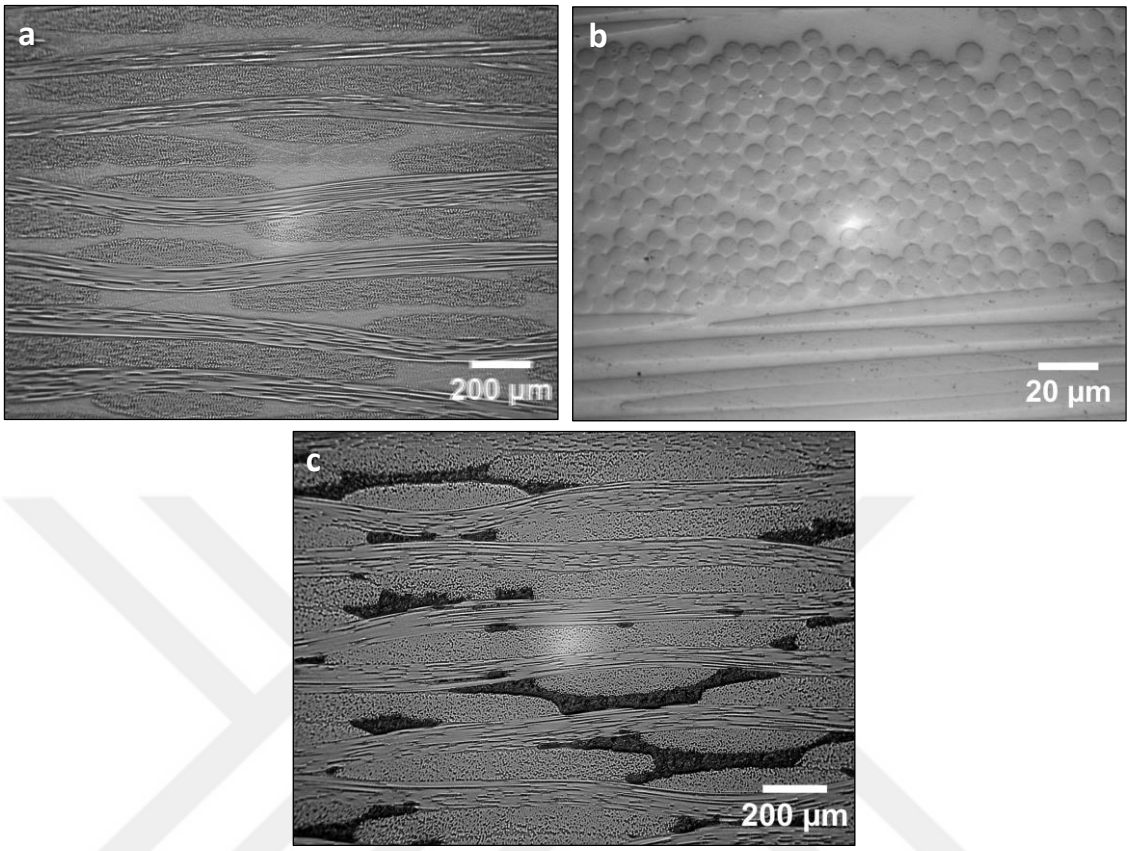

Figure 4.11 - Micrographs of (a) a void free section, (b) a void free tow, and (c) a section with voids

In Section 3.5.3, it was mentioned that a small number of voids were seen in 6-ply laminates and most of the analyzed cross-section was void free especially when P_{ext}<138 kPa. Here, in 12- and 18-ply laminates similar trend was observed as shown in Figure 4.11(a). Regardless of the P_{ext} level and number of plies, no voids were noticed in the tows located in transverse direction to flow (i.e., weft direction) (see Figure 4.11(b)). Moreover, voids were seen as localized and entrapped clusters in inter-tow regions rather than being evenly distributed along the samples' cross-section (see Figure 4.11(c)) which was also valid for 6-ply laminates. This implied that when voids were being removed during flushing, external pressurization further compacted the fabric layers and caused the inter-tow regions to shrink which squeezed and encapsulated the mobilized voids. In addition, the flushed resin amount was reduced when external pressure was applied as

seen in Figure 4.6 and removal of voids with the excessive resin flow was limited as discussed in Section 3.5.2.

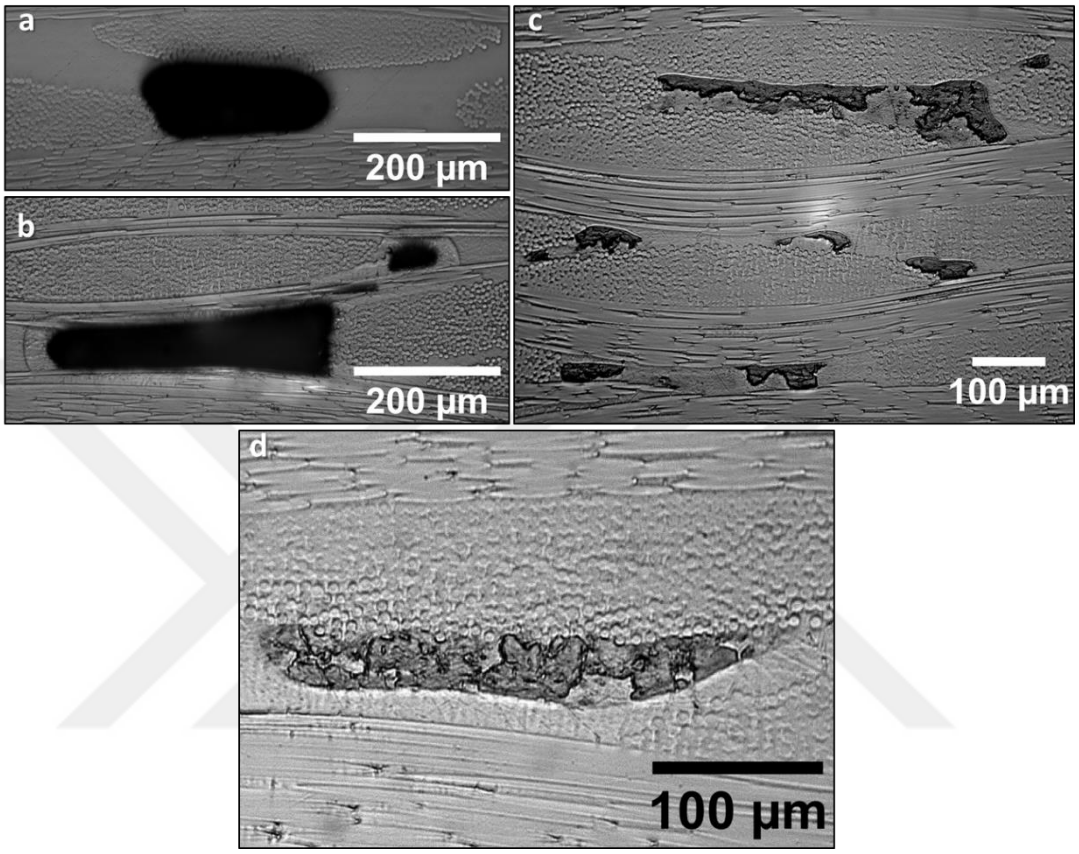

Figure 4.12 - Micrographs of voids with various shapes and morphology

Figure 4.12(a) and (b) shows micrographs taken from a non-pressurized and pressurized (P_{ext} = 69 kPa) 18-ply laminate, respectively. The effect of external pressure on fabric consolidation and thus, void shape is clearly seen when these micrographs are compared. The void in Figure 4.12 (a) was not compressed to elongate in the inter-tow region and had a less aspect ratio. On the other hand, the void shown in Figure 4.12(b) was compressed and enclosed by the tows around it due to external pressure and took the shape of the inter-tow region. Such elongated voids with higher aspect ratio were mostly seen when P_{ext} = 138 kPa and it should be highlighted that only very few voids as seen in Figure 4.12(a) were noticed when P_{ext} < 138 kPa. Another phenomenon about the shape of voids was observed in a 12-ply laminate manufactured under P_{ext} = 138 kPa. Figure

4.12(c) and (d) shows that sinuous voids with such different shapes and textures could be formed during manufacturing. These voids seemed to be formed due to the large voids being broken into smaller arbitrarily shaped voids in which the light colored areas were resin residuals. The penetration of resin was possibly due to external pressure causing increased hydrostatic pressure around the voids. Figure 4.12(d) shows one of these voids in detail, however, it was not clear whether these voids adjacent to the tows penetrated into the tows or not. Therefore, the interface between voids and tows were analyzed under a higher magnification as seen in Figure 4.12(a).

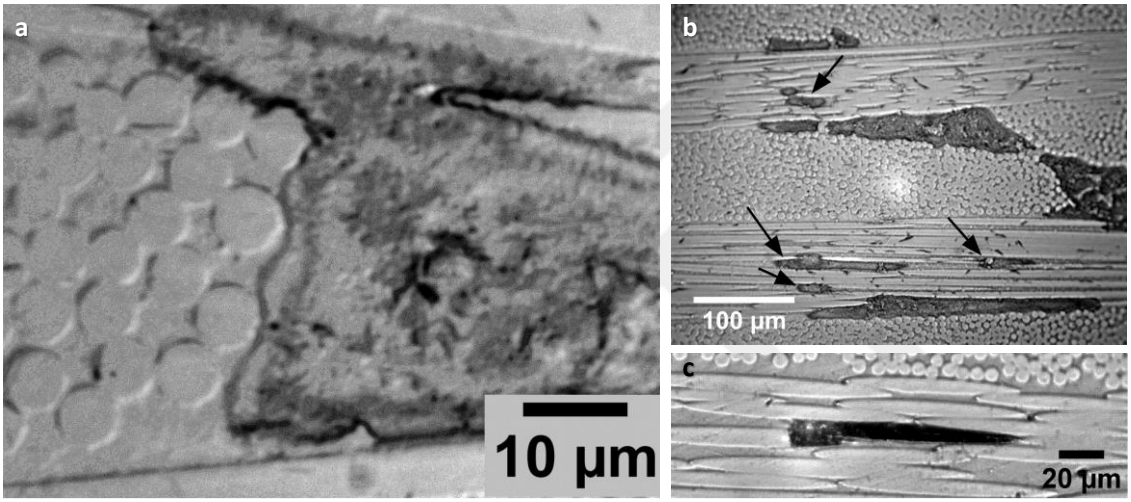

Figure 4.13 - (a) a void next to a tow in transverse direction to the flow direction (b) intra-tow voids in tows along the flow direction, and (c) broken fibers during cutting and polishing

Figure 4.13(a) clearly shows that the voids were not diffused into the weft tows even under the highest P_{ext}. This was a strong sign that the mobilized voids were moving through more permeable paths along the preform which could be the inter-tow regions and warp tows rather than the transverse tows. However, in various locations where voids were densely seen and tows were highly compacted, some large voids penetrated through the warp tows and seen as intra-tow voids as shown with arrows in Figure 4.13(b). It should be highlighted that these voids were not present in in areas where inter-tow voids were not seen which implied that intra-tow voids were not formed due to capillary effects but diffusion of large voids into the warp tows. Moreover, when conducting the

microscopy analysis one should be careful not to misinterpret the broken fibers (see Figure 4.13(c)) as intra-tow voids.

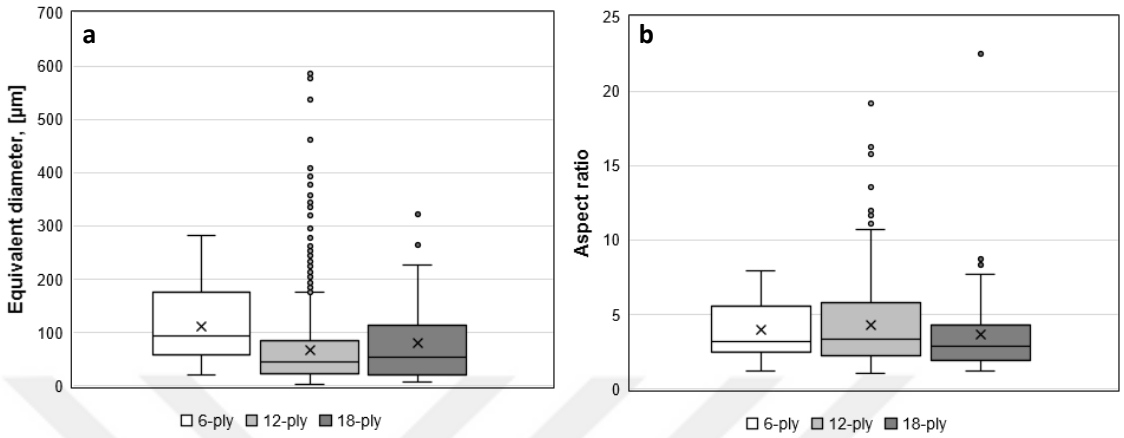

Figure 4.14 - Microscopy analysis of voids in 6-, 12-, and 18-ply laminates manufactured under Pext = 138 kPa: (a) equivalent diameter and (b) aspect ratio of the voids

Figure 4.14(a) and (b) presents the size and aspect ratio of the voids captured in microscopy examinations, respectively. Since, almost no-voids were seen at P_{ext}<138 kPa, laminates manufactured under P_{ext} = 138 kPa were analyzed. To capture and measure the dimensional properties of voids, image processing software, ImageJ was used. Equivalent diameter of the void, D_{eq} which corresponds to the diameter of the circle with the same area of the void was calculated and depicted in Figure 4.14(a). The average D_{eq} was 110 µm, 66 µm and 80 µm in 6-, 12-, and 18-ply laminates (labeled with x in Figure 4.14 (a)). This figure shows that significant variation in void size was observed regardless of the number of plies. 12-ply laminates had the smallest average D_{eq} because of the presence of (i) small intra-tow voids with D_{eq}<10 µm shown in Figure 4.13(b), and (ii) broken large voids resulting in smaller sinuous shaped voids as presented in Figure 4.12(c). Another observation was the variation in number of voids in different samples due to the localized voids being randomly distributed in the laminate. Since the samples were taken from same location in every laminate, some had more voids and some had less. For instance, 36 voids were captured in 6- and 18-ply whereas it was 1382 for 12 plies. This was specifically due to very small intra-tow voids being diffused into warp

tows and broken voids which increased the number of voids drastically in 12-ply laminates. Furthermore, the void content was also calculated by dividing the total void area to the total area of the sample and 0.27%, 1.50% and 0.07% void content were calculated for 6-, 12-, and 18-ply laminates, respectively. These values were plausibly comparable to the resin burn-off method results presented in Figure 4.10. The average aspect ratio of voids was calculated by fitting an ellipse to the selected void and dividing the major axis to the minor axis of the fitted ellipse. The results are presented in Figure 4.14(b) which shows that the average aspect ratio in all laminates were close to each other and slightly under 5. This implied that voids were mostly elongated due to P_{ext} rather than being circular as discussed previously. However, in 12- and 18- ply laminates some extreme values (AR > ~20) were noticed which were the outliers well above the whiskers.

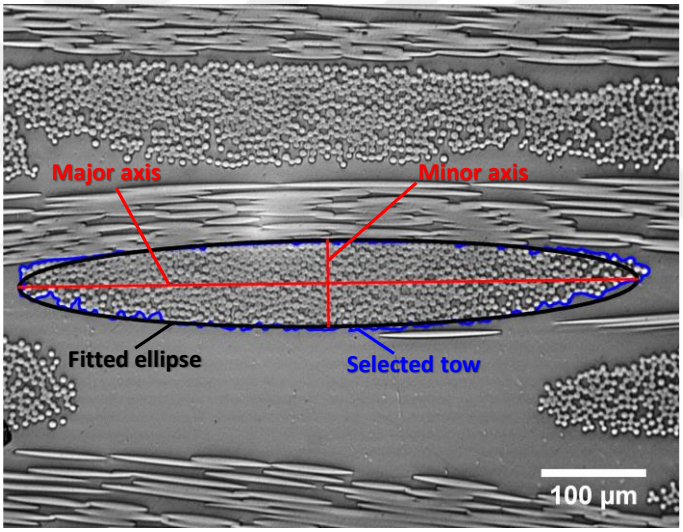

Figure 4.15 - Analysis of tow properties using image processing tool

The thickness reduction under external pressure is driven by two major factors which can be categorized as (i) closing the gap between fabric layers (i.e., nesting) and (ii) compaction of tows. The former was clearly observed by naked eye when Figure 4.11(a) and (c) were compared. It was seen that the resin rich inter-tow regions in the non-pressurized laminate was shrunk in the externally pressurized laminate which led to an overall thickness reduction. On the other hand, compaction of tows was not recognized readily. Therefore, ~120 weft tows were analyzed from each pressure configuration by selecting the periphery of the tows and fitting an ellipse to the selected tow as shown in

Figure 4.15. The minor axis of the fitted ellipse was assumed to be the height of the tow, h_{tow}. Regardless of the number of plies, average h_{tow} was decreased with the increasing P_{ext} as shown in Figure 4.16. Average h_{tow} was decreased by 9.2%, 10.5%, and 7.1% in 6-,12- and 18-ply laminates manufactured under 138 kPa of external pressure. Such decrease in tow height was also observed and modelled for plain-woven fabrics in the literature [64,73,74]. However, it could be stated that the effect of tow consolidation on overall fabric compaction was not as significant as nesting of fabric layers since the per-ply thickness of 6-, 12- and 18 ply laminates were very similar. Moreover, the large variation in h_{tow} could be explained by the 8 harness satin woven architecture of the fabric in which tows contacted each other at different locations causing non-uniform compaction.

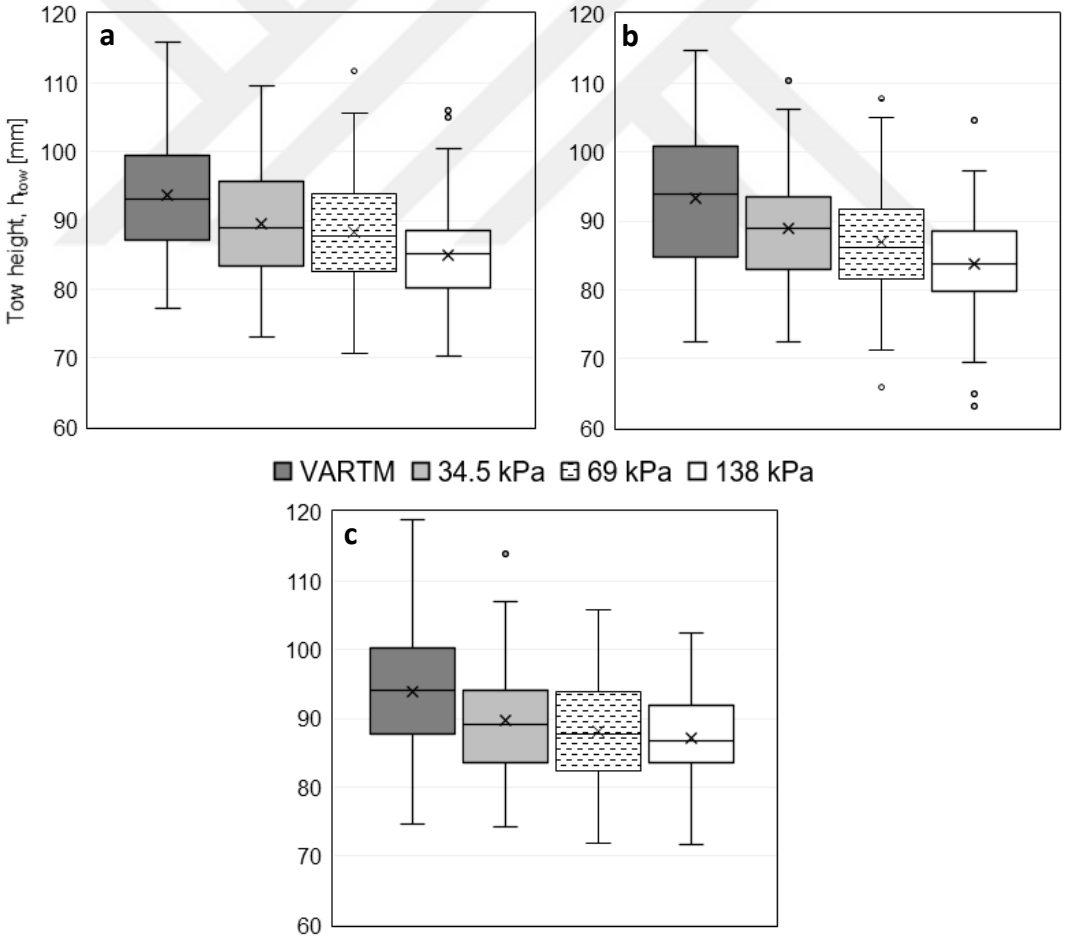

Figure 4.16 - Change in tow height with external pressure in (a) 6-, (b) 12- and (c) 18-ply laminates

4.4.3. Mechanical properties

Flexural strength and stiffness of 6 samples from each laminate were determined according to ASTM D 790. The results are presented in Figure 4.17(a) and (b) for 12- and 18-ply laminates, respectively.

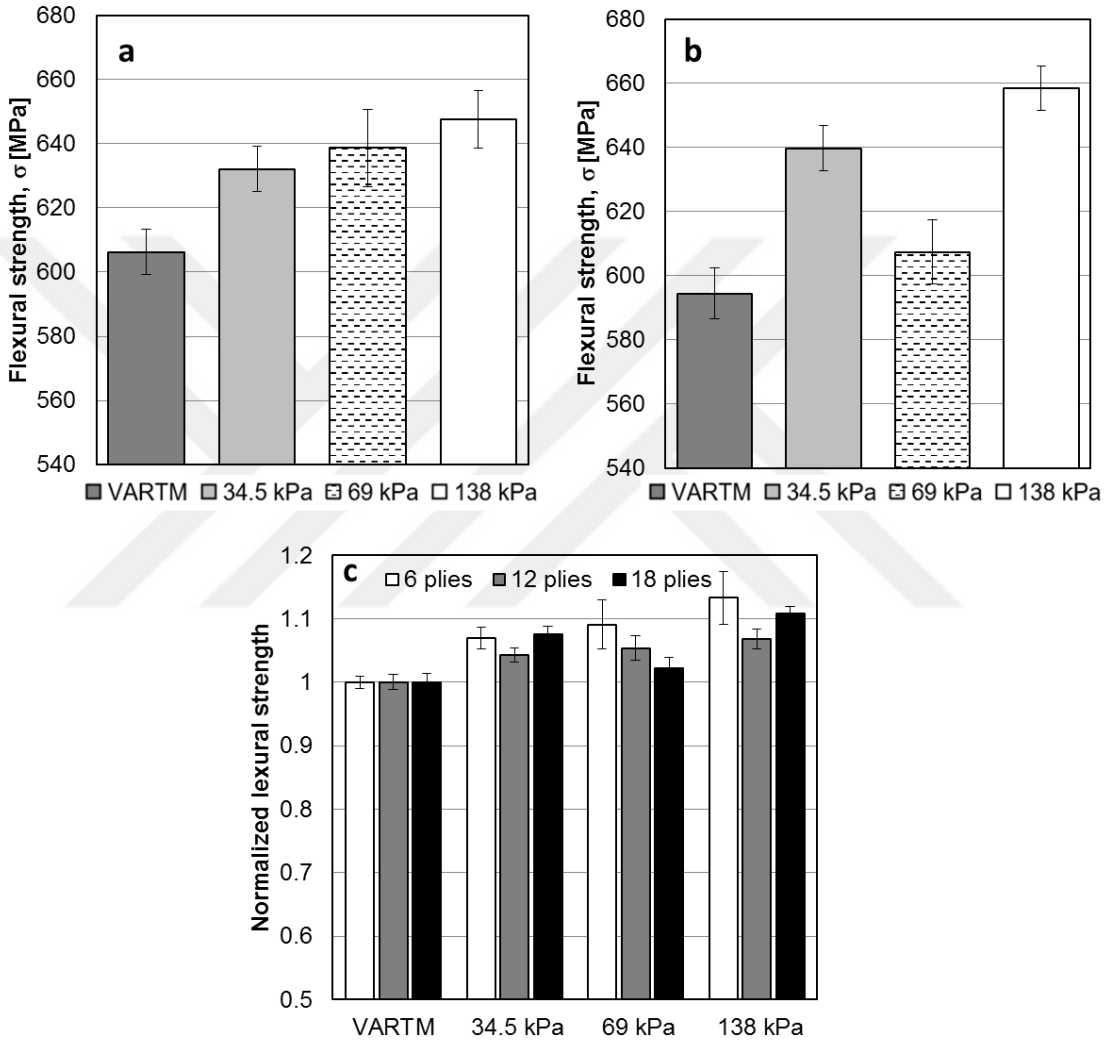

Figure 4.17 - Flexural strength of laminates made of a) 12 and b) 18 plies. c) comparison of normalized flexural strength of 6-, 12-, and 18-ply laminates

The effect of external pressurization on the flexural strength of both 12- and 18-ply laminates was apparent and similar to that of 6-ply laminates. Even under P_{ext} = 34.5 kPa, a noteworthy increase in flexural strength was observed in all ply configurations. As Figure 4.17(c) shows, the increase in flexural strength was 7% and 11% in 12- and 18-

ply laminates, respectively whereas it was reported as 13% in 6-ply laminates under P_{ext} = 138 kPa. Various studies investigated the effect of voids on the mechanical properties of composites and reported that voids significantly reduced the flexural strength [75,76]. The reason for relatively less improvement in 12-ply laminates manufactured under P_{ext} = 138 kPa could be correlated to the shape and size of the voids in the laminates. Even though Figure 4.14(a) showed that very large voids (D_{eq} >200 µm) were outliers and rarely seen in 12-ply laminates, they could still cause degradation of flexural properties since, even at the same void content larger voids decrease the flexural strength and stiffness [76]. Likewise, the increase under P_{ext} = 69 kPa in 18-ply laminates was not as high expected which could possibly be due to voids which were only noticed in 18-ply laminates under this pressure level (Figure 4.12(b)). Figure 4.18 illustrates the flexural stiffness of the laminates made of different number of plies. The flexural stiffness increased from 24.0 GPa to 28.4 GPa for 12- and 18-ply laminates which was similarly valid for 6-ply laminates (increased from 24.3 GPa to 29.1 GPa) in Section 3.5.4.

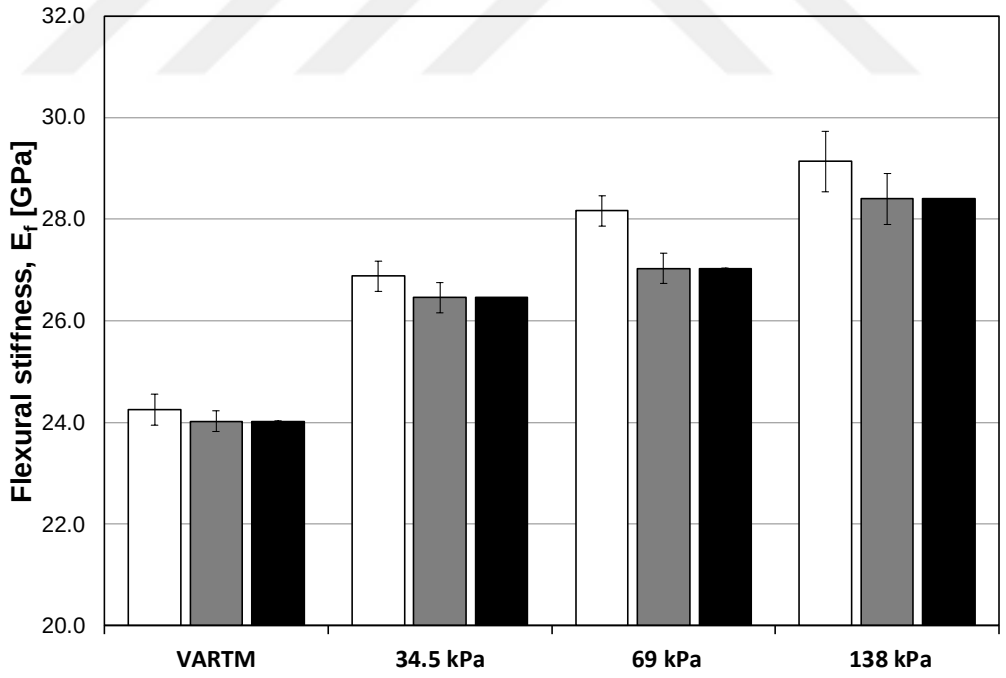

Figure 4.18 - Flexural stiffness of 6-, 12-, and 18-ply laminates

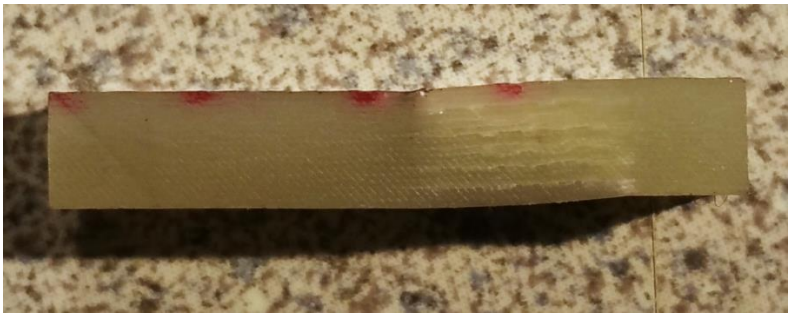

Figure 4.19 - Short beam test specimen after failure

Short beam shear testing for 12- and 18-ply laminates were conducted according to ASTM D 2344 to investigate the effect of external pressurization on the shear strength of the laminates. Since the thickness of 6-ply laminates did not satisfy the requirements of the ASTM standard, they were not tested. 6 samples from each laminate were tested at span to thickness ratio of 4:1 which was adjusted within ±1% of the calculated value. A sample broken under inter-laminar shear is shown in Figure 4.19.

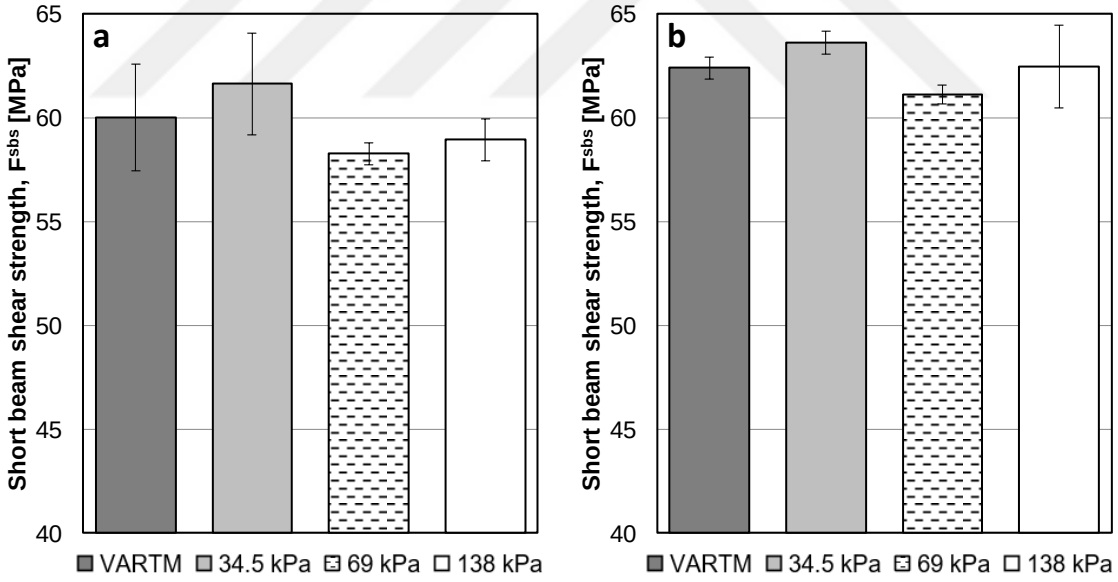

Figure 4.20 - Short beam shear strength of (a)12- and (b)18-ply laminates

Figure 4.20 shows that although external pressurization increased V_f, it did not lead to a significant change in shear strength of the laminates. For 12- and 18-ply laminates under P_{ext} = 0, 34.5, 69, and 138 kPa, short beam strength was measured as 60.0±2.6, 61.6±2.4, 58.3±0.5, and 58.9±1.0 MPa whereas, it was 62.4±0.5, 63.6±0.5, 61.1±0.5, and 62.5±2.0

MPa, respectively. Similar behavior was also observed and discussed in another study by emphasizing that cracks were formed in the matrix and shear strength did not depend on V_f which ranged between 40 - 60% among the tested samples [77]. On the contrary, it was also reported that the shear strength was reduced with the increased V_f simply by reducing the thickness of a laminate [78]. Since the shear strength of a composite laminate is a matrix governed property [55], it is significantly related to matrix properties and matrix-fiber interface. Moreover, effect of voids on shear strength is another factor which was widely investigated in previous studies showing that an increase in void content caused reduction in shear strength [55,78,79]. However, not only the void content but also location, shape and size of the voids play a significant role in terms of crack initiation and propagation. For instance, it was shown that triangular voids with sharp edges which were located in inter-tow regions of woven fabric reinforced laminates (similar to the voids presented in this study) caused initiation and propagation of inter-laminar cracks [55] whereas large and smoother voids did not cause initiation of cracks [78]. It was also shown that as the length of defects increased, shear strength significantly decreased [78] which could address the slight decrease in 12-ply laminates containing voids with high aspect ratio. Furthermore, it was observed that there was a critical V_v value depending on the resin and fabric type, below which voids did not significantly affect the shear strength [61,80]. Regarding these outcomes in the literature, at various V_f similar shear strength values were acceptable and the slight decrease of shear strength (<3%) under various external pressure levels could be explained by the presence of the voids. However, it should be highlighted that since pressurized and heated VARTM led to very low void content (i.e., $V_v < 1\%$), the reduction in shear strength was negligible.

5. IMPLEMENTATION OF A LOW TEMPERATURE RESIN SYSTEM AND FLOW ENHANCEMENT WITH PRESSURE CHAMBER

5.1. Objective of the study

Since conventional VARTM process is usually performed at room temperature and the mold may not be suitable for heating, pressurized VARTM will be implemented to low temperature processed resin systems in this section. The objective of this study is to

- investigate the applicability of pressurized VARTM on low temperature resin systems with higher viscosity,
- enhance resin flow by using the external chamber to relax the fabric preform,
- investigate the effect of pressurization and flow enhancement on the laminate properties.

5.2. Laminate manufacturing

6-ply laminates were manufactured using the same fabric and PRO-SET INF 114 epoxy resin. Resin properties are presented in Table 5.1, together with the EPON 862 resin.

Table 5.1 - Resin properties [50,81]

	EPON 862	**PRO-SET INF 114**
Curing agent	EPIKURE Curing agent W	PRO-SET INF 211
Mold temperature	121 °C	30 °C
Curing	4 hr at 121 °C	8 hr at 60 °C
Viscosity at 25 °C	~ 21-23 P	~ 245 cP
Viscosity at mold temp.	on the order of 10 cP	~ 190 cP
Complete mold filling time for 6-ply laminates	~ 2 min (no resistance tubing) ~ 10 min (with resistance induced by using a tube with diameter of 1.6 mm)	~ 50 min
Flexural strength	127 MPa	121 MPa
Flexural stiffness	3.42 GPa	3.41 GPa
Glass transition temp., T_g	113 °C	91 °C
Cured density	1.195±0.000 g/cm^3	1.142±0.001 g/cm^3

The mold temperature was set to 30 ºC which was slightly above the room temperature to ensure that all experiments were manufactured at the same temperature which eliminated the effect of varying room temperature at the laboratory. At 30 ºC, the pot life of the resin is 64-80 minutes according to the manufacturer's datasheet which also lists various cure schedules such as 2 weeks at 25 ºC, 8 hours at 49 ºC, or 60 ºC or 82 ºC. In this study, 8 hours at 60 ºC was chosen which was faster than curing at room temperature while keeping the process temperature at a moderate level. Curing was started 60 minutes after the beginning of infusion by increasing the mold temperature to 60 ºC.

5.2.1. Effect of resin removal through inlet port during external pressurization on thickness variation

Regarding the viscosity and gel time of the resin, process parameters used for EPON 862 was revised. Figure 5.1 shows the preliminary manufacturing scheme with PRO-SET INF 114. Before mixing the resin with the hardener, neat resin was degassed for 1 hour to remove the air bubbles which were formed while pouring the resin from the container into the cup. The resin and hardener were mixed for 5 minutes at 350 rpm which was shorter but at a higher mixing rate than that of EPON resin due to limited working time of PRO-SET. Then, the mixture was degassed for 10 minutes at ~100 kPa of gauge vacuum pressure.

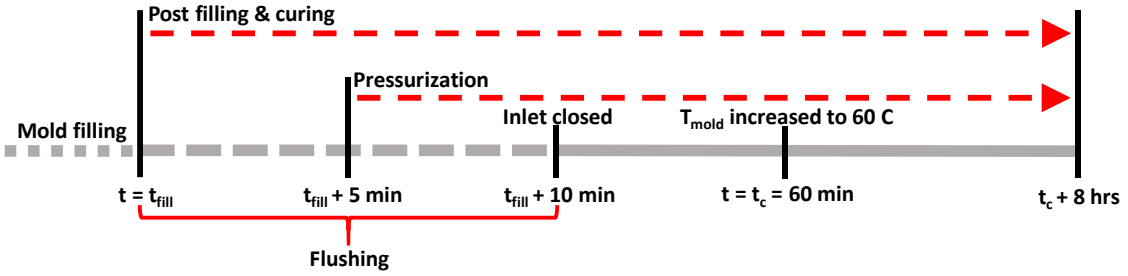

Figure 5.1 - Preliminary process outline for PRO-SET resin

The complete mold filling time was approximately 50 minutes with this resin system. Initially, flushing time was determined as 10 minutes and for pressurized laminates, P_{ext} was applied at the 5th minute of flushing (i.e., t_{fill} + 5 min). The same P_{ext} levels (0, 34.5, 69, and 138 kPa) were applied to compare the thickness reduction of laminates with the

previous ones manufactured using EPON resin. Additionally, the pressure was increased to 276 kPa to investigate whether significant decrease in laminate thickness compared to P_{ext} =138 kPa could be achieved or not. Resin mass at the inlet was monitored and recorded during the process and an example is given in Figure 5.2.

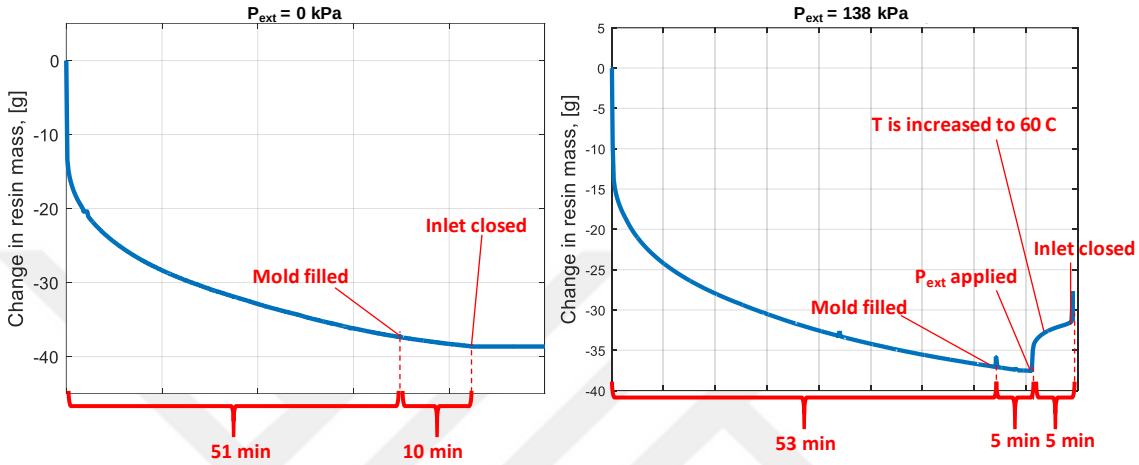

Figure 5.2 - Resin mass at the inlet resin reservoir in preliminary manufacturing experiments using PRO-SET resin: (a) non-pressurized, and (b) pressurized laminate

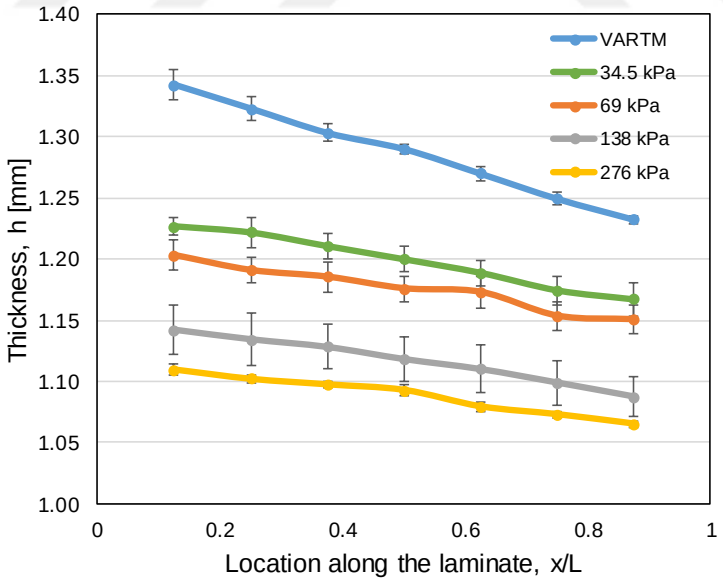

Figure 5.3 - Effect of preliminary process parameters for PRO-SET resin on thickness distribution along the laminate

Figure 5.3 shows the thickness distribution in laminates manufactured by following the preliminary process outline described in Figure 5.1. It was observed that the average thickness of non-pressurized laminates was reduced from 1.287 mm to 1.088 mm at P_{ext} = 276 kPa. However, significant thickness gradient along the laminate was observed as shown in Figure 5.3. Regardless of the pressurization level, inlet side of the laminates were thicker than the exit side. As seen in Figure 5.2(b), when inlet was closed, there was still resin removal through the inlet. This was a strong sign of insufficient excess resin removal through the inlet port which caused the laminates to be thicker at the inlet side. This also indicated that after closing the inlet port, the excess resin could not be removed through exit port which was most probably due to the increase in resin viscosity at the exit side caused by curing reaction.

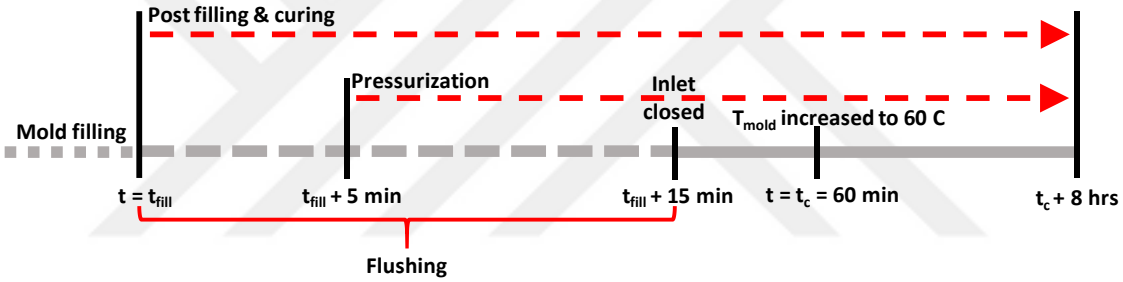

Figure 5.4 - Process outline for uniform thickness distribution using PRO-SET resin

It was aimed to reduce thickness variation by extending the total flushing time as shown in Figure 5.4. Compared to the case presented in Figure 5.3(b), more resin was evacuated through inlet by keeping inlet port open for a longer duration as seen in Figure 5.5(b). However, when flushing was extended, more resin was infused in non-pressurized case, which could cause thicker non-pressurized laminates compared to the ones presented in Figure 5.3.

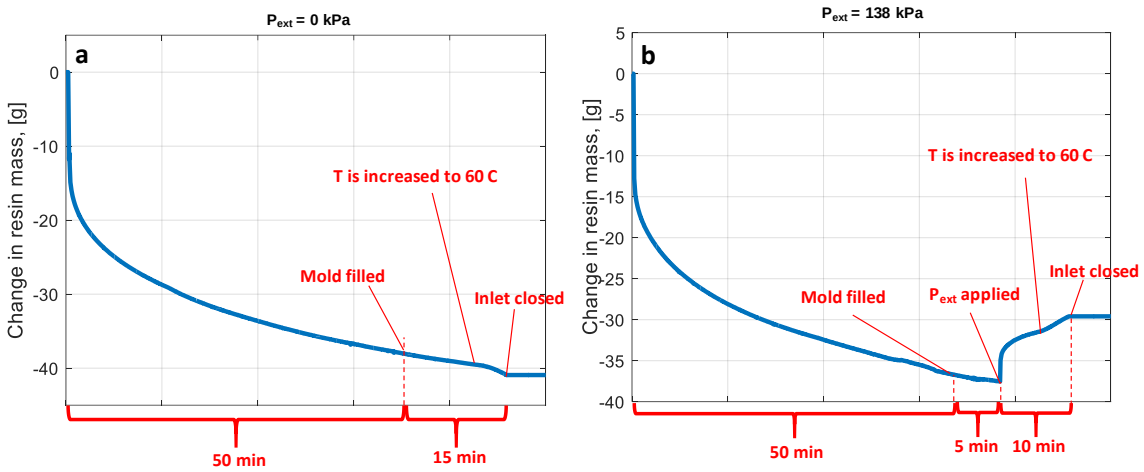

Figure 5.5 - Resin mass at the inlet resin reservoir in extended flushing of PRO-SET resin: (a) non-pressurized, and (b) pressurized laminate

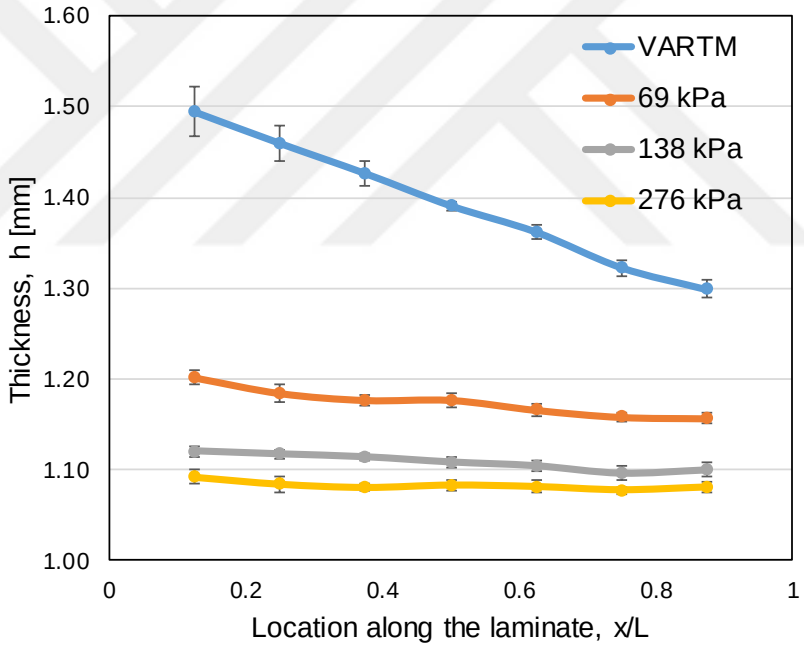

Figure 5.6 - Effect of extended flushing time on thickness distribution along the PRO-SET laminates

Figure 5.6 shows that, extended resin removal through the inlet significantly reduced the thickness variation along the laminates compared to the ones presented in Figure 5.3. On the contrary, non-pressurized laminates still had the variation and their overall thickness

increased due to excess resin intake. However, it is important to highlight that pressurization led to almost uniform laminates with minor thickness variation.

Using the revised process outline with extended flushing presented in Figure 5.4, two laminates for each P_{ext} level (0, 69, 138, and 276 kPa) were manufactured. Their properties will be presented in Section 5.3. An example of PRO-SET laminate is illustrated in Figure 5.7 which shows that PRO-SET resin resulted in more transparent laminates compared to EPON resin.

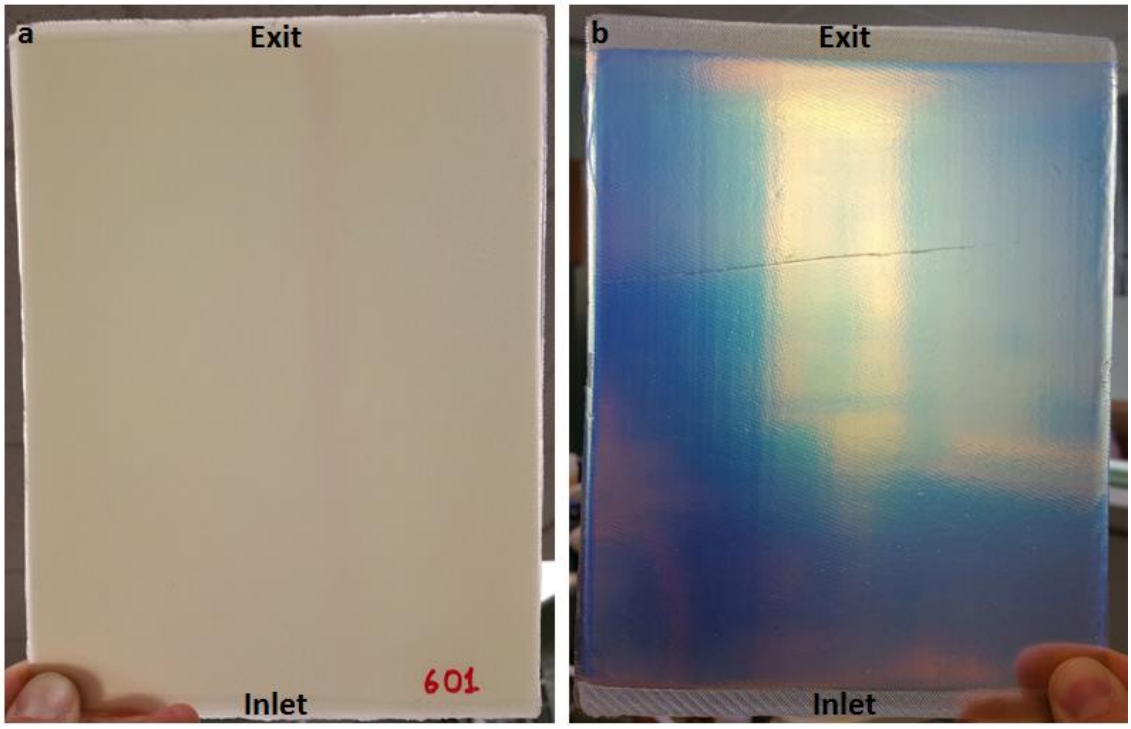

Figure 5.7 - View of laminates manufactured with (a) EPON and (b) PRO-SET resins

5.2.2. Flow enhancement by using the pressure chamber

The infusion of PRO-SET resin with high viscosity at the processing temperature of 30 ºC, resulted in very long mold filling time compared to EPON resin processed at high temperatures as presented in Table 5.1. For PRO-SET resin, it was not possible to reduce the viscosity further by increasing the process temperature because of pre-mature gelation of resin would occur before complete mold filling. In this case, flow enhancement methods such as placement of a highly permeable distribution medium on the preform

(as done in SCRIMP) could be implemented to enhance the resin flow as discussed in detail in Introduction section. However, the conventional SCRIMP method requires use of an additional distribution layer on top of the preform. In this study, an approach similar to FFC was applied by applying vacuum pressure in the chamber. The experimental set-up was revised by adding a vacuum pressure regulator (SMC ITV-2090 21N2BL5) and an additional solenoid valve as shown in Figure 5.8. The Labview user interface was also revised to control the additional equipment.

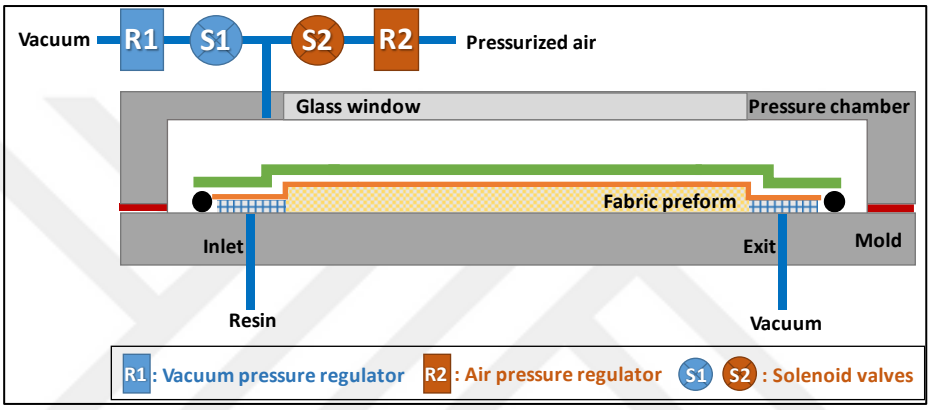

Figure 5.8 - Revision of the experimental setup for flow enhancement

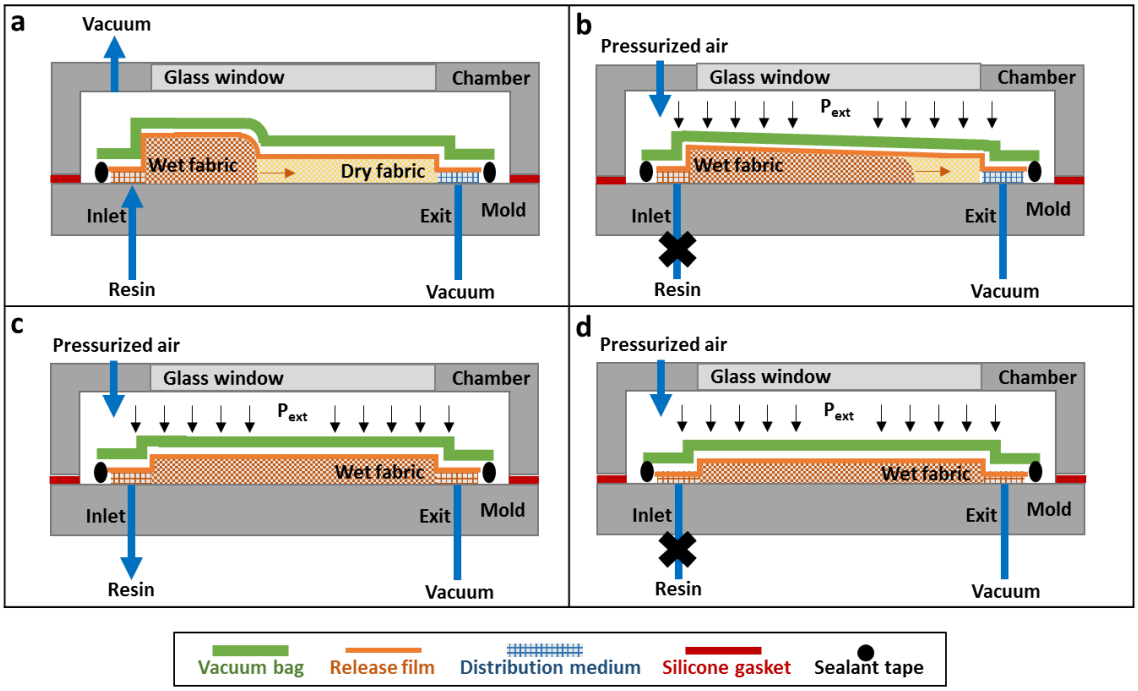

Figure 5.9 - Flow enhancement process

In Figure 5.9, the steps of flow enhancement and pressurization processes are schematically described. After preparation of the mold as previously described in Section 3.1 and mounting of the chamber, 5 kPa of gauge vacuum pressure was applied into the chamber by opening the first solenoid valve. The inlet port was opened and fabric preform was rapidly impregnated at the inlet side as shown in Figure 5.9(a) due to relaxation of the preform under vacuum. It was observed that at this stage, the vacuum bag was swollen by the resin pressure. This was due to resin pressure being higher than the compaction pressure on the preform due to the vacuum applied in the chamber. Regarding the resin mass intake in Figure 5.5(a), 40 g of resin was infused at this stage and the inlet was clamped. Then, the solenoid valve, S1 was closed and S2 was opened to pressurize the partially wetted preform and distribute the resin accumulated at the inlet side along the laminate as demonstrated in Figure 5.9(b). After complete mold filling, resin was bled for 5 minutes only through the exit, and then, the inlet port was opened for 10 minutes to remove excess resin through the inlet (see Figure 5.9(c)) similar to manufacturing of pressurized laminates shown in Figure 5.5(b). After flushing was completed, the inlet was clamped and the part was cured for 8 hours at 60 ºC under external pressure as shown in Figure 5.9(d). Mold temperature was increased to 60 ºC at $t = t_c = 60$ min (i.e., 60 minutes after the infusion was started) as described in the previous section. An example of resin mass change at the inlet reservoir for flow-enhanced manufacturing of laminates is presented in Figure 5.10(b) together with the mass change during the regular pressurized laminate manufacturing in Figure 5.10(a). The properties of the laminates and the effect of flow enhancement on the mold filling time will be presented in Section 5.3.

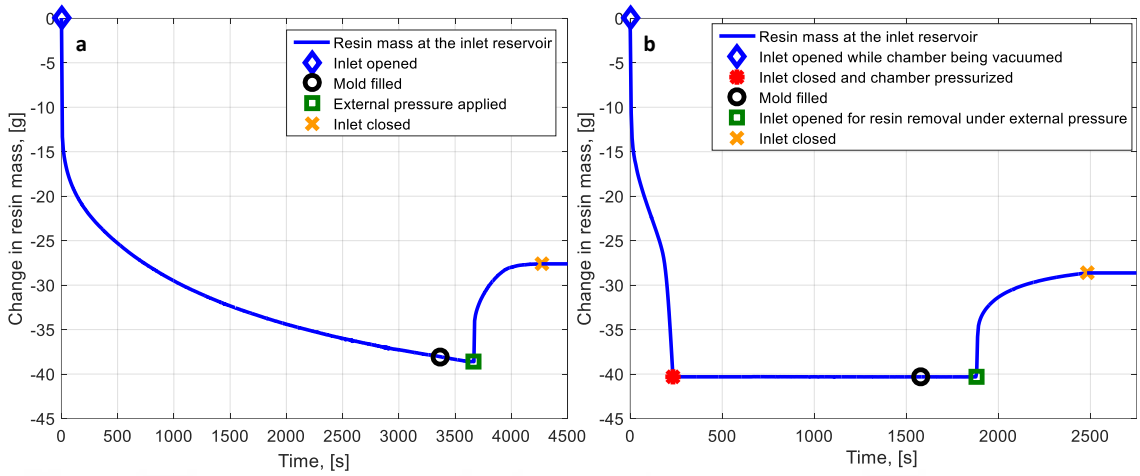

Figure 5.10 – Mass change at the inlet reservoir during manufacturing of (a) the regular pressurized (P_{ext} =276 kPa), and (b) flow enhanced pressurized laminate

5.3. Results and discussion

5.3.1. Effect of flow enhancement on the mold filling time

The aim of flow enhancement was to reduce the mold filling time by relaxing the fabric preform and enabling rapid resin intake into the mold. The infused resin was distributed along the laminate by applying P_{ext} at various levels. Effect of P_{ext} on mold filling time and laminate properties was investigated. Figure 5.11(a) shows the flow front position with respect to time under P_{ext} = 0, 69, 138, and 276 kPa.

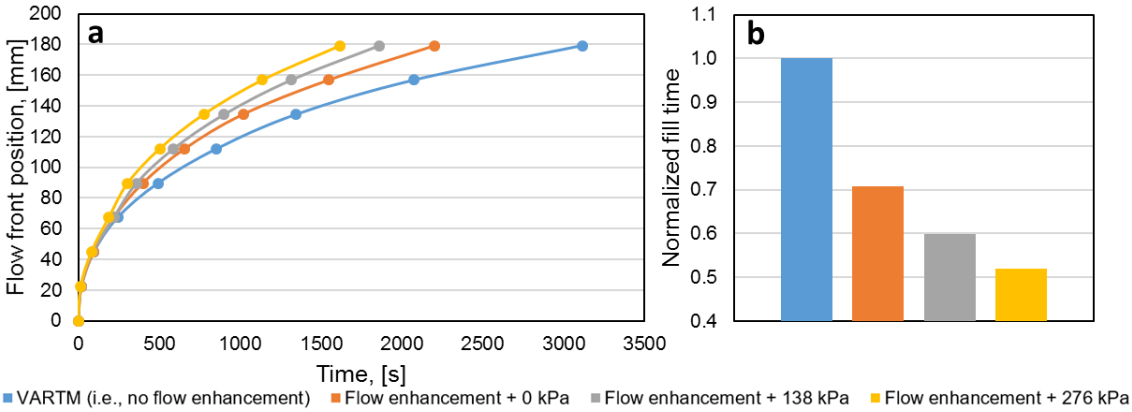

Figure 5.11 - Effect of flow enhancement and various P_{ext} on (a) flow front propagation and (b) mold filling time

It was observed that the mold filling time was significantly reduced by flow enhancement method. Average mold filling time was reported as 3115 seconds for VARTM process with no flow enhancement. Flow enhancement without application of P_{ext} after resin intake reduced the mold filling time to 2206 seconds. At P_{ext} = 138 and 276 kPa after resin intake, fill time was further reduced to 1862 and 1620 seconds, respectively. Figure 5.11(b) illustrates the normalized mold filling times with respect to VARTM mold filling time. It shows that the mold filling time was reduced by 29, 40%, and, 48% at P_{ext} = 0, 138 and 276 kPa, respectively.

When vacuum was applied in the chamber for preform relaxation, vacuum bag was swollen since the resin pressure at the inlet (~100 kPa) was higher than the compaction pressure on the vacuum bag ($P_c \approx 100 - 5$ kPa). This led to rapid resin intake at the inlet side which resulted in swollen vacuum bag with excess resin. After the inlet port was clamped, resin was distributed by the compaction pressure on the vacuum bag. Increasing P_{ext} led to higher resin pressure which resulted in reduced mold filling time. It could be argued that the increase in P_{ext} would reduce permeability of the dry fabric due to increased V_f and cause more resistance to flow which would result in higher mold filling time. According to the extrapolated dry compaction characterization shown in Figure 5.12, V_f of dry fabric does not increase significantly between 100 and 376 kPa. This indicates that permeability of the dry fabric was not significantly affected by P_{ext} and apparently, the increase in resin pressure with P_{ext} had a more dominant effect on mold filling compared.

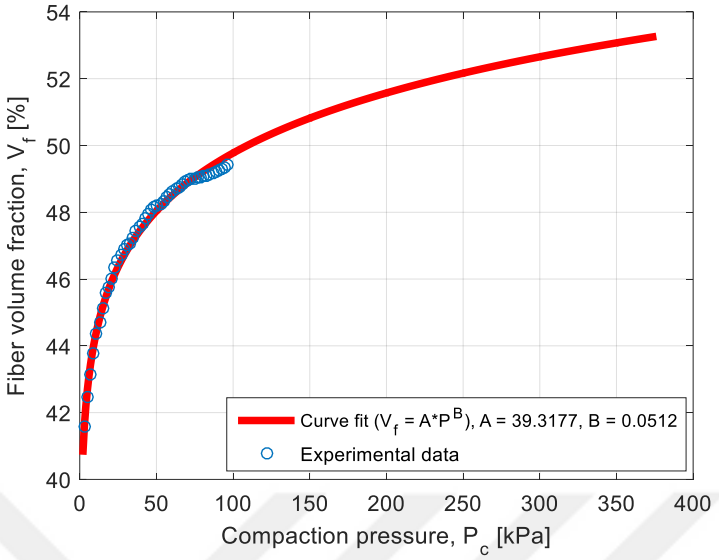

Figure 5.12 - Dry compaction characterization of 6 plies of fabric

5.3.2. Laminate thickness

The effect of external pressurization on laminate thickness is presented in Figure 5.13. 34.5 kPa laminates were not manufactured with PRO-SET resin, therefore, only EPON results are shown at that P_{ext}. On the other hand, P_{ext} was increased to 276 kPa to investigate if further pressurization would cause significant change in laminate thickness.

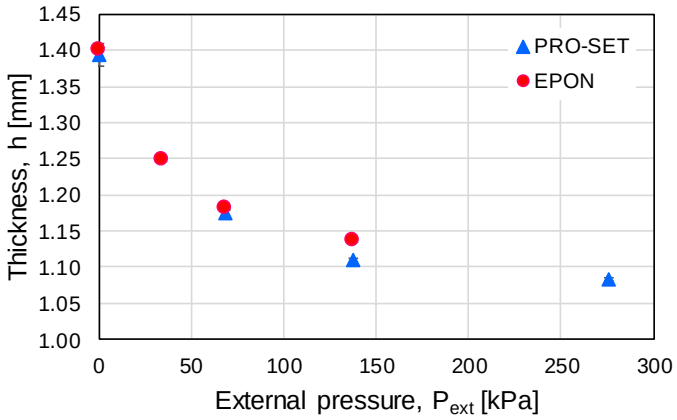

Figure 5.13 - Average thickness of laminates manufactured using PRO-SET and EPON resins under various P_{ext}

It was observed that the average thickness of laminates manufactured using PRO-SET resin decreased similar to the EPON-laminates under the same P_{ext}. At P_{ext} = 69 and 138

kPa, thickness reduction was reported as 16% and 19% for EPON-lamiantes whereas it was 16% and 20% for PRO-SET-laminates. Pressurization at P_{ext} = 276 kPa reduced the thickness by 22%. The average thickness values for EPON-laminates at P_{ext} = 0, 34.5, 69, and 138 kPa were 1.401±0.003 mm, 1.249±0.004 mm, 1.181±0.003 mm and 1.134±0.003 mm whereas, at P_{ext} = 0, 69, 138, and 276 kPa average laminate thickness was documented as 1.393±0.017 mm, 1.174±0.004 mm, 1.109±0.003 mm, and 1.083±0.002 mm, respectively. These results indicate that, regardless of the resin type, thickness reduction could be successfully achieved in pressurized VARTM.

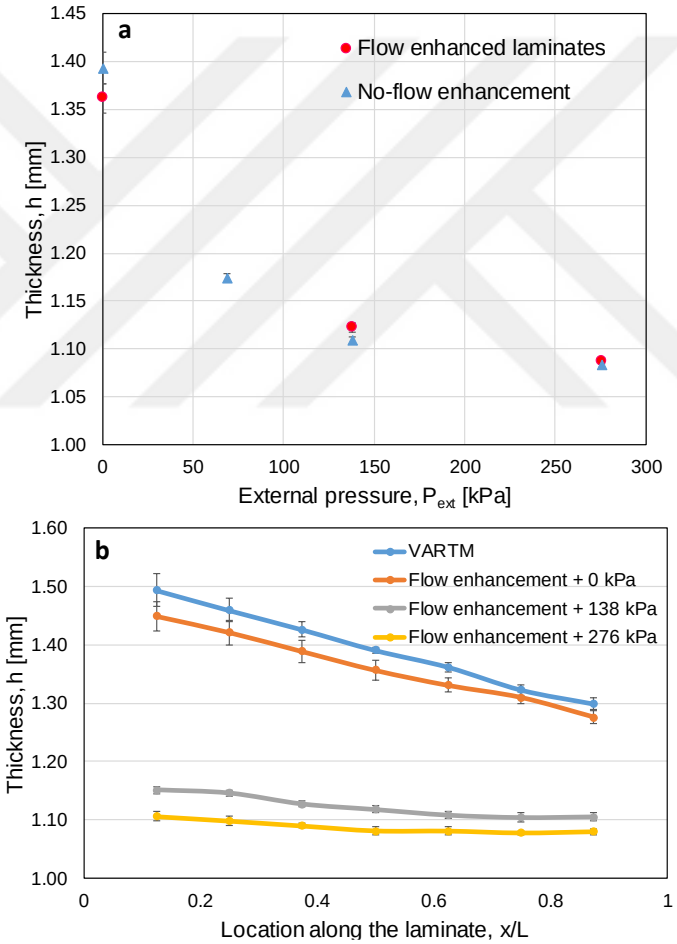

Figure 5.14 - Effect of flow enhancement on (a) average laminate thickness and (b) thickness distribution along the laminates

Effect of flow enhancement process on the laminate thickness is presented in Figure 5.14. It was observed that flow enhancement with no external pressurization resulted in slightly

thinner laminates (1.338±0.017 mm) than VARTM laminates (1.393±0.017 mm). However, the thickness gradient was not eliminated. On the other hand, flow enhanced and pressurized laminates had minimal thickness gradient. Moreover, average thicknesses of flow enhanced and pressurized laminates were similar to that of regular pressurized laminates. Under same the P_{ext} (i.e., 138 and 276 kPa), average thicknesses of flow enhanced laminates were 1.123±0.005 mm and 1.087±0.003 mm whereas, regular pressurized laminates were 1.109±0.003 mm and 1.083±0.002 mm, respectively.

Regarding these results, it could be concluded that with external pressurization not only thickness reduction was obtained but also thickness gradient along the laminate was eliminated. In addition, flow enhancement and pressurization enabled similar thickness reduction while significantly reducing the fill time.

5.3.3. Fiber volume fraction and void content

V_f and V_v of laminates were determined by following the ASTM D 3171 standard as described in Section 3.5.2. Nine samples from each laminate were cut and burned-off. The results for V_f at various P_{ext} and flow enhancement are presented in Figure 5.15.

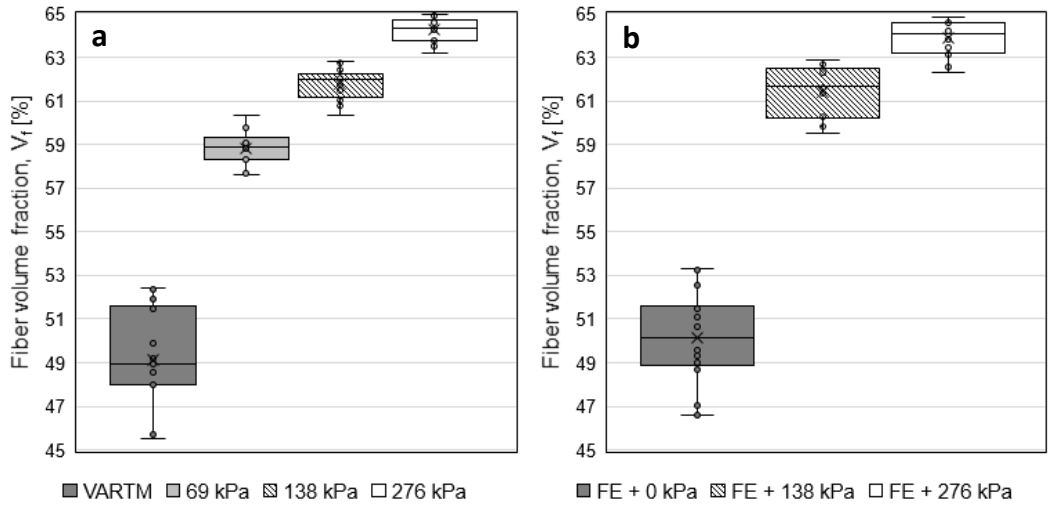

Figure 5.15 - Fiber volume fraction of laminates manufactured (a) under various P_{ext} and (b) with flow enhancement (FE)

Figure 5.15(a) shows that at P_{ext} = 0, 69, 138, and 276 kPa, V_f of laminates were 49, 59, 62, and 64%, respectively. The same V_f values were obtained for laminates manufactured

using EPON resin at the same P_{ext} as well. Flow enhanced (FE) laminates' V_f are presented in Figure 5.15(b). It was observed that V_f increased similarly as in non-FE laminates. In both FE and non-FE laminates, without pressurization it was observed that variation of V_f was relatively higher which was due to the thickness gradient as presented in Figure 5.6 and Figure 5.14.

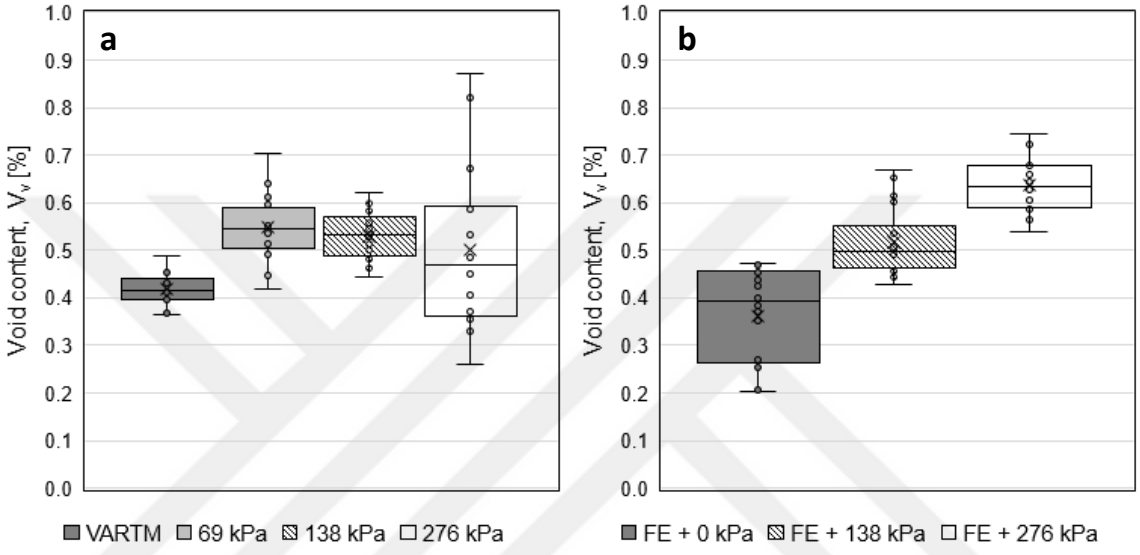

Figure 5.16 – Void content of laminates manufactured (a) under various P_{ext} and (b) with flow enhancement (FE)

Figure 5.16 shows the void content of PRO-SET laminates manufactured under various P_{ext} and with flow enhancement (FE). This figure clearly presents that the void content of all laminates were below 1% and slight increase in V_v was observed due to pressurization which was also seen in EPON laminates. Moreover, flow enhancement and pressurization resulted in V_v below 1% as well which was a promising outcome of the process.

5.3.4. Mechanical properties

Flexural properties of laminates were determined by following the ASTM D 790 standard as in previous sections. The results are presented in Figure 5.17 and Figure 5.18.

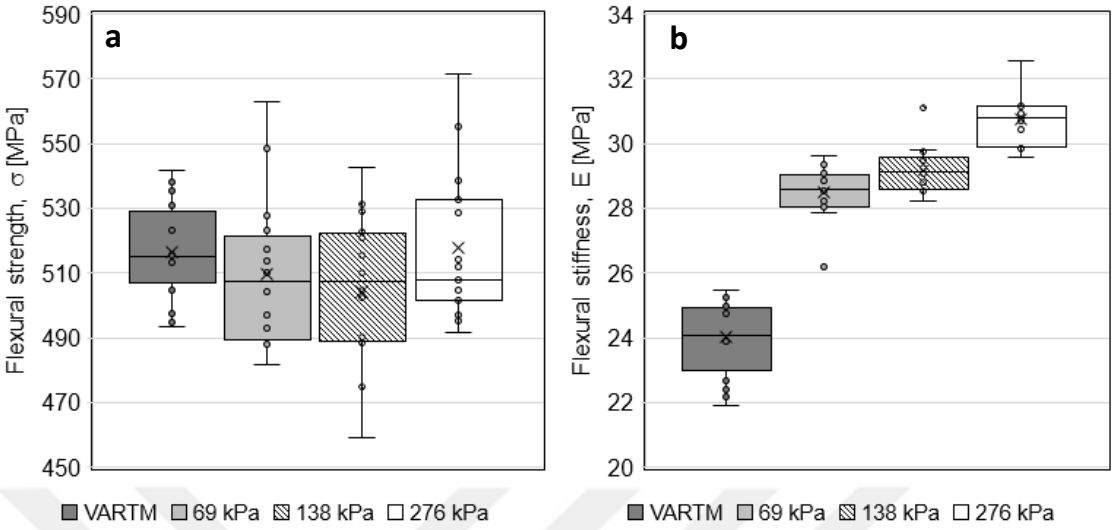

Figure 5.17 - Effect of external pressurization on (a) flexural strength and (b) flexural stiffness of PRO-SET laminates

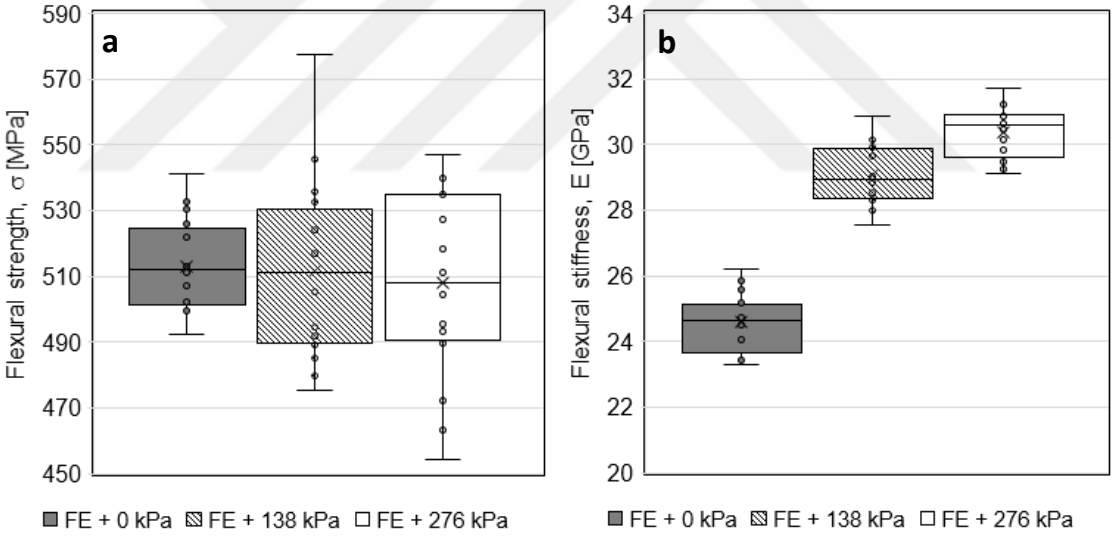

Figure 5.18 - Effect of flow enhancement and external pressurization on (a) flexural strength and (b) flexural stiffness of PRO-SET laminates

Although it was expected to achieve an increase in flexural strength with increasing V_f, it was observed that external pressurization did not cause any significant change in flexural strength of laminates as seen in Figure 5.17. A similar trend was observed for flow enhanced laminates as well in Figure 5.18. This was unlike the results obtained for laminates with EPON resin. This could not be explained by the presence of voids since

the void content was very low and microscopy examinations for PRO-SET laminates showed that almost no voids were present in the laminates. Possible causes of this phenomenon could be (i) improper bonding in between the fiber-matrix interface, and (ii) premature failure of matrix. The former could be investigated by analyzing the increase in flexural stiffness. Stiffness of a composite laminate, E can be expressed with the rule of mixtures: $E = V_f E_{fiber} + (1\text{-}V_f) E_{matrix}$ where V_f is the fiber volume fraction and E_{fiber} and E_{matrix} (3.41 GPa as documented in [81]) are the stiffness of fibers and matrix, respectively. This equation shows that the stiffness of composite, E is linearly related to V_f. However, if significant voids and/or defects in resin-fiber interface are present in the laminate, the linear relation will not be valid. Therefore, the linearity of E vs. V_f was analyzed to investigate the resin-fiber interface.

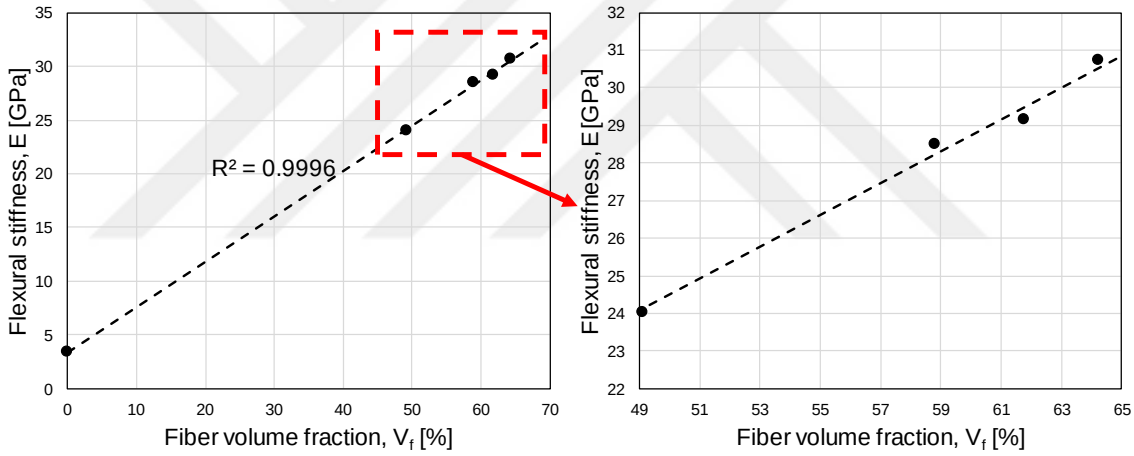

Figure 5.19 - Rule of mixtures analysis to investigate the quality of fiber-matrix interface

Figure 5.19 shows the linear relation between V_f and flexural stiffness which indicates that the fiber-matrix interface was properly formed. Therefore, the second argument (i.e., premature failure of matrix) could address the unchanging flexural strength with increasing fiber volume fraction. As Table 5.1 shows, flexural properties of both EPON and PRO-SET resin were very similar, therefore, one would expect to achieve similar flexural properties for laminates manufactured with both resins. Regardless of V_f, average flexural strength of PRO-SET laminates was ~510 MPa which was much lower than

EPON laminates (from 650 MPa to 695, 709 and 736 MPa at P_{ext} = 0, 34.5, 69, and 138 kPa, respectively). Premature failure of the matrix may be due to incomplete curing of the composite laminates. The manufacturer's datasheet recommends various cure schedules as mentioned in Section 5.2. It recommends room temperature gelation which was claimed as 8 hours in the datasheet. Since this would increase the total processing time enormously, mold temperature was increased 60 minutes after the infusion was started. In addition, 8 hours of curing time was started at this moment whereas, the manufacturer recommends 8 hours of curing at 60 ºC after room temperature gelation. Moreover, manufacturer stated that additional post-curing might be required. However, this was not clearly explained in the datasheet. Regarding all these arguments, it could be concluded that it was highly possible that the matrix was not completely cured which caused premature failure of composite laminates resulting in relatively low flexural strength. After clarifying the cure schedule with the manufacturer, this issue could be eliminated and improvement in flexural strength would be achieved with the low temperature resin as well.

6. CONCLUSIONS AND FUTURE WORK

6.1. Conclusions

In this study, an alternative composite manufacturing method (Pressurized VARTM) was developed to improve the quality and mechanical performance of composite laminates. Effect of process parameters, number of fabric layers, and resin type on the laminate properties and microstructure were investigated.

In Section 3, externally pressurized variant of heated VARTM process was presented by manufacturing 6-ply laminates made of 8-harness satin woven fabric and high temperature resin, EPON 862. A preliminary study was presented to investigate the effect of resin flushing on the laminate properties. It was observed that, voids were formed in between the tows due to dual-scale flow and they were entrapped and could not be removed if the inlet port was closed right after mold filling. Resin flushing was implemented to remove the voids and improve quality of the laminates. It was documented that flushing reduced the void content of laminates below 1% which was as high as 4.7% when flushing was not performed. In addition, effect of pressurization on laminate properties was studied and it was highlighted that external pressurization on its own reduced the void content to 1.4% which was further reduced below 1% when pressurization and flushing were applied together. It was also highlighted that external pressure should be applied at the right time to facilitate these improvements. When the external pressure was applied too late in the process, evacuating the excess resin was difficult as the resin viscosity increased with time which caused thickness gradient along the laminates. External pressurization increased the compaction pressure on the vacuum bag (limited to ~100 kPa in typical VARTM process) and caused the part to be considerably thinner than those made by conventional VARTM. Hence, fiber volume fraction of 6-ply lamianates was increased from 50 to 56, 59 and 62% at external pressure levels of 34.5, 69 and 138 kPa, respectively. The increase in fiber volume fraction yielded to 7, 9, and 13% improvement of flexural strength and 11, 17, and 20% improvement of flexural stiffness at the corresponding external pressure levels.

Effect of external pressurization on physical and mechanical properties of thicker laminates made of 12, and 18 plies of woven glass fabric were investigated and compared with 6-ply laminates. To understand the effect of number of plies on the consolidation of fabric layers, compaction characterization of fabric preforms was conducted. It was observed that thickness per layer decreased (and thus, V_f increased) as N increased and reached an almost steady value. 6-, 12-, and 18-ply preforms had similar compaction behavior (i.e., for large N, thickness per layer reached a steady value). This implied that the effect of nesting was not causing further compaction as the number of layers increased. The effect of external pressurization on thickness reduction and increase in V_f of laminates were also similar in 6, 12, and 18 plies. At 138 kPa of external pressure, fiber volume fraction increased from 50, 51, and 50% to 62, 62, and 61% for 6-, 12-, and 18-ply laminates, respectively which improved flexural strength and stiffness of all laminates. Microstructural analysis showed that overall compaction of the laminates was governed by the nesting of fabric layers and consolidation of fiber tows. It was shown that the increase in number of plies did not cause a significant change in void content which was achieved below 1% in all laminates regardless of the external pressure level. However, the increase in external pressure slightly increased the void content in all 6-, 12-, and 18-ply laminates due to entrapment of mobilized voids in between the fiber tows which were squeezed under external pressurization. Although, intra-tow voids were not seen in most of the laminates, some of laminates manufactured under high external pressurization had them in weft tows at locations where inter-tow voids were densely entrapped. This implied that the voids were not formed due to dual-scale flow but diffusion of inter-tow voids into the tows. It was also shown that the short beam strength of 12- and 18-ply laminates manufactured under various external pressure levels were not significantly affected by the increase in fiber volume fraction and slight variation in void content. As a conclusion, externally pressurized and heated VARTM led to similar improvement in laminate properties at increased laminate thickness while achieving low void content below 1%.

A low temperature processed resin (PRO-SET INF 114) was implemented to pressurized VARTM and it was investigated whether similar improvements in laminate properties would be achieved or not. Since the viscosity of PRO-SET resin was much higher than EPON resin which was processed at high temperatures, fill time increased from ~8 minutes to ~52 minutes. Thus, the post filling time was shortened since the viscosity of resin was already increased due to cross-linking reaction at complete mold filling. Therefore, duration of flushing was reduced from 30 minutes to 15 minutes to remove the voids and equalize the thickness along the laminate before resin gelation. Average thickness of laminates were reduced under external pressurization similar to EPON laminates. Thus, fiber volume fraction was increased similarly as well. It was reported that at external pressure levels of 0, 69, and 138 kPa, fiber volume fraction of laminates were 49, 59, and 62%, respectively. In addition, external pressure was increased to 276 kPa to investigate whether further reduction in laminate thickness and improvement in laminate properties would be achieved or not. At 276 kPa, thickness was slightly reduced and fiber volume fraction was increased up to 64%. It was also noted that with PRO-SET resin, thickness gradient observed in non-pressurized laminates was minimized by external pressurization. Regardless of external pressure level, void content of all laminates was measured and documented below 1%. Moreover, a flow enhancement method was implemented to shorten mold filling time by vacuuming the pressure chamber which reduced the pressure on the vacuum bag and enabled rapid intake of resin. The infused resin was distributed by applying various external pressure levels, 0, 138, and 276 kPa which reduced the average fill time of 52 minutes to 37, 31, and 27 minutes, respectively. Similar fiber volume fraction and void content values compared to non-flow enhanced laminates were reported. Flexural testing of laminates were also conducted. While the flexural stiffness of laminates increased from 24 GPa up to 31 GPa at 276 kPa of external pressure, no improvement in flexural strength was documented. The most possible explanation of this phenomenon was the premature failure of the matrix which was possibly due to incomplete curing of laminates. Since very few voids were observed in the laminates and the fiber-resin interface was maintained properly as the increase in

stiffness indicated, incomplete curing of laminates could be the cause of the early failure of laminates.

Aside from all of these outcomes concluded above, few remarks on the applicability and possible disadvantages of the pressurized VARTM could be discussed. The use of chamber and mold which can withstand pressurization increase the tooling costs and it can be argued that RTM or Compression RTM (C-RTM) may be more convenient manufacturing methods since high compaction pressure levels can also be achieved in those processes by the solid upper mold. However, machining a double sided and matching mold would be much more costly than a single sided mold and a relatively simple pressure chamber as the part dimensions increase. Furthermore, RTM requires an injection machine which also introduces additional costs whereas pressurized VARTM requires only a vacuum pump and a compressor for pressurization. The use of autoclave molding can also be suggested instead of the pressurized and heated VARTM, since both high pressure and high temperature are achieved in an autoclave. However, an autoclave requires very high initial investment and operating costs, whereas heating and pressurization of a mold can be more cost effective in terms of initial investment and energy consumption. In addition, prepreg materials for autoclave molding are more expensive and require more demanding storage conditions (i.e., sub-zero temperature, sealed storage, and low humidity environment) compared to VARTM consumables.

Moreover, as the planar dimensions of the part increase, the required clamping force and mold rigidity increase as well. Therefore, while implementing pressurized VARTM, two factors are critical: (i) the level of external pressure and (ii) tool design. Both should be carefully performed so that conventional equipment for clamping and materials for manufacturing the tools can be used. While it is possible to apply pressurized VARTM to very large-scale parts such as boat hulls (e.g., planar dimensions of 30 m x 10 m), it is not practical to pressurize such large molds due to challenges in chamber design and durability. Therefore, it is recommended to use pressurized VARTM up to mid-scale parts of various industrial applications (e.g., aerospace, automotive, marine and etc.) with few meters of planar dimensions.

As a conclusion, it can be stated that pressurized VARTM is a compelling alternative for RTM and, in some cases, for autoclave molding by manufacturing parts with high fiber volume fractions, low void contents, and sufficiently high mechanical properties.

6.2. Future work

Pressurized VARTM as a newly developed process has a great potential for research and industrial application. Further research can be pursued on pressurized VARTM to investigate the effect of:

- External pressurization on properties of larger laminates:
    - Since the laminate dimensions significantly affect the resin flow within the mold, resin flow and removal through the ports of mold can be different from the studied cases in this thesis. This can cause varying properties in the laminate.
    - Gel time of resin may not be adequate for mold filling, therefore, flow enhancement method can be studied for larger laminates or use of distribution medium can be implemented to pressurized VARTM.
- Cyclic pressurization on thickness reduction and void removal:
    - Cyclic pressurization of impregnated fabric may further reduce the thickness of laminates by enhancing the nesting of fibers.
    - The entrapped voids due to pressurization may be removed due to cyclic relaxation of preform and almost void-free laminates can be manufactured.
- External pressurization on the parts with curvatures:
    - Pressurization may eliminate the resin accumulation at the bend corners of mold by further draping and compressing the fabric into the curvature.
- Use of various types of fabrics on laminate consolidation and properties:
    - Non-crimp and 3D woven fabrics may be worthy of investigating, since their structure and compaction behavior is different from the fabric used in this study.

In addition to these, process modeling of pressurized VARTM can be developed to predict mold filling time, pressure application duration, resin gelation, final thickness and fiber volume fraction of laminates.

7. REFERENCES

[1] Advani SG, Sozer EM. Process Modeling in Composites Manufacturing. 2nd ed. London: Taylor & Francis; 2010.

[2] Miracle DB, ASM International HC, Donaldson SL, editors. ASM Handbook Composites Volume 21. 10th ed. Ohio: ASM International; 2001.

[3] Abraham D, Matthews S, McIlhagger R. A comparison of physical properties of glass fibre epoxy composites produced by wet lay-up with autoclave consolidation and resin transfer moulding. Compos Part A Appl Sci Manuf 1998;29:795–801.

[4] Andersson HM, Lundstrom TS, Gebart BR, Langstrom R. Flow-enhancing layers in the vacuum infusion process. Polym Compos 2002;2:895–901.

[5] Mathur R, Heider D, Hoffmann C, Gillespie Jr. J, Advani SG, Fink BK. Flow front measurements and model validation in the vacuum assisted resin transfer molding process. Polym Compos 2001;22:477–90.

[6] Seemann WH. Plastic transfer molding techniques for the production of fiber reinforced plastic structures. 4902215, 1990.

[7] Kuentzer N, Simacek P, Advani SG, Walsh S. Correlation of void distribution to VARTM manufacturing techniques. Compos Part A Appl Sci Manuf 2007;38:802–13.

[8] Sas HS, Simacek P, Advani SG. A methodology to reduce variability during vacuum infusion with optimized design of distribution media. Compos Part A Appl Sci Manuf 2015;78:223–33.

[9] Allende M, Mohan R V., Walsh SM. Experimental and numerical analysis of flow behavior in the FASTRAC liquid composite manufacturing process. Polym Compos 2004;25:384–96.

[10] Curtis PT, Whitehead DL. The effect of fabrication-induced surface roughness on the compressive and flexural properties of carbon fibre-reinforced plastics. Compos Manuf 1990;1:235–41.

[11] Hammami A, Gebart BR. Analysis of the vacuum infusion molding process. Polym Compos 2000;21:28–40.

[12] Alms JB. Flow manipulation and control methodologies for vacuum infusion processes. University of Delaware, 2010.

[13] Alms J, Advani SG. Simulation and experimental validation of flow flooding chamber method of resin delivery in liquid composite molding. Compos Part A Appl Sci Manuf 2007;38:2131–41.

[14] Alms JB, Advani SG, Glancey JL. Liquid composite molding control methodologies using vacuum induced preform relaxation. Compos Part A Appl Sci Manuf 2011;42:57–65.

[15] Alms JB, Glancey JL, Advani SG. Mechanical properties of composite structures fabricated with the vacuum induced preform relaxation process. Compos Struct 2010;92:2811–6.

[16] Mall S, Katwyk DW, Bolick RL, Kelkar AD, Davis DC. Tension–compression fatigue behavior of a H-VARTM manufactured unnotched and notched carbon/epoxy composite. Compos Struct 2009;90:201–7.

[17] Fu X, Zhang C, Liang R, Wang B, Fielding JC. High temperature vacuum assisted resin transfer molding of phenylethynyl terminated imide composites. Polym Compos 2008;16:101–13.

[18] Anderson JP, Kelly AJ, Altan MC. Fabrication of composite laminates by vacuum-assisted resin transfer molding augmented with an inflatable bladder. Proc. Am. Soc. Compos. 28th Tech. Conf., 2013.

[19] Bolick R, Kelkar A. Heat vacuum assisted resin transfer molding processes for manufacturing composite materials. US 2009/0189320, 2009.

[20] Menta V, Vuppalapati R, Chandrashekhara K, Schuman T, Sha J. Elevated-temperature vacuum-assisted resin transfer molding process for high performance aerospace composites. Polym Int 2013;62:1465–76.

[21] Ghose S, Watson K a., Cano RJ, Britton SM, Jensen BJ, Connell JW, et al. High temperature VARTM of phenylethynyl terminated imides. High Perform Polym 2009;21:653–72.

[22] Shinde D, Kimbro E, Mohan R, Kelkar A. Mechanical properties of woven fiberglass composite interleaved with glass nanofibers. 19TH Int. Conf. Compos. Mater., 2013, p. 1–12.

[23] Michaud V. A review of non-saturated resin flow in liquid composite moulding processes. Transp Porous Media 2016:1–21.

[24] Ruiz E, Achim V, Soukane S, Trochu F, Bréard J. Optimization of injection flow rate to minimize micro/macro-voids formation in resin transfer molded composites. Compos Sci Technol 2006;66:475–86.

[25] Hamidi YK, Dharmavaram S, Aktas L, Altan MC. Effect of fiber content on void morphology in resin transfer molded e-glass/epoxy composites. J Eng Mater Technol 2009;131:21014-1-021014–11.

[26] Zhan-Sheng Guo, Ling Liu, Bo-Ming Zhang, Shanyi Du. Critical void content for thermoset composite laminates. J Compos Mater 2009;43:1775–90.

[27] Costa ML, de Almeida SFM, Rezende MC. Critical void content for polymer composite laminates. AIAA J 2005;43:1336–41.

[28] Kang MK, Lee W Il, Hahn HT. Formation of microvoids during resin-transfer molding process. Compos Sci Technol 2000;60:2427–34.

[29] Lo J, Anders M, Centea T, Nutt SR. The effect of process parameters on volatile release for a benzoxazine-epoxy RTM resin. Compos Part A Appl Sci Manuf 2016;84:326–35.

[30] Afendi M, Banks WM, Kirkwood D. Bubble free resin for infusion process. Compos Part A Appl Sci Manuf 2005;36:739–46.

[31] Kedari VR, Farah BI, Hsiao K-T. Effects of vacuum pressure, inlet pressure, and mold temperature on the void content, volume fraction of polyester/e-glass fiber

composites manufactured with VARTM process. J Compos Mater 2011;45:2727–42.

[32] Olivero KA, Barraza HJ, O'Rear EA, Altan MC. Effect of injection rate and post-fill cure pressure on properties of resin transfer molded disks. J Compos Mater 2002;36:2011–28.

[33] Lundström T, Gebart B. Influence from process parameters on void formation in resin transfer molding. Polym Compos 1994;15:25–33.

[34] Sudarisman, Davies IJ. The effect of processing parameters on the flexural properties of unidirectional carbon fibre-reinforced polymer (CFRP) composites. Mater Sci Eng A 2008;498:65–8.

[35] Kaynak C, Akgul E, Isitman NA. Effects of RTM mold temperature and vacuum on the mechanical properties of epoxy/glass fiber composite plates. J Compos Mater 2008;42:1505–21.

[36] Brouwer WD, Van Herpt ECFC, Labordus M. Vacuum injection moulding for large structural applications. Compos Part A Appl Sci Manuf 2003;34:551–8.

[37] Li W, Krehl J, Gillespie JW, Heider D, Endrulat M, Hochrein K, et al. Process and performance evaluation of the vacuum-assisted process. J Compos Mater 2004;38:1803–14.

[38] Yalcinkaya MA, Sozer EM. Effect of part thickness variation on the mold filling time in vacuum infusion process. J Reinf Plast Compos 2014;33:2136–50.

[39] Yenilmez B, Senan M, Sozer EM. Variation of part thickness and compaction pressure in vacuum infusion process. Compos Sci Technol 2009;69:1710–9.

[40] Tackitt KD, Walsh SM. Experimental study of thickness gradient formation in the VARTM process. Mater Manuf Process 2005;20:607–27.

[41] Simacek P, Eksik O, Heider D, Gillespie JW, Advani S. Experimental validation of post-filling flow in vacuum assisted resin transfer molding processes. Compos Part A Appl Sci Manuf 2012;43:370–80.

[42] Caglar B, Yenilmez B, Sozer EM. Modeling of post-filling stage in vacuum infusion using compaction characterization. J Compos Mater 2015;49:1947–60.

[43] Timms J, Bickerton S, Kelly PA. Laminate thickness and resin pressure evolution during axisymmetric liquid composite moulding with flexible tooling. Compos Part A Appl Sci Manuf 2012;43:621–30.

[44] Simacek P, Heider D, Gillespie JW, Advani S. Post-filling flow in vacuum assisted resin transfer molding processes: Theoretical analysis. Compos Part A Appl Sci Manuf 2009;40:913–24.

[45] Govignon Q, Bickerton S, Kelly P. Experimental investigation into the post-filling stage of the resin infusion process. J Compos Mater 2012;47:1479–92.

[46] Causse P, Ruiz E, Trochu F. Experimental Study of Flexible Injection to Manufacture Parts of Strong Curvature. Polym Compos 2011:882–95. doi:10.1002/pc.

[47] Daqoune T, Ruiz E. Study of the compaction chamber geometry for manufacturing of composite by flexible injection. 9th Int. Conf. Flow Process. Compos. Mater., 2008.

[48] Fibreglast. Style 7781 E-Glass. 2010.

[49] Aktas L, Bauman DP, Bowen ST, Saha MC, Altan MC. Effect of distribution media length and multiwalled carbon nanotubes on the formation of voids in VARTM composites. J Eng Mater Technol 2011;133:41006-1-041006–9.

[50] Resolution performance products. Epikote Resin 862/ Epikure Curing Agent W System. 2001.

[51] White E. Surface free energy measurements of epon 828 and m-Phenylenediamine as a curing agent of epon 828. Atlanta University, 1983.

[52] Park CH, Lebel A, Saouab A, Bréard J, Lee W Il. Modeling and simulation of voids and saturation in liquid composite molding processes. Compos Part A Appl Sci Manuf 2011;42:658–68.

[53] Park CH, Lee W Il. Modeling void formation and unsaturated flow in liquid composite molding processes: a survey and review. J Reinf Plast Compos 2011;30:957–77.

[54] Patel N, Rohatgi V, Lee LJ. Modeling of void formation and removal in liquid composite molding. Part II: Model development and implementation. Polym Compos 1996;17:104–14.

[55] Almeida M De, Cerqueira M, Leali M. The influence of porosity on the interlaminar shear strength of carbon / epoxy and carbon / bismaleimide fabric laminates. Compos Sci Technol 2001;61:2101–8.

[56] Nedanov PB, Advani SG. A method to determine 3D permeability of fibrous reinforcements. J Compos Mater 2002;36:241.

[57] Correia NC, Robitaille F, Long AC, Rudd CD, Simacek P, Advani SG. Analysis of the vacuum infusion moulding process: I. analytical formulation. Compos Part A Appl Sci Manuf 2005;36:1645–56.

[58] Chen D, Arakawa K, Uchino M. Effects of the addition of a cover mold on resin flow and the quality of the finished product in vacuum-assisted resin transfer molding. Polym Compos 2016;37:1435–42.

[59] Hamidi YK, Aktas L, Altan MC. Three-dimensional features of void morphology in resin transfer molded composites. Compos Sci Technol 2005;65:1306–20.

[60] Pearce N, Guild F, Summerscales J. A study of the effects of convergent flow fronts on the properties of fibre reinforced composites produced by RTM. Compos Part A Appl Sci Manuf 1998;29:141–52.

[61] Koushyar H, Alavi-Soltani S, Minaie B, Violette M. Effects of variation in autoclave pressure, temperature, and vacuum-application time on porosity and mechanical properties of a carbon fiber/epoxy composite. J Compos Mater 2012;46:1985–2004.

[62] Yenilmez B, Sozer EM. Compaction of e-glass fabric preforms in the Vacuum Infusion Process, A: Characterization experiments. Compos Part A Appl Sci

Manuf 2009;40:499–510.

[63] Lomov S V., Verpoest I, Peeters T, Roose D, Zako M. Nesting in textile laminates: Geometrical modelling of the laminate. Compos Sci Technol 2003;63:993–1007.

[64] Saunders R a., Lekakou C, Bader MG. Compression and microstructure of fibre plain woven cloths in the processing of polymer composites. Compos Part A Appl Sci Manuf 1998;29:443–54.

[65] Chen B, Cheng AH, Chou T. A nonlinear compaction model for fibrous preforms. Compos Part A Appl Sci Manuf 2001;32:701–7.

[66] Yalcinkaya MA, Caglar B, Sozer EM. Effect of permeability characterization at different boundary and flow conditions on vacuum infusion process modeling. J Reinf Plast Compos 2016.

[67] Govignon Q, Bickerton S, Kelly PA. Simulation of the reinforcement compaction and resin flow during the complete resin infusion process. Compos Part A Appl Sci Manuf 2010;41:45–57.

[68] Robitaille F, Gauvin R. Compaction of textile reinforcements for composites manufacturing. I: Review of experimental results. Polym Compos 1998;19:198–216.

[69] Saunders RA, Lekakou C, Bader MG. Compression in the processing of polymer composites 1. A mechanical and microstructural study for different glass fabrics and resins. Compos Sci Technol 1999;59:983–93.

[70] Young W. Consolidation and cure simulations for laminated composites. Polym Compos 1996;17:142–8.

[71] Robitaille F, Gauvin R. Compaction of textile reinforcements for composites manufacturing. III: Reorganization of the fiber network. Polym Compos 1999;20:48–61.

[72] Somashekar AA, Bickerton S, Bhattacharyya D. Exploring the non-elastic compression deformation of dry glass fibre reinforcements. Compos Sci Technol

2007;67:183–200.

[73] Chen B, Chou T. Compaction of woven-fabric preforms: nesting and multi-layer deformation. Compos Sci Technol 2000;60:2223–31.

[74] Chen B, Lang EJ, Chou TW. Experimental and theoretical studies of fabric compaction behavior in resin transfer molding. Mater Sci Eng A 2001;317:188–96.

[75] Suhot MA, Chambers AR. The effect of voids on the flexural fatigue properties of carbon/epoxy composites. 16th Int. Conf. Compos. Mater., 2007.

[76] Olivier P, Cottu JP, Ferret B. Effects of cure cycle pressure and voids on some mechanical properties of carbon/epoxy laminates. Composites 1995;26:509–15.

[77] Esnaola A, Tena I, Aurrekoetxea J, Gallego I, Ulacia I. Effect of fibre volume fraction on energy absorption capabilities of E-glass/polyester automotive crash structures. Compos Part B Eng 2016;85:1–7.

[78] Wisnom MR, Reynolds T, Gwilliam N. Reduction in interlaminar shear strength by discrete and distributed voids. Compos Sci Technol 1996;56:93–101.

[79] Hernandez S, Sket F, Molina-Aldareguia JM, Gonzalez C, LLorca J. Effect of curing cycle on void distribution and interlaminar shear strength in polymer-matrix composites. Compos Sci Technol 2011;71:1331–41.

[80] Jeong H. Effect of voids on the mechanical strength and ultrasonic attenuation of laminated composites. J Compos Mater 1997;31:276–92.

[81] Prosetepoxy. PRO-SET INF-114 / INF-211 Technical Data. 2015.

8. APPENDIX

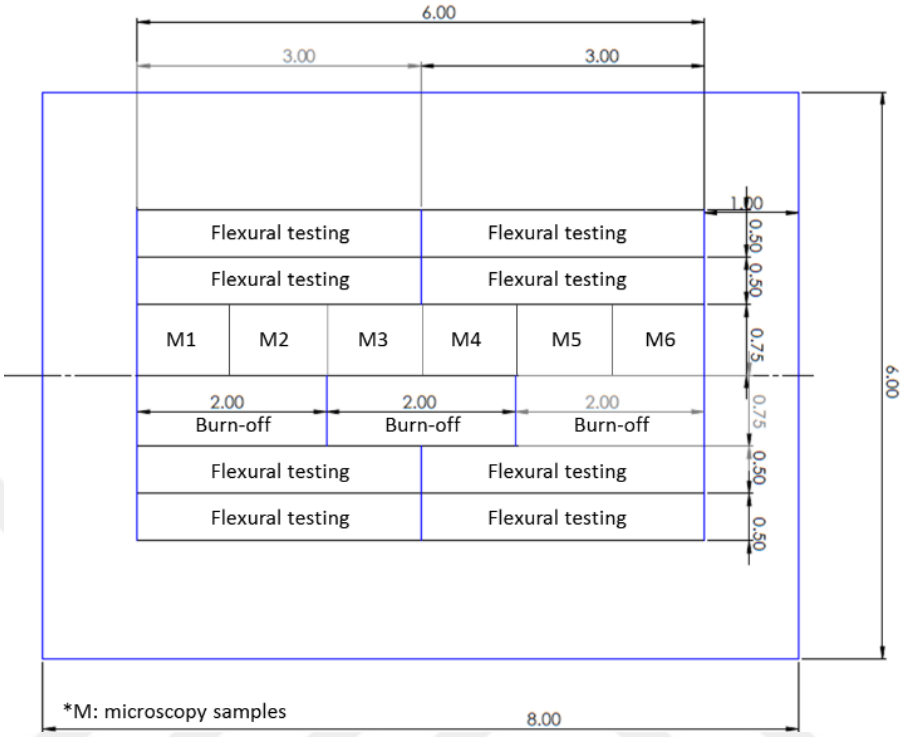

Figure A.1 - Cutting template for 6-ply laminates

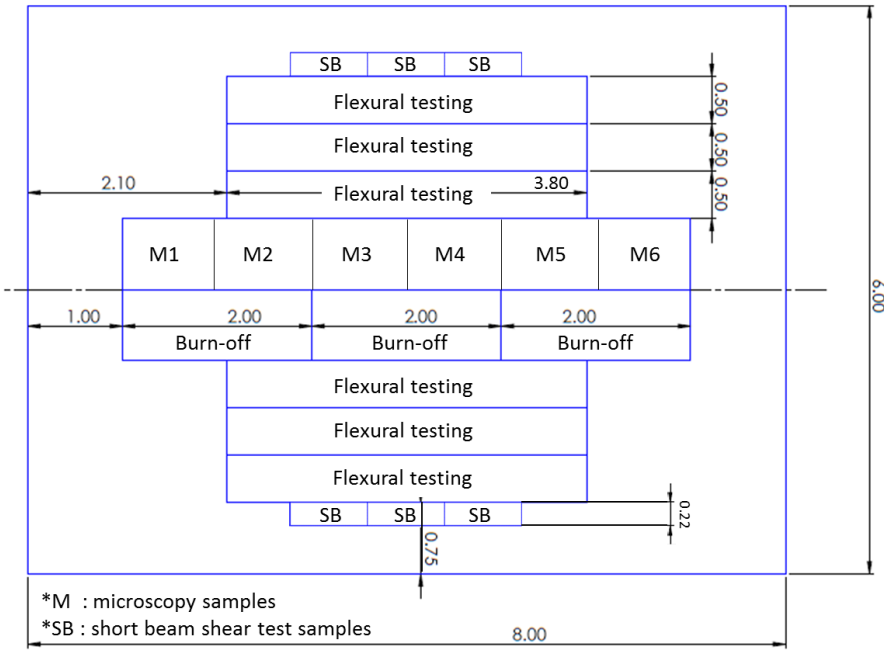

Figure A.2 - Cutting template for 12-ply laminates

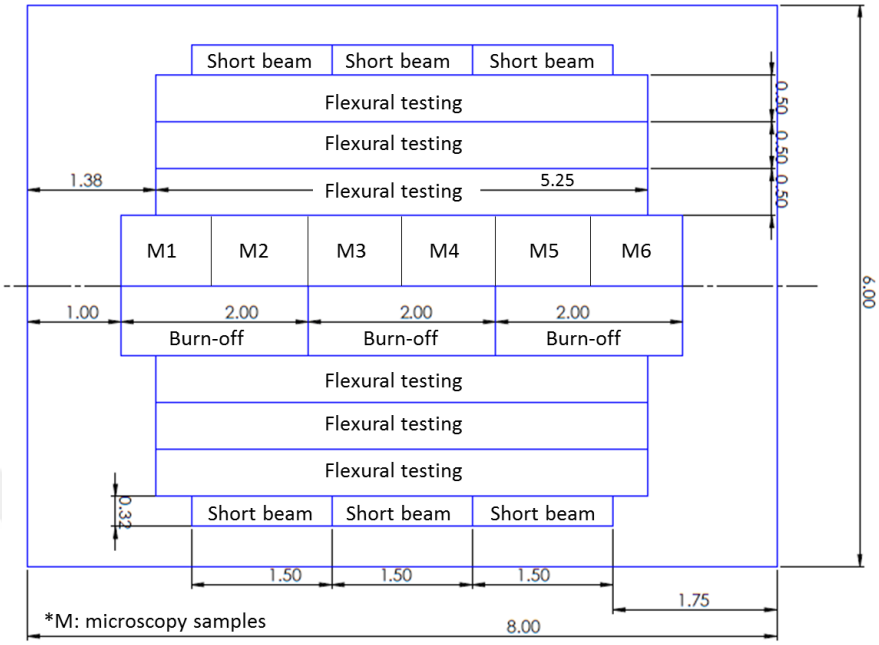

Figure A.3 - Cutting template for 18-ply laminates

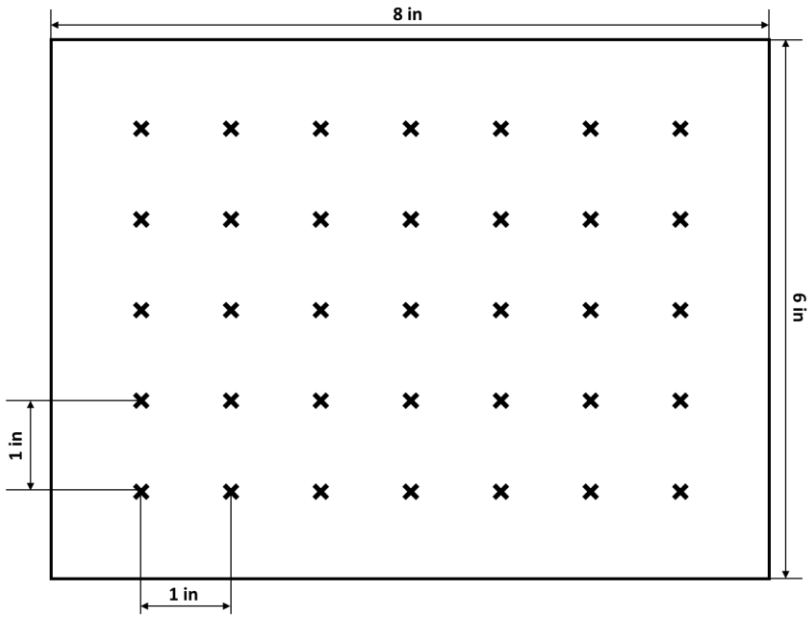

Figure A.4 – Thickness measurement template for all laminates

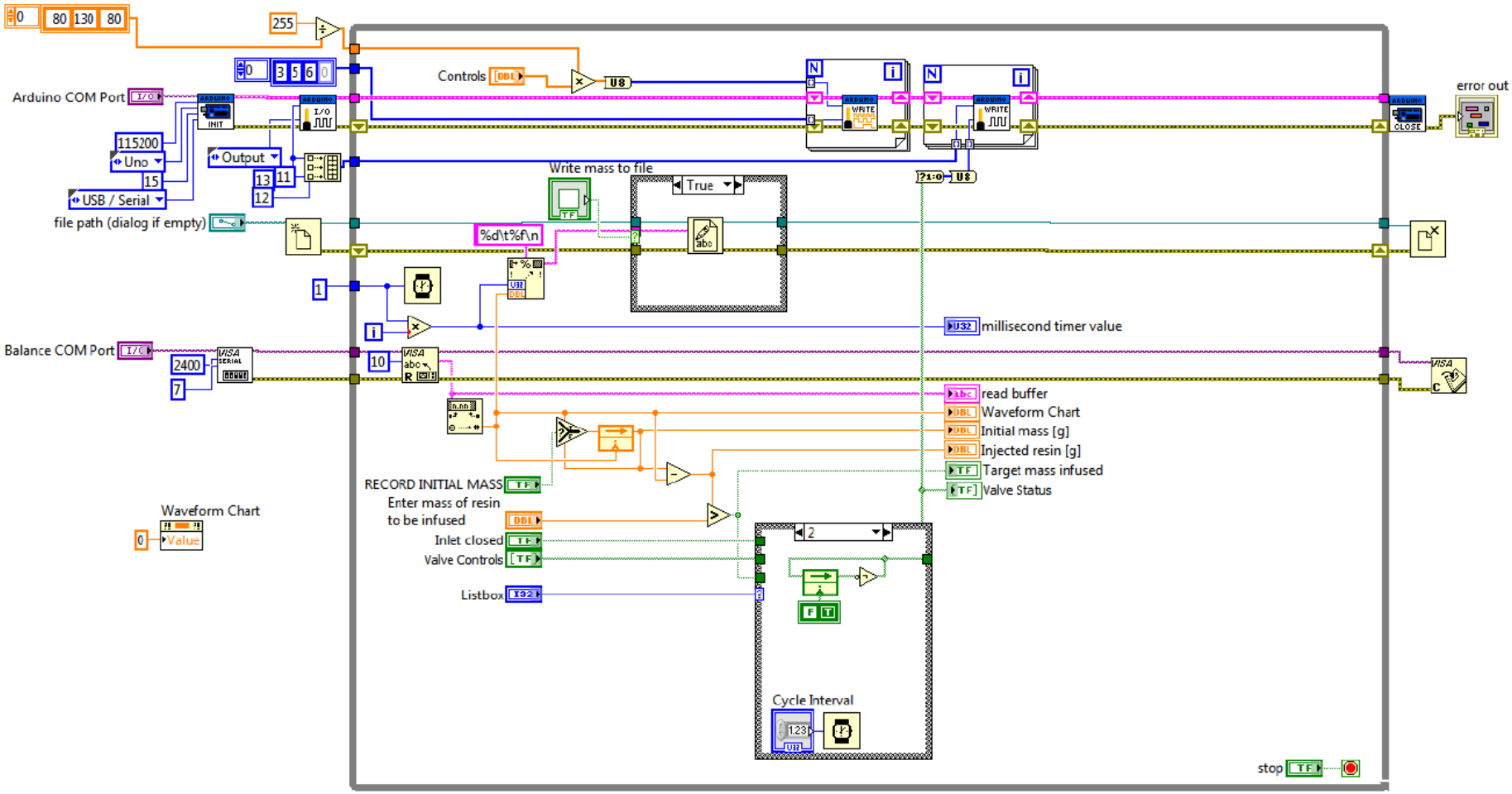

Figure A.5 – Labview block diagram for the control of experimental setup

Box and Whisker plot:

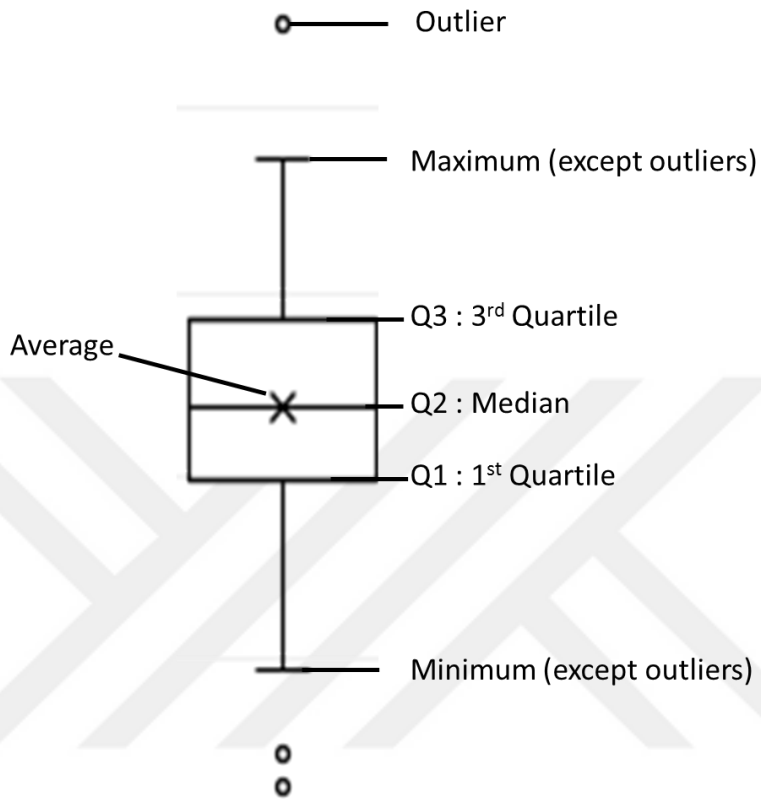

Figure A.6 - Box and Whisker plot

- 25% of the data is in between **Minimum** and **Q1** (Quartile 1)
- 25% of the data is in between **Q1** and **Q2**
- 25% of the data is in between **Q2** and **Q3**
- 25% of the data is in between **Q3** and **Maximum**
- The range between **Q1** and **Q3** is called Interquartile range, **IQR**
- Outliers are in **3 x IQR**

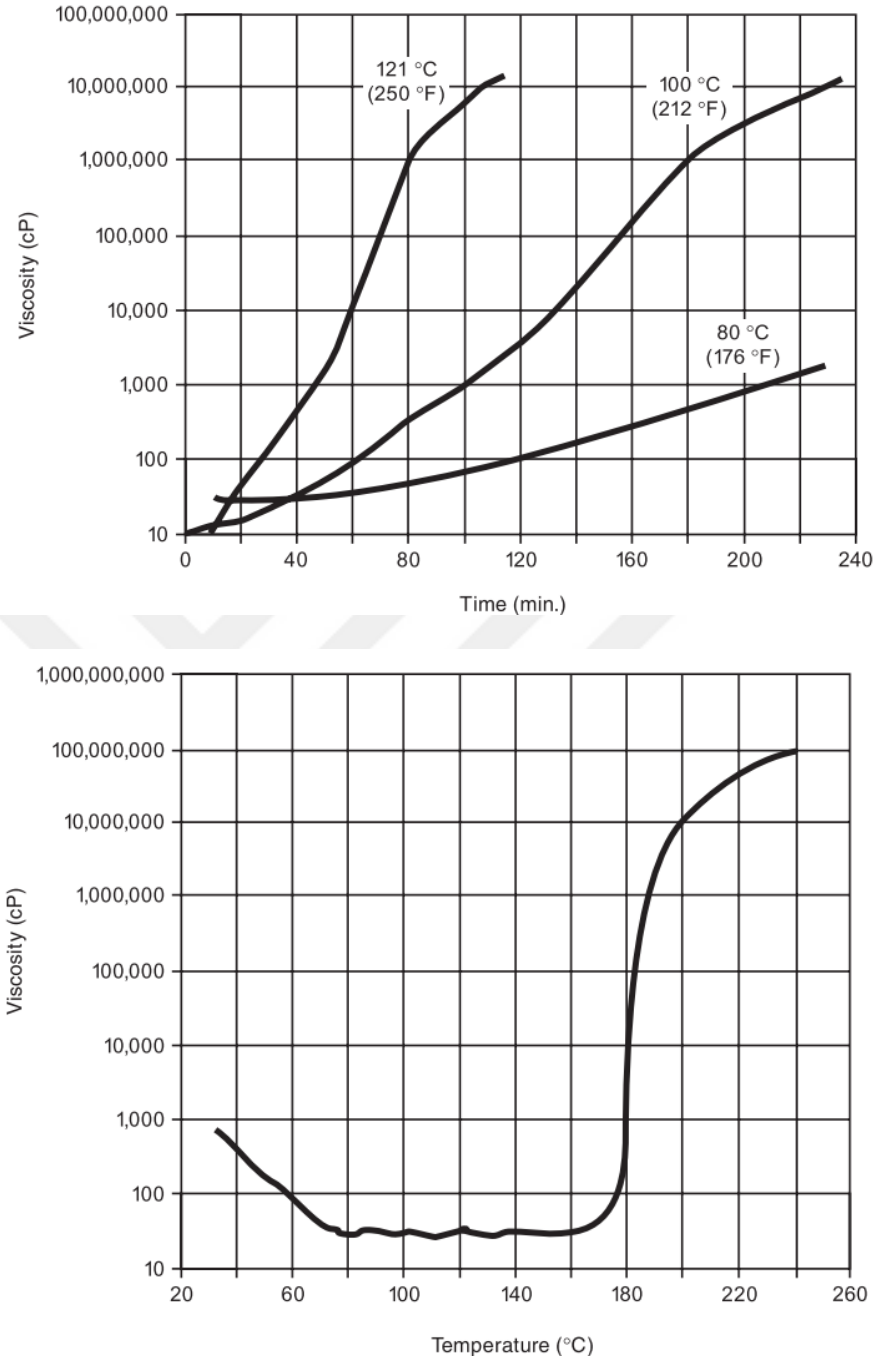

Figure A.7 – Change in viscosity of EPON 862 with time and temperature [50]